Nano Research

ISSN 1998-0124 CN 11-5974/O4
https://doi.org/10.26599/NR.2026.94908821

Review Article

Evolution of next-generation guided bone regeneration barrier membranes: Biodegradable materials, advanced structural designs, and intelligent integrated systems

Jiahua Ni[1], Tiantian Chen[2], Xin Guan[1], Chenxi Wang[1], Nianzhe Wu[1], Jing Lu[1], Xingyu Gao[1], Lei Zhang[3], Wenhui Wang[1](✉), Zhe Zhao[1](✉), Xiaonong Zhang[4,5]

[1] College of Biological Science and Medical Engineering, Donghua University, Shanghai 201620, China

[2] Shanghai Xuhui District Dental Center, Shanghai 200030, China

[3] College of Information Science and Technology, Donghua University, Shanghai 201620, China

[4] State Key Laboratory of Metal Matrix Composites, School of Materials Science and Engineering, Shanghai Jiao Tong University, Shanghai 200240, China

[5] Suzhou Origin Medical Technology Co. Ltd., Suzhou 215513, China

Nano Res., **Just Accepted Manuscript** • https://doi.org/10.26599/NR.2026.94908821

https://www.sciopen.com/journal/1998-0124 on May. 6, 2026

Review Article

Evolution of next-generation guided bone regeneration barrier membranes: Biodegradable materials, advanced structural designs, and intelligent integrated systems

Jiahua Ni[1], Tiantian Chen[2], Xin Guan[1], Chenxi Wang[1], Nianzhe Wu[1], Jing Lu[1], Xingyu Gao[1], Lei Zhang[3], Wenhui Wang[1]✉, Zhe Zhao[1]✉, and Xiaonong Zhang[4,5]

[1] College of Biological Science and Medical Engineering, Donghua University, Shanghai 201620, China

[2] Shanghai Xuhui District Dental Center, Shanghai 200030, China

[3] College of Information Science and Technology, Donghua University, Shanghai 201620, China

[4] State Key Laboratory of Metal Matrix Composites, School of Materials Science and Engineering, Shanghai Jiao Tong University, Shanghai 200240, China

[5] Suzhou Origin Medical Technology Co. Ltd., Suzhou 215513, China

Received: 19 March 2026; **Revised:** 14 April 2026; **Accepted:** 6 May 2026

✉Address correspondence to Wenhui Wang, wenhuiwang@dhu.edu.cn; Zhe Zhao, zhezhao@dhu.edu.cn

Cite this article: *Nano Research*, 2026, 19, 94908821 https://doi.org/10.26599/NR.2026.94908821

ABSTRACT: Successful osseointegration and long-term stability of dental implants depend on sufficient healthy bone tissue at the surgical site. Guided bone regeneration (GBR) has emerged as a critical treatment modality for alveolar bone defects, utilizing physical barrier membranes to selectively inhibit soft tissue cell migration and create a favorable environment for osteoblast proliferation. This review provides a comprehensive overview of recent advancements in GBR barrier membranes, specifically focusing on biodegradable polymers, biodegradable metals, and novel intelligent systems. We first detail the application of absorbable polymers, categorizing natural (e.g., collagen, chitosan, silk fibroin) and synthetic (e.g., polylactic acid (PLA), poly(lactic-co-glycolic acid) (PLGA), polycaprolactone (PCL)) materials, and discussing strategies to optimize their degradation kinetics and mechanical stability. A significant portion of this review is dedicated to the burgeoning field of biodegradable metals, particularly magnesium (Mg)- and zinc (Zn)-based alloys, which offer superior space-maintaining capacity and inherent bioactivity without the need for secondary removal. Furthermore, we explore novel GBR membranes characterized by advanced structural designs, such as asymmetric and bioinspired architecture, and smart responsive systems that respond to pH, light, or enzymes. Special emphasis is placed on the integration of electroactive materials, nanotechnology, and the emerging role of artificial intelligence (AI) and flexible sensing for real-time postoperative monitoring. By synthesizing progress across material science and digital technology, this review outlines the transition of GBR membranes from passive barriers to active, intelligent therapeutic platforms for precision bone tissue engineering.

KEYWORDS: guided bone regeneration, barrier membranes, biodegradable materials, intelligent integrated systems, artificial intelligence

Contents

1 Introduction

Dental implantation has become a pivotal solution for the treatment of tooth loss, and adequate bone volume is a prerequisite for achieving ideal osseointegration of implants [1, 2]. The primary causes of alveolar bone defects include: congenital developmental anomalies, severe periodontal disease, bone loss due to periapical lesions, traumatic injuries, secondary defects following tumor/cyst resection, and disuse atrophy resulting from prolonged tooth loss [3]. Currently, the commonly employed clinical methods for alveolar bone augmentation include ridge expansion, maxillary sinus floor elevation, distraction osteogenesis, autologous bone grafting, and guided bone regeneration (GBR) technology [4, 5].

GBR is widely used in the reconstruction of alveolar bone defects in edentulous areas. Its principle (**Figure 1**) involves the placement of a mechanical barrier membrane to isolate the bone defect from surrounding connective tissues, thereby preventing the infiltration of non-osteogenic cells and providing a stable environment for osteogenic cell growth [6, 7]. By the 1990s, GBR technology had gradually matured. It involved the use of barrier membranes to prevent the invasion of soft tissue cells into bone defects, with or without the combination of bone grafts/substitutes (such as autografts, allografts, or xenografts), to create optimal conditions for bone regeneration. This established GBR as an effective method for alveolar bone augmentation, offering new options for patients with inadequate bone volume [8]. Currently, GBR technology is widely used in oral implantology. Clinical data indicate that approximately 40% of implant patients require GBR surgery due to bone defects [9].

Given the rapid emergence of digital healthcare, in this review, we propose that the evolution of GBR barrier membranes is categorized into four generations: ① First-generation (non-resorbable): e-PTFE and titanium-reinforced membranes offer superior space maintenance but require secondary surgery and face high exposure/infection risks (30%-40%) [10]. ② Second-generation (resorbable): Natural collagen and synthetic polymers (e.g., polylactic acid (PLA)) eliminate removal surgery, though balancing degradation with mechanical support remains critical [11, 13]. ③ Third-generation tissue-engineered membranes: These utilize novel materials (biodegradable metals (BMs), biomimetic

nanofibers, and functional modifications), and advanced technologies (e.g., electrospinning), and additives (e.g., growth factors (BMP-2) or antimicrobial agents) to obtain dual-functional support [11, 12]. Most third-generation membranes are currently in laboratory or pre-clinical stages. ④ Fourth-generation intelligent membranes (in early stages): These integrate flexible sensing technology and artificial intelligence (AI) to construct intelligent monitoring systems capable of tracking bone regeneration progress in real-time and optimizing postoperative management. The absorbable materials and novel materials employed in GBR barrier membranes are depicted in **Figure 1**.

Following GBR surgery, the barrier membrane orchestrates a specialized microenvironment through four key biological phases (**Figure 1**): Inflammatory phase & fibrin clot formation (24 h): A hematoma and fibrin clot form, rich in growth factors (bone morphogenetic protein-2 (BMP-2), transforming growth factor-beta (TGF-β)) that drive subsequent cell migration and angiogenesis [13]. Cell migration & angiogenesis: Osteoblasts and mesenchymal stem cells (MSCs) infiltrate the defect via new vasculature. Cluster of differentiation 68-positive ($CD68^+$) macrophages and osteoprogenitor cells secrete vascular endothelial growth factor (VEGF) and bone morphogenetic proteins (BMPs) to direct bone remodeling. Vascular synergy: Early vascularization is critical for osteogenesis and anti-infection capacity. Even if membranes are exposed, they can support functional vascularization essential for regeneration [12, 14]. Bone remodeling equilibrium: Osteoblasts and osteoclasts maintain a dynamic equilibrium during matrix synthesis and mineralization [13].

Clinical GBR membranes face several critical complications: Exposure and infection, leading to microbial colonization [15]. Degradation mismatch, where rapid resorption or acidic by-products cause structural collapse and inflammation [12, 16]. Mechanical failure, particularly graft displacement in vertical augmentation [10]. Bioactivity deficiencies, specifically lacking antibacterial and osteoinductive components; and surgical trauma, including nerve injury. Success requires balancing material properties, technique, and patient-specific factors [17].

Based on the aforementioned analysis, an ideal GBR membrane should possess the following characteristics [18]: ① Biocompatibility: Elicit a moderate tissue response without interfering with therapeutic outcomes. ② Space-maintaining capacity: Exhibit sufficient mechanical strength and structural integrity to resist compression by soft tissues. ③ Barrier sealing function: Prevent fibrous

tissue infiltration, bacterial invasion, and bone resorption while permitting the exchange of oxygen and nutrients. ④ Bioactivity: Accelerate natural bone healing through pro-angiogenic, osteoinductive, or similar functionalities. ⑤ Clinical operability: Be easily shaped during surgery without tearing, maintain its morphology after implantation, and avoid causing soft tissue damage due to excessive rigidity. ⑥ Antibacterial functionality: Actively inhibit bacterial adhesion and biofilm formation; ⑦ Degradation matching: Demonstrate degradation kinetics synchronized with the bone regeneration period (typically recommended to be 16 to 24 weeks) and mechanical support requirements. ⑧ Low complication risk: Minimize adverse events such as membrane exposure, infection, and inflammation. Guided by these criteria, current research has developed various barrier membranes to enhance the predictability of GBR therapy, reduce complications, and shorten surgical duration.

This review specifically focuses on biodegradable GBR materials and novel GBR membranes, which are currently in the research stage. We propose a fourth-generation classification characterized by intelligent monitoring systems that integrate flexible sensing and AI. This work evaluates the respective advantages and limitations of these GBR membrane materials and explores how interdisciplinary innovations (such as three-dimensional (3D) and four-dimensional (4D) printing, stimulus-responsive mechanisms, and AI-driven diagnostics) can address current clinical challenges. By synthesizing advances in materials science and digital technologies, this review outlines a strategic roadmap toward more precise, predictable, and intelligent bone regeneration therapies.

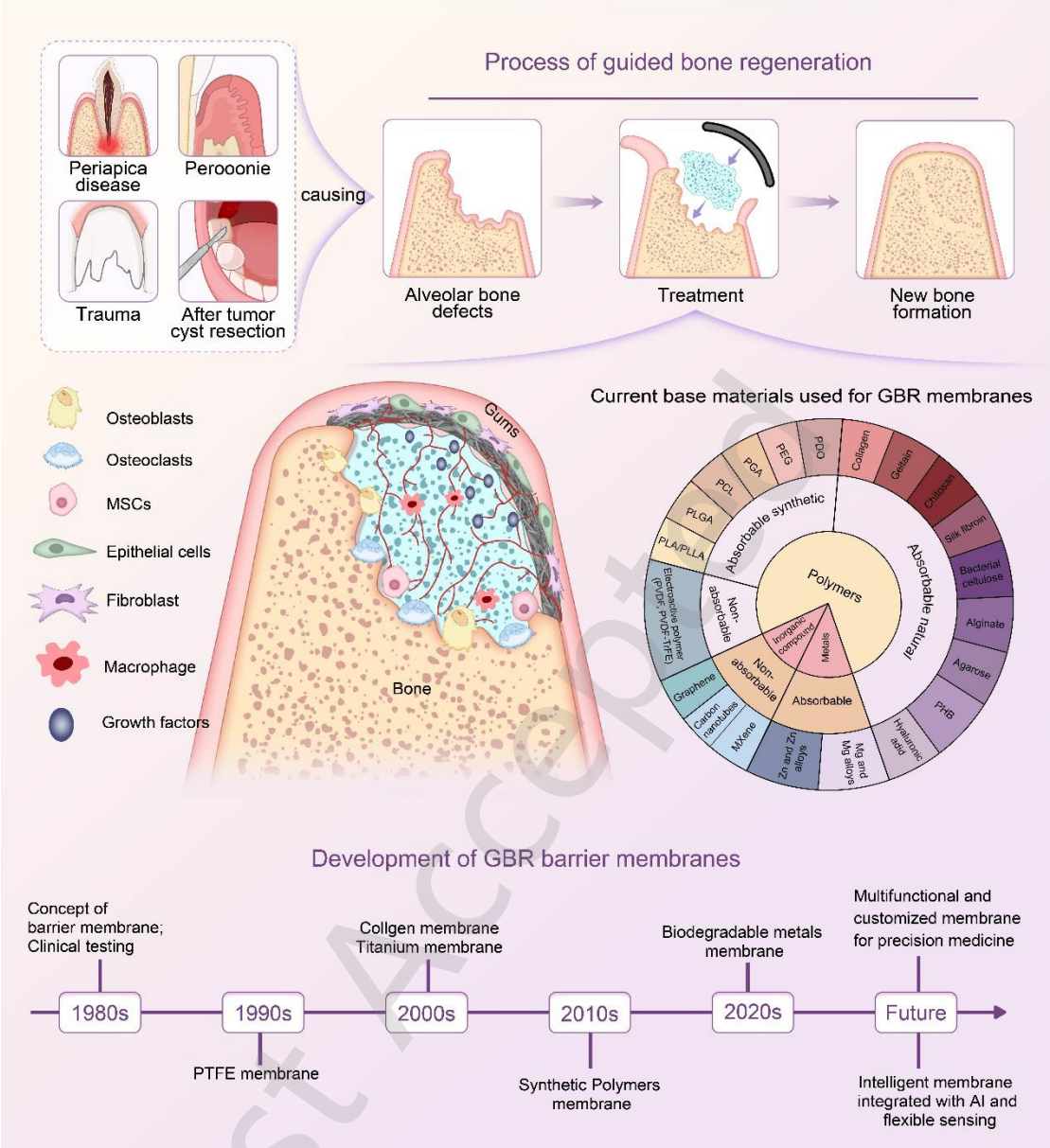

Figure 1 Process, principle, current materials and development of GBR barrier membranes.

2 Absorbable polymer GBR membranes

Absorbable GBR membranes are clinically preferred as they eliminate secondary surgeries, reduce costs, and provide osteogenic capacity comparable to non-resorbable alternatives [19-21]. However, they often face challenges regarding dimensional stability and mechanical strength [11]. Precisely matching degradation kinetics with the bone regeneration cycle remains essential to avoid clinical failure [22]. These membranes are generally categorized into natural polymers (e.g., collagen) and synthetic polymers (e.g., PLA) [23].

2.1 Natural polymers

Natural polymers offer inherent bioactivity [24, 25]. Nevertheless, they present challenges such as potential immunogenicity, complex purification, risk of zoonotic disease transmission, and highly variable mechanical or degradation profiles [26].

2.1.1 Collagen membranes

Collagen is the gold standard for natural GBR membranes and the most widely used animal-derived barrier in clinical practice [27, 28]. Since the 1995 launch of Bio-Gide® [29], collagen has dominated the market due to its excellent biocompatibility and absorbability [28]. Collagen membranes are classified by: ① Source: Primarily xenografts (porcine/bovine); allografts are rare due to ethical and cost constraints. ② Processing Technique: Decellularized matrix (retains extracellular matrix (ECM) structure), purified Type I collagen, or recombinant collagen (lower immunogenicity but higher cost). ③ Crosslinking Characteristics: Cross-linked membranes offer enhanced strength and a 3-6 month degradation period for large defects [30]. Non-cross-linked membranes degrade rapidly (2-4 weeks) but offer superior biocompatibility for short-term repair [31].

2.1.1.1. Non-crosslinked collagen membranes

The classic Bio-Gide® features a bilayer structure: a dense outer layer to block fibroblasts and a porous inner layer to facilitate osteoblast migration (**Figure 2a**) [10, 32, 33]. While the dense layer remains intact for 60 days, the porous layer often resorbs within 4-8 weeks [92]. Limitations include insufficient rigidity for vertical augmentation [34], rapid enzymatic degradation [12], immune responses or transmitting zoonotic diseases [29], and unpredictable batch-to-batch consistency.

2.1.1.2. Cross-linked collagen membrane

Cross-linking chemically interconnects polymer chains to extend the biodegradation period and improve stability [35]. While this improves space maintenance, excessive cross-linking can increase stiffness and hinder vascular infiltration [35]. Current methods include physical, chemical, and biological cross-linking [35, 36].

2.1.1.3. Strategies for improving the functionality of collagen membranes

Osteogenic optimization: To overcome the inherent limitations of pure collagen in bone induction, various functionalization strategies have been developed to transform passive barriers into bioactive

scaffolds: (a) Loading growth factors (e.g., BMPs, platelet-derived growth factor-BB (PDGF-BB), stromal cell-derived factor-1 alpha (SDF-1α)) or autologous bone marrow mesenchymal stem cells (BMSCs) creates a pro-osteogenic microenvironment. (b) Doping with metal ions such as strontium (Sr), Zn, or Mg enhances bioactivity. For instance, magnesium oxide (MgO)-deposited membranes provide sustained magnesium ion (Mg^{2+}) release and antibacterial properties, achieving near-complete bone healing in 28 days (**Figure 2b**) [37-39]. (c) Incorporating hydroxyapatite (HAp), bioactive glass, or silicon nanoparticles modifies surface porosity and ion release [40, 41]. A Janus bilayer membrane mineralized with strontium-apatite and poly(caprolactone) methacrylate (PCLMA) promoted stem cell recruitment and M2 macrophage polarization, repairing defects within 12 weeks (**Figure 2c**) [42]. (d) The mechanical and functional profile of collagen can be refined through polymer blending**.** Integrating collagen with chitosan (CS) improves mechanical strength and adds antibacterial functionality (**Figure 2d**) [41].

Antibacterial and immunomodulatory properties: the clinical success of GBR membranes depends heavily on their ability to manage the host immune response and microbial challenges. (a) While collagen is biocompatible, it can still trigger a foreign body reaction (FBR). Epigallocatechin gallate (EGCG)-modified membranes mitigate FBR by promoting M2 macrophage polarization, upregulating VEGF, BMP-2, and Runt-related transcription factor 2 (RUNX2) to facilitate superior osteogenesis (**Figure 2e**) [43-46]. (b) To prevent infection during membrane exposure, agents like silver nanoparticles (AgNPs), amoxicillin, or curcumin are frequently utilized [47]. To address concerns regarding dose-dependent toxicity and drug resistance, antimicrobial peptides (AMPs) are gaining traction as novel alternatives due to their low resistance risk and design flexibility [47]. (c) The smart coatings that provide on-demand protection are designed. Innovative membranes like PO/4-BPBA/Mino@COL (PBMC) provide smart antibacterial defense (**Figure 2f**) [48]. Similarly, the Janus membrane utilizes dual-drug release (chlorhexidine and curcumin) to provide rapid bactericidal action and sustained anti-inflammatory effects via the Interleukin-1 (IL-1)/TGF-β pathway (**Figure 2g**) [49] .

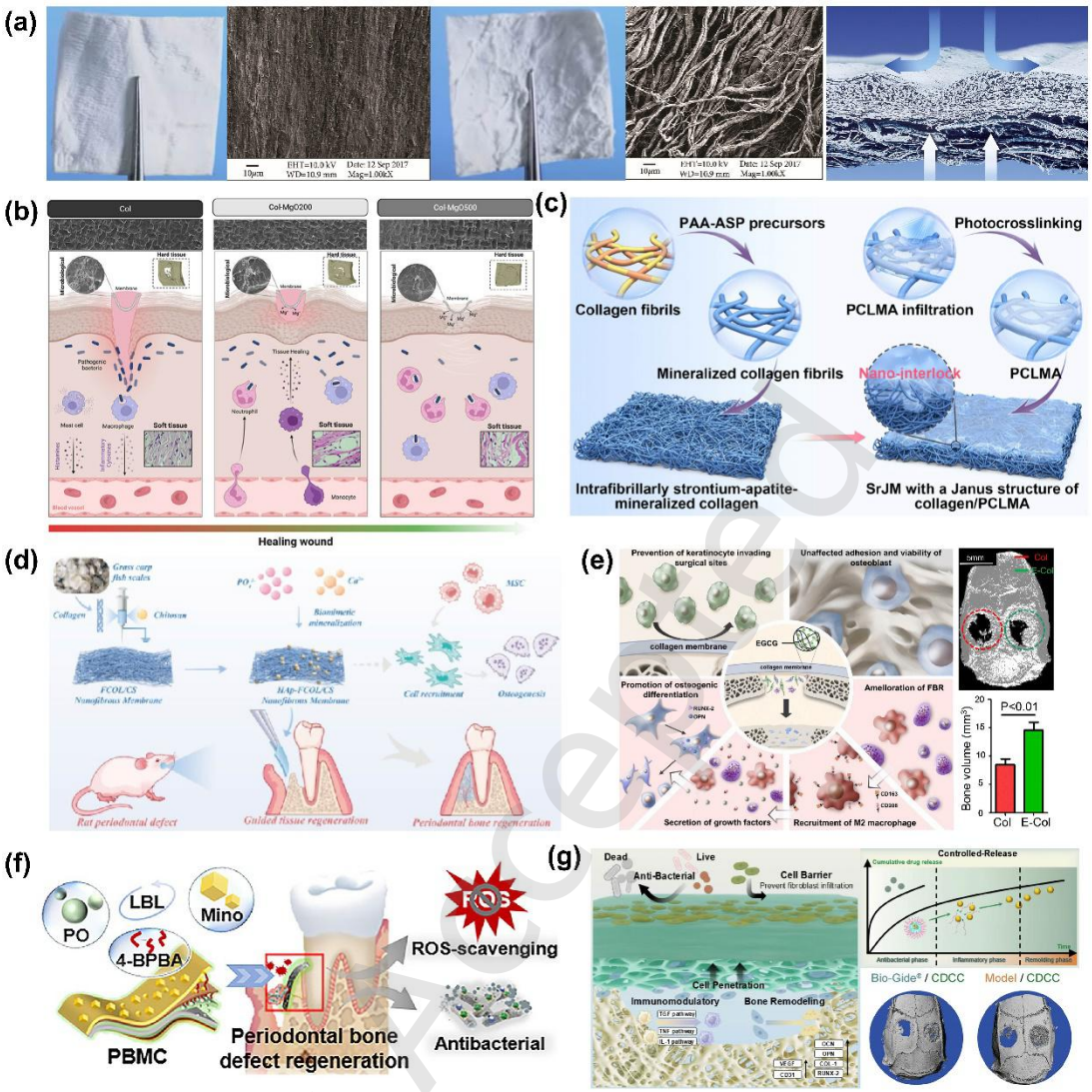

Figure 2 Commercial collagen GBR membranes and functional modification of collagen GBR membranes. (a) Bio-Gide® membrane: left to right: Upper surface macro- and micro-morphology, lower surface macro- and micro-morphology, cross-sectional micro-morphology. Reproduced with permission from Ref. [32], © Wiley 2018. (b) Collagen membrane functionalized with MgO via room-temperature atomic layer deposition. Reproduced with permission from Ref. [39], © Elsevier 2023. (c) Janus membrane with intrafibrillarly strontium-apatite-mineralized collagen membrane. Reproduced with permission from Ref. [42], © American Chemical Society 2024. (d) Collagen-CS blended cross-linked membrane. Reproduced with permission from Ref. [41], © American Chemical Society 2024. (e) Schematic illustration on the function of EGCG-modified collagen membrane. Reproduced with permission from Ref. [44], © Elsevier 2019. (f) A novel intelligent oral barrier membrane PBMC was prepared by combining polyphenols (PO), the commercial bifunctional linker 4-

(bromomethyl)phenylboronic acid (4-BPBA), and the antimicrobial drug minocycline (Mino) through layer-by-layer assembly technology. Reproduced with permission from Ref. [48], © Oxford University Press 2024. (g) Based on the collagen-based Janus bilayer membrane, through the controlled release of two drugs (chlorhexidine for rapid bactericidal effect and curcumin for long-term anti-inflammatory action) and the regulation of the IL-1/TGF-β signaling pathway, the membrane facilitates the polarization of macrophages towards the M2 phenotype. Reproduced with permission from Ref. [49], © Yang, D. et al. 2025.

2.1.2 Gelatin

Gelatin is derived from the partial hydrolysis of collagen. Its peptide chains retain some arginyl-glycyl-aspartic acid (RGD) sequence fragments, but the cell adhesion activity is significantly lower than that of natural collagen [50, 51]. Gelatin is a material certified by the U.S. Food and Drug Administration (FDA) for internal use. Currently, the three-layer composite membrane, Wennuo® augmented Gingival Matrix, made from gelatin and PCL via electrospinning, has been approved by the National Medical Products Administration (NMPA) of China for Class III medical device registration.

Research progress of gelatin-based GBR membranes:

Improving biocompatibility: The loss of activity is often compensated for by methods such as cross-linking RGD short peptides (e.g., grafting CGRGDS) to enhance adhesion and combining with active factors (e.g., BMP-2) to synergistically promote osteogenesis.

Doping or chemical modification can expand additional functionalities: *Drug delivery functionalization*: For instance, loading simvastatin (Sim) into PLGA microspheres combined with a gelatin-CS composite significantly enhanced osteogenic differentiation (demonstrated by a 50% increase in alkaline phosphatase activity) and angiogenesis [52]. *Antioxidant modification*: Gelatin grafted with caffeic acid (GelCA) exhibited enhanced antioxidant properties [53]. *Doping with nanomaterials and metal ions*: Examples include incorporating nano-HAp (nHAp) [54] or Cu ion [55]. Myoung Hwan Kim et al. [56] fabricated a gelatin GBR membrane containing silicon-substituted Hap (Si-HAp) using 3D printing. This membrane featured an interconnected porous structure to support cellular activities.

Multi-layer structure design (e.g., Janus structure [54] or multilayer gradient structure). Qingbin Han et al. [57] prepared the composite barrier membrane of gelatin methacrylate (GelMA)/HAp/HAp membrane, which achieves the dual functions of barrier function and osteogenesis promotion through a double-layer structure (**Figure 3a**).

Improve mechanical properties: Pure gelatin membranes exhibit drawbacks such as low mechanical strength and an uncontrollable degradation rate; therefore, they are often combined with polymers like CS, PLA, or sodium alginate [58]. Additionally, chemical and enzymatic cross-linking techniques are employed to enhance their mechanical properties [58, 59]. For example, sodium alginate/gelatin/two-dimensional (2D) transition metal carbides, nitrides, and carbonitrides (MXenes) composite membranes can reach a tensile strength of 41 MPa, a 48-hour swelling rate of 1012%, and a 28-day degradation rate of 40% [60]. Mengmeng Jin et al. [61] prepared a polydopamine-coated copper-doped mesoporous silica (PDA-Cu/MSN)/gelatin-waterborne polyurethane composite GBR membrane, achieving the integration of mechanical properties, degradation balance, antibacterial activity, pro-angiogenesis, and osteogenic functions (**Figure 3b**)

2.1.3 Chitosan (CS)

Chitosan (CS), a cationic polysaccharide derived from chitin, is valued for its excellent biocompatibility, hydrophilicity, and film-forming ability [62, 63]. Its unique cationic nature confers inherent anti-inflammatory and antibacterial properties against oral pathogens like *P. gingivalis* [64, 65]. Additionally, CS undergoes lysozyme-mediated degradation into non-toxic products.

To address the low mechanical strength and rapid degradation of pure CS, current research focuses on: Composite Modification: Incorporating inorganic fillers (HAp, β-tricalcium phosphate (β-TCP), bioactive glass) or carbon-based materials (GO, CNTs) enhances structural integrity and bioactivity [64]. For instance, an injectable silk-fibroin-reinforced carboxymethyl chitosan (CMCS) hydrogel functionalized with bioactive glass demonstrated osteogenic performance comparable to Bio-Gide® while inhibiting infection (**Figure 3c**) [66]. Therapeutic Integration: CS membranes serve as local delivery vehicles for statins, antibiotics, or growth factors (BMP-2/6) [67]. A Janus-type CS membrane featuring a mineralized/BMP-6-loaded porous surface and a PCL-nanofiber-coated dense

surface effectively meets GBR requirements (**Figure 3d**) [18, 67]. Functional Grading: Multilayered or asymmetric configurations further optimize cell growth and barrier function [52].

2.1.4 Silk fibroin (SF)

Silk fibroin (SF), a fibrous protein composed of 18 amino acids, is an FDA-approved biomaterial that degrades into non-toxic metabolites without immunogenic risk [68]. Its mechanical properties and degradation kinetics are highly tunable by modulating the β-sheet (silk-II) content through ethanol, ultrasonic, or thermal treatments [69]. Notably, SF membranes exhibit a wet-state elastic modulus (up to 45 MPa) and tensile strength (8.39 MPa) significantly superior to traditional collagen membranes (3.3 MPa), effectively preventing structural collapse during healing [70, 71]. Current research focuses on optimizing SF for GBR through: Bilayer or trilayer asymmetric structures [72, 73]: Multi-layered designs feature a dense layer to block bacteria (reducing *S. aureus* adhesion by 70%) and a porous layer to promote osteogenesis. For example, a sandwich membrane (nZnO/SF; SF; nHA/SF) demonstrated potent antibacterial activity and enhanced bone regeneration in periodontal defect models (**Figure 3e**) [74]. Bio-inspired Design [75]: Spider silk-inspired membranes utilize conical micropores to facilitate directional fluid transport, improving nutrient supply to the bone defect. Functional Compositing: Hybridizing SF with HAp, MgO, graphene, antibacterial nanoparticles (silver, curcumin, ZnO), or LAPONITE® further synergizes osteogenic and antimicrobial properties [74, 76, 77]. Mechanical Property Optimization: Sequential cross-linking (photo-cross-linking followed by ethanol treatment) produces hydrogel membranes with high compressive strength (>1 MPa) and stable 12-week degradation profiles (**Figure 3f**) [78].

2.1.5 Bacterial cellulose (BC)

Bacterial cellulose (BC) is a high-purity nanofibrous material produced via microbial fermentation, characterized by high crystallinity and a unique 3D network [79, 80]. BC demonstrates excellent biocompatibility and mechanical properties [81, 82]. Its electrospun fiber diameters (20-100 nm) form a highly porous structure (porosity >90%) that facilitates nutrient permeation and cell adhesion [83]. Notably, BC exhibits a wet-state tensile strength of 100-200 MPa, significantly surpassing collagen (5-50 MPa), providing superior space maintenance for bone defects.

Current research focuses on structural design and surface functionalization to optimize BC for GBR [81, 84]. Janus Membranes: Hongling Zhou et al. [84] fabricated a bilayer BC/Ti3C2Tx MXene membrane featuring a dense barrier layer and a porous osteogenic layer. This composite achieved a tensile strength of 15.0 MPa (19.5 times that of pure MXene) and a degradation rate (25% over 8 weeks) that matches the bone regeneration cycle (**Figure 3g**). Surface functionalization: Shuyi Wu et al.[83] developed an asymmetric membrane by grafting polyacrylamide onto a dense BC layer, followed by chlorination (BC-g-PNCl) to provide multi-mechanism antibacterial properties. A loose CS-HAp layer was then integrated via freeze-drying to promote osteogenic cell infiltration. This system demonstrated mechanical properties matching gingival tissue while effectively blocking fibroblast invasion and accelerating bone repair in vivo (**Figure 3h**).

2.1.6 Alginate

Alginate, a polysaccharide derived from alginic acid, is valued for its biocompatibility and ability to form ECM-like hydrogels through ionic cross-linking [85, 86]. While its flexible structure allows it to serve as an effective barrier, pure alginate membranes often lack the mechanical rigidity to prevent collapse into defect sites, which can compromise osteogenesis [10, 18]. To address these limitations, several optimization strategies are employed: Material compositing: Reinforcing alginate with polymers or inorganic particles (e.g., chitosan, nHA, β-TCP) significantly enhances viscosity and compressive strength [60, 87-89]. Specifically, nHA increases network branching, reducing plasticity while improving structural stability [90]. In situ gelation: injecting alginate solutions for *in situ* ionic cross-linking with $CaCl_2$ allows the membrane to conform precisely to complex bone defect geometries [90]. Advanced functional compositing: Xiaoli Qin et al. [60, 91] developed sodium alginate/gelatin/MXene (SGM) films featuring a double-cross-linked network. These films achieved a high tensile strength (41 MPa) and demonstrated significant promotion of rBMSC proliferation and mineralization (**Figure 3i**). By incorporating glycerol as a plasticizer, the researchers increased the elongation at break to 360%, providing the high flexibility required for clinical handling while MXene enhanced the membrane's HAp-deposition capacity (**Figure 3j**).

2.1.7 Agarose

Agarose, a seaweed-derived polysaccharide, forms a 3D hydrophilic network that mimics the extracellular matrix, offering excellent biocompatibility and low immunogenicity [92, 93]. Its high permeability and scaffold-forming ability provide essential structural support for cell migration and proliferation in bone defects. To overcome the rapid degradation (days to weeks) and mechanical fragility of pure agarose in hydrated states, research focuses on composite reinforcement. Integrating agarose with HAp or polylactide significantly enhances its compressive strength, allowing the membrane to withstand soft-tissue pressure and maintain space stability while synergistically promoting the osteogenic differentiation of mesenchymal stem cells [304]. Specifically, agarose/poly(D, L-lactide) composites have successfully demonstrated the ability to guide bone regeneration in rabbit femoral models.

2.1.8 Poly(3-hydroxybutyrate) (PHB)

PHB is a microbial polyester that degrades into β-hydroxybutyrate, a non-cytotoxic human metabolite [94, 95]. With an elastic modulus of 3.5 GPa, PHB matches the mechanical support of cortical bone. However, its high crystallinity (> 60%) and brittleness (5% elongation) necessitate toughening via plasticizers or blending with PCL, which also recalibrates the 12-24 month degradation period to a more clinically relevant 3-6 months [96-98]. While electrospun PHB nanofibers (100-500 nm) effectively mimic the ECM, the polymer's inherent hydrophobicity (contact angle > 90°) requires surface amination or PEG-blending to facilitate cell adhesion. Furthermore, PHB lacks intrinsic bioactivity; thus, functionalization with BMP-2 or silver nanoparticles is essential to provide osteoinductive and antibacterial properties [99, 100]. Despite processing challenges like a narrow thermal window, modified PHB remains a potent candidate for space-maintaining GBR scaffolds.

2.1.9 Hyaluronic acid (HA)

Hyaluronic acid (HA), a major ECM component composed of D-glucuronic acid and N-acetylglucosamine, is highly hydrophilic and non-immunogenic [101]. Its capacity to promote bone healing and periodontal mineralization is comparable to collagen membranes, making it an ideal GBR candidate [18, 102-104]. When combined with allografts, HA membranes effectively accelerate bone defect repair [105]. For enhanced functionality, Kaichi Chang et al. developed gelatin/HA membranes

cross-linked with genipin and loaded with hinokitiol [106]. These scaffolds achieved a high cross-linking degree (> 84%), providing delayed degradation and potent antibacterial activity against *S. aureus* and *E. coli* without sacrificing tensile properties or biocompatibility.

Gelatin

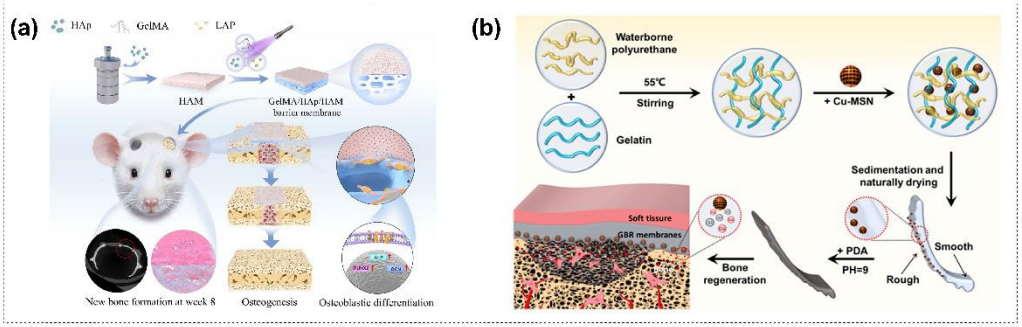

Chitosan

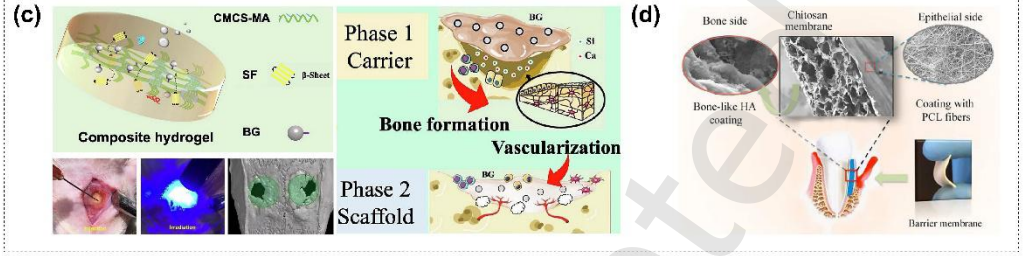

Silk Fibroin

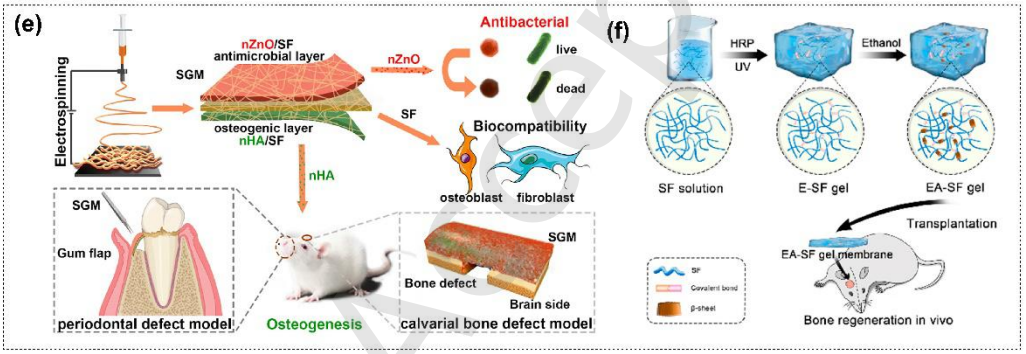

Bacterial Cellulose

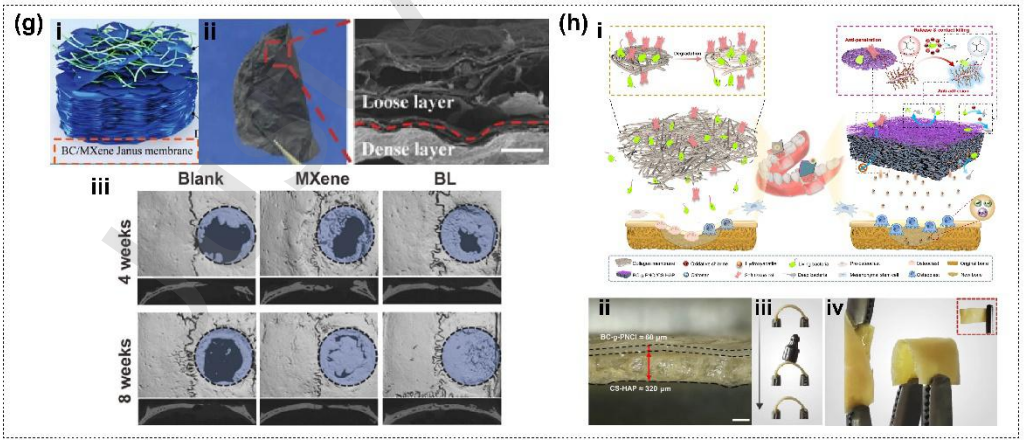

Alginate

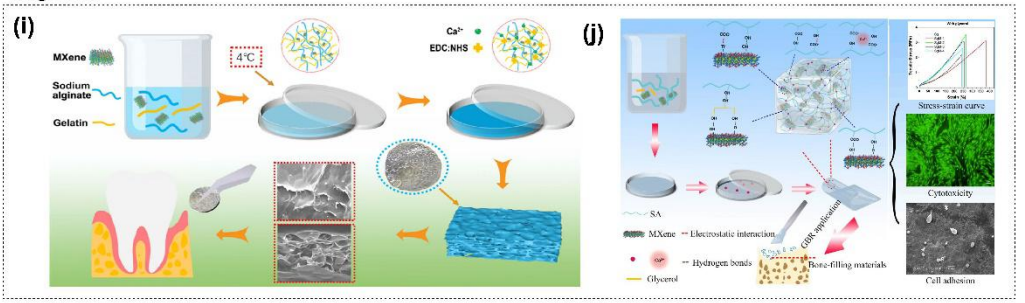

Figure 3 Research status of natural polymer barrier membranes. (a) GelMA/HAp/HAM barrier membranes. Reproduced with permission from Ref. [57], © Elsevier 2025. (b) Schematic representation of Cu-MSN/GP-PDA GBR membrane. Reproduced with permission from Ref. [61], © Jing, M. et al 2025. (c) Schematic illustration of A photo-thermal dual crosslinked chitosan-based hydrogel membrane. Reproduced with permission from Ref. [66], © Elsevier 2025. (d) Chitosan-based double-faced barrier membrane coated with functional nanostructures and loaded with BMP-6. Reproduced with permission from Ref. [67], © SpringerLink 2020. (e) Sandwich-like nanocomposite (nZnO, nHA) electrospun silk fibroin membrane. Reproduced with permission from Ref. [74], © Elsevier 2022. (f) Silk fibroin hydrogel membranes. Reproduced with permission from Ref. [78], © Elsevier 2023. (g) A Janus, robust, biodegradable BC/Ti3C2Tx MXene bilayer membranes for GBR: (i) schematic illustration of the janus BC/MXene membrane, (ii) SEM cross-section microstructure morphology of the BL membranes, (iii) Representative micro-CT images of the rat calvaria defects in Blank group, MXene group, and BC/Ti3C2Tx MXene bilayer membranes at 4-week and 8-week post-surgery. Reproduced with permission from Ref. [84], © Elsevier 2024. (h) BC-g-PNCl/CS-HAP membranes: (i) Schematic illustration of structures and protective behaviors in commercial collagen membrane and BC-g-PNCl/CS-HAP; (ii) Side view macroscopic image showing asymmetric bilayer structure and thickness of BC-g-PNCl/CS-HAP (scale bar = 200 μm), (iii) digital photos of BC-g-PNCl/CS-HAP before, during, and after the application of a load of 1 g in the wet state, (iv) Digital photos of bending and twisting for BC-g-PNCl/CS-HAP (inset: digital photo after bending and twisting). Reproduced with permission from Ref. [83], © Wu, S. et al. 2024. (i) The preparation process of the Sodium Alginate/Gelatin/MXene Composite Membrane **(**SGM) composite membranes. Reproduced with permission from Ref. [60], © Informa UK Limited 2023. (j) The preparation process of the Sodium alginate/glycerol/MXene (SgM) composite membrane, stress-strain curve, cytotoxicity, and cell adhesion of SgM membranes. Reproduced with permission from Ref. [91], © Elsevier 2024.

2.2 Synthetic polymers

Synthetic aliphatic polyesters are favored for their highly tunable morphology, mechanical strength, and degradation [107]. However, acidic by-products can trigger inflammation, and slow degradation, such as PCL's 2-year timeline, may mismatch bone healing [108]. Next-generation GBR

research focuses on multi-component composites to synergistically optimize biocompatibility, mechanical support, and synchronized resorption [109, 110].

2.2.1 Polylactic acid (PLA)

PLA is a semi-crystalline aliphatic polyester derived from lactic acid monomers. In GBR, the most common isoforms are PLLA (semi-crystalline, high strength, > 5 year degradation) and PDLLA (amorphous, 4-12 month degradation), the latter of which better aligns with the bone regeneration cycle [111, 112]. While PLA is cost-effective and widely used, its inherent brittleness and acidic degradation by-products necessitate specific optimization strategies.

① Physicochemical and mechanical optimization: a) Hydrophilicity and plasticity: Hydrophilicity & Plasticity: Pure PLA is hydrophobic and rigid. Incorporating hydrophilic substances like silk fibroin or softeners (e.g., NMP, PNIPAAm, lauric acid) enhances its flexibility, allowing it to conform to complex bone defects without mandatory titanium nail fixation [113]. b) Degradation Control: PLA degrades via ester bond hydrolysis into CO_2 and H_2O. To prevent localized inflammation caused by PLLA's slow resorption or to extend PDLLA's barrier function, researchers use blending or copolymerization to tune the resorption rate [114]. Notably, PLA maintains space longer than collagen membranes (which often resorb within 3-4 months), making it superior for cases where bone grafts require stable protection beyond 6 months [115].

② Bio-functionalization: a) Osteoinductivity: Bioactive agents such as pearl powder, bioglass, HAp, or growth factors (e.g., BMP-2) are incorporated to shift PLA from a passive barrier to an active scaffold [116]. Asymmetric PLA/HAp@MnO_2 membranes catalyze H_2O_2 into O_2, reducing oxidative stress and promoting M_2 macrophage polarization [117]. Double-sided porous membranes modified with copper-tannic acid networks (PLAM-MPN) inhibit pro-inflammatory signals and promote angiogenesis in periodontal defects [118]. b) Antibacterial properties: Since pure PLA lacks antimicrobial properties (1.28% inhibition against *E. coli*), surface modifications with polydopamine, nano-silver, or antibiotics are employed to prevent postoperative infection [119].

③ 3D Printing: Precise, personalized GBR membranes can be fabricated using PLA/HA composites based on patient CT data. These printed membranes and their corresponding absorbable PLA screws provide excellent mechanical stability and fit (**Figure 4a-c**) [120]. Fused deposition

modeling (FDM)-printed porous PLA structures exhibit significantly higher mechanical strength than traditional solvent-casted films [121, 122].

Clinically established products include GUIDOR® (pure PLA) and Resolut Adapt® (PLA/PGA copolymer) [123].

2.2.2 Poly(lactic-co-glycolic acid) (PLGA)

PLGA is a random copolymer of lactic acid (LA) and glycolic acid (GA) [124]. Its degradation cycle is highly tunable (1 month to 1 year) by adjusting the LA/GA ratio; higher GA content accelerates resorption but increases localized acidity, necessitating neutralization via alkaline additives like HAp [125]. Compared to PLA, PLGA features an amorphous structure with superior hydrophilicity, flexibility, and cell adhesion, though its mechanical strength diminishes more rapidly during degradation [126].

Current design strategies of PLGA GBR membranes mainly focuses on: Hydrogel-Integrated Membranes: Yuting Wang, et al [127] developed the PLGA-PGN membrane by infiltrating electrospun PLGA with a photocrosslinkable hydrogel (PEGDA/GelMA/nanosilicates). This composite exhibits exceptional wet-state space-maintaining properties, exceeding those of commercial membranes by 55 times, and significantly enhances early-stage bone formation (**Figure 4d**). Asymmetric multilayers functionalization: Vivian Inês dos Santos et al. [128] combined dry phase inversion with electrospinning to create a dense PLGA/HAp barrier layer and a porous PLGA/HAp/β-TCP scaffold layer. This design successfully prevents fibroblast infiltration while facilitating osteoblast migration (**Figure 4e**). 3D printing customized design: Beyond traditional casting, 3D printing via multi-head deposition systems (MHDS) allows for the fabrication of PCL/PLGA/β-TCP membranes with fully interconnected pores and biomimetic surface roughness, offering precise anatomical adaptation [129] (**Figure 4f**).

2.2.3 Polycaprolactone (PCL)

PCL is a semi-crystalline aliphatic polyester known for its high flexibility (elongation at break 400-600%) and low melting point [130, 131], While it offers superior ductility compared to PLA, its low rigidity (tensile strength 15-30 MPa) and slow degradation (2-3 years) often mismatch the 3-6 month bone regeneration cycle [132].

Current research focuses on optimizing PCL for GBR applications: Degradation & Hydrophilicity: To accelerate resorption and reduce foreign body retention, PCL is typically copolymerized with PLA/PGA or blended with natural polymers (e.g., gelatin, silk fibroin) [133-135]. Introducing hydrophilic groups (-OH, -COOH) can overcome PCL's inherent hydrophobicity to improve cell adhesion. Mechanical Reinforcement: While flexible enough to fit complex bone contours, PCL requires additives like silica nanoparticles or carbon nanotubes to enhance its resistance to sustained mechanical loads [136, 137]. Bio-functionalization: To impart osteoinductivity and antibacterial properties, PCL is combined with bioactive ceramics (nHA, β-TCP), growth factors (BMP-2), or antibiotics (metronidazole) [87, 138]. Abdullrahman M. Al-Bishari et al. [377] engineered a triple-layer electrospun PCL/Gelatin membrane (MFM/Van-Sr-Qk) that achieves 21-day sustained release of vancomycin, strontium, and Qk peptide. This system synergistically enhances angiogenesis, osteogenesis, and antibacterial defense against *S. aureus*. Manufacturing & clinical status: PCL's versatility allows for the fabrication of porous scaffolds or nanofibers via electrospinning [139], 3d printing (**Figure 4g**) [140, 141] etc. Although PCL offers a long-acting barrier function, it remains largely in the experimental stage, with few approved commercial GBR products currently available. Balancing its degradation rate with mechanical support remains the primary hurdle for large-scale clinical translation.

2.2.4 Polyglycolic acid (PGA)

PGA is a high-strength synthetic polyester characterized by rapid degradation (1-3 months) and a high melting point (> 200°C), making it suitable for load-bearing surgical applications [142, 143]. While its tensile strength (110 MPa) is double that of PLA, its fast resorption and acidic by-products often necessitate modification to match the bone regeneration cycle [142]. Currently, the commercially available Cytoflex® Resorb membrane is made of PGA, PLA, and PLGA copolymers with good biocompatibility. Preclinical studies have shown that it maintains the barrier function within 8 weeks and can be completely absorbed within 6 months [13].

At present, the optimization directions and research status of PGA for GBR membranes are as follows: Degradation and stability: To synchronize resorption with bone healing, PGA is often copolymerized (as seen in the commercial Cytoflex® Resorb) or blended with collagen and HAp [144].

HA further serves to neutralize the acidic environment generated during GA hydrolysis [145]. Structural design: Advanced manufacturing, including electrospinning and 3D printing, creates porous architectures that facilitate nutrient exchange [146]. Byung Nam Kim et al. [146] developed an SF-PGA hybrid scaffold by compounding electrospun silk fibroin (SF) with a 3D-printed PGA frame. The SF layer acts as a stable barrier (0.1% degradation at 8 weeks), while the PGA scaffold (48% degradation) promotes robust pre-osteoblast proliferation, significantly increasing new bone volume in rabbit models (**Figure 4h**). Cijun Shuai, et al [145] utilized laser 3D printing to fabricate PLLA/PGA/HAp composite scaffolds. The inclusion of PGA enhances hydrophilicity and weight loss (25% at 28 days), promoting HAP exposure and apatite deposition (**Figure 4i**). Surface coating modification: Coating PGA with materials like PHB or chitosan reduces the localized concentration of acidic products, thereby mitigating inflammatory reactions while enhancing the membrane's epithelial barrier function.

Currently, most PGA-based GBR research is in the preclinical phase. Future efforts require multi-center clinical trials to validate the long-term safety and efficacy of these high-strength, fast-resorbing barriers before widespread adoption.

2.2.5 Polyethylene glycol (PEG)

PEG is a linear, hydrophilic polymer linked by ether bonds, offering exceptional biocompatibility, injectability, and the ability for *in situ* molding to fit complex defect contours [147]. Clinically, PEG membranes effectively reduce bone resorption during alveolar ridge preservation, performing particularly well in the coronal region compared to traditional collagen barriers [148]. Their resorbable nature eliminates secondary surgeries, reducing infection risks and patient discomfort.

Despite these benefits, PEG membranes often exhibit low mechanical strength, making space maintenance difficult in high-stress areas. Precise control over degradation rates remains challenging, and some studies suggest PEG may be slightly inferior to collagen regarding early soft-tissue healing, with potential risks of dehiscence [149].

Current research focuses on enhancing PEG's structural and biological performance. Composite Systems: Blending or copolymerizing PEG with PLA or PCL and introducing inorganic fillers (e.g., HAp) significantly improves mechanical stiffness and osteoblast differentiation [150, 151]. For instance,

electrospun PEG/PCL composites outperform pure PCL in lateral ridge defects due to PEG's superior hydrophilicity, which facilitates cell adhesion [152]. Cross-linking and smart hydrogels: PEG can be cross-linked into hydrogel membranes via enzymatic or photo-initiated processes [153, 154]. Advanced smart hydrogels are being developed with pH, ROS, or enzyme responsiveness to enable on-demand antibacterial and anti-inflammatory functions [155].

The commercially available Straumann® MembraGel is applied as a liquid that conforms precisely to the defect before solidifying within 20—50 seconds, stabilizing the bone graft and providing an immediate tissue barrier (**Figure 4j**) [148, 156]. Future translation will prioritize 3D printing and gradient structures to achieve personalized, multi-functional GBR solutions.

2.2.6 Polydioxanone (PDO)

PDO is a synthetic polymer offering excellent flexibility, mechanical strength, and a predictable 6—8 month degradation cycle that matches the bone regeneration window [157-159]. Unlike collagen, PDO is produced uniformly, carries no risk of zoonotic disease transmission, and avoids immunogenic reactions, making it an ideal alternative for patients with specific religious or ethnic restrictions regarding animal-derived materials [159, 160].

Current research focuses on enhancing its inherent bioactivity through modification: Antibacterial Functionalization: Victoria L. Abdo et al. [161] used glow discharge plasma to load amoxicillin onto PDO membranes (AMX-PDO). This system maintains the substrate's tensile strength while significantly reducing oral pathogen infiltration (e.g., *P. intermedia*). Composite Strategies: Blending with bioactive ceramics (e.g., HA) or utilizing electrospinning to create 3D nanofibrous networks further optimizes osteoconductivity and cell guidance [159].

The commercially available Plenum® Guide membrane resorbs fully via cellular metabolism within 6—12 months, yielding new bone microstructure comparable to traditional collagen barriers (Figure 4f) [162].

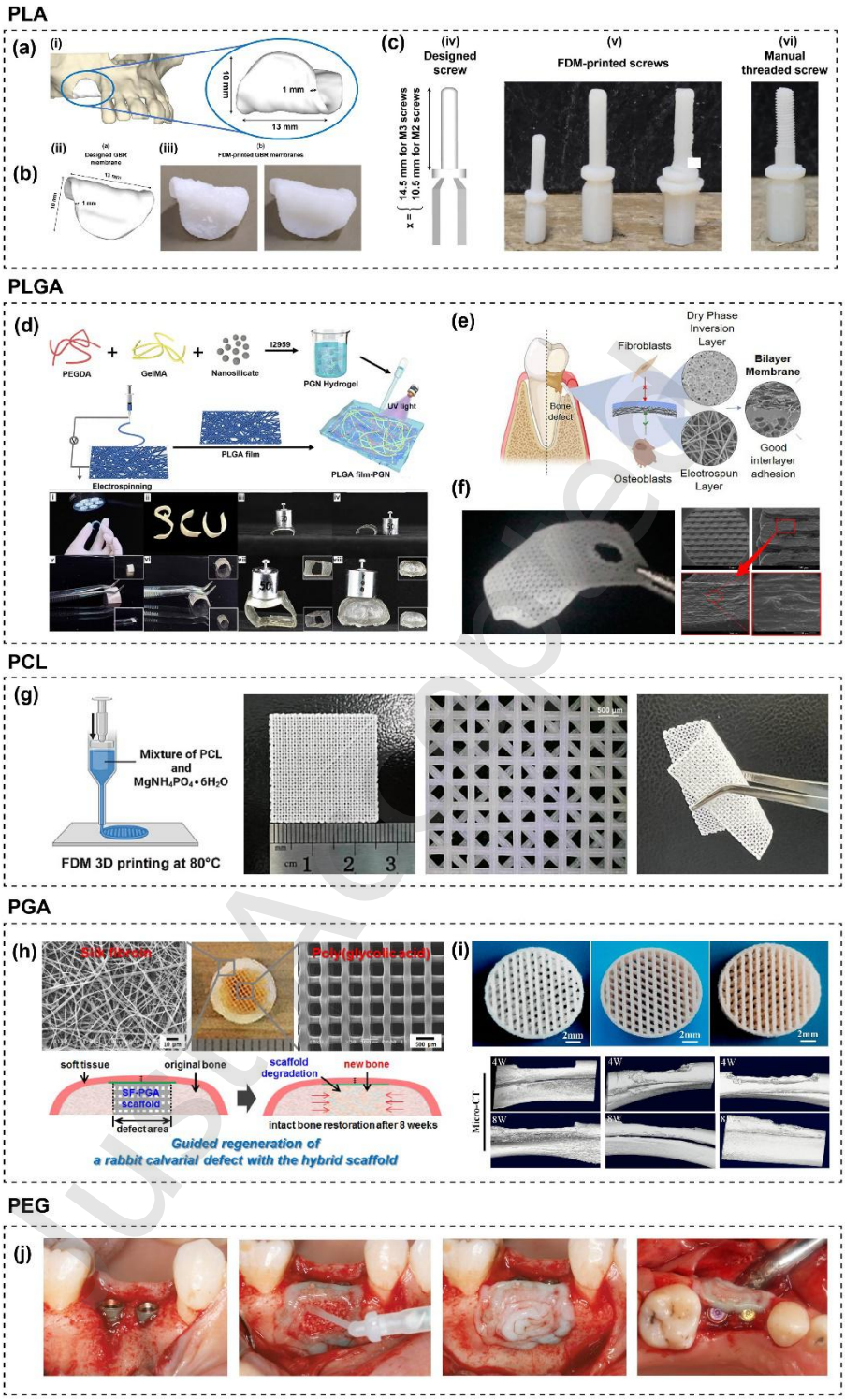

Figure 4 Research progress of synthetic polymer GBR membranes. (a-c) Design of the custom PLA GBR membrane (i-iii) and screws (iv-vi). FDM-printed GBR membranes in two different configurations (ii, iii). Designed screw (iv); (v) from left to right M2 and M3 screw manufactured in horizontal configuration and 3 mm screw 3D-printed in vertical configuration and (vi) M3 screw FDM-printed in

horizontal configuration after the manual threading process. Reproduced with permission from Ref. [120], © Elsevier 2025. (d) Schematic presentation of the fabrication of electrospun PLGA film into PGN hydrogel. Evaluation of film plasticity (i-viii). Reproduced with permission from Ref. [127], © Wang, Y. et al. 2024. (e) Illustration of the placement of a bilayer membrane of PLGA/HAp/β-TCP bilayer membrane. The dry phase inversion layer prevents fibroblast infiltration, whereas the electrospun layer improves osteoblastic adhesion and proliferation. Reproduced with permission from Ref. [128], © Elsevier 2020. (f) PCL/PLGA/β-TCP membrane produced using 3D printing technology. Pores were triangularly structured and completely interconnected. SEM images of the prepared PCL/PLGA/β-TCP membrane, and a rough surface, which was produced by incorporating TCP powder. Reproduced with permission from Ref. [163], © Shim, J. et al. 2015. (g) 3D printed $MgNH_4PO_4 \cdot 6H_2O$ (MNP) and polycaprolactone (PCL) composite GBR membrane (from left to right): Schematic illustration of the 3D-printing fabrication of the MNP-PCL membrane; The macroscopic view of the 3D printed membrane; The microscopic view of the 3D printed membrane; Flexibility and thermo-plasticity of 3D printed membrane. Reproduced with permission from Ref. [141], © Elsevier 2024. (h) SF-PGA hybrid scaffold (including silk fibroin nanofiber membrane prepared by electrospinning and PGA scaffold with 400 μm pore size prepared by hot-melt 3D printing). Reproduced with permission from Ref. [146], © American Chemical Society 2019. (i) Typical optical images of the PLLA/HAp, 1PLLA/1PGA/HAp, and PGA/HAp scaffolds seen from the top, and micro-CT images of the PLLA/HAp, 1PLLA/1PGA/HAp, and PGA/HAp scaffolds after 4 and 8 weeks of implantation. Reproduced with permission from Ref. [164], © Elsevier 2021. (j) Photograph series showing the dehiscence defect at the implant, the application of the bone substitute material and the placement of the PEG membrane (PEG group), and final contouring of the PEG membrane according to the study protocol. The membrane overlapped the walls of the defect by at least 2 mm. The thickness was approximately 1 mm. No fixation was needed as the gel adheres to the surrounding tissues. Reproduced with permission from Ref. [156], © Wiley 2020.

2.3 Design strategies for polymer GBR membranes

Current strategies for polymer GBR membranes focus on transitioning from passive barriers to bioactive, structurally optimized scaffolds (**Figure 5**).

The core design principle involves hybridizing natural and synthetic polymers to achieve performance complementarity. Natural polymers (e.g., collagen, CS) offer superior biocompatibility and cell affinity but suffer from poor mechanical control. Synthetic polymers (e.g., PLA, PCL) provide excellent processability and tunable degradation. Mainstream strategies, such as PCL/collagen composites, retain the mechanical integrity of synthetics while incorporating the biological signaling of natural materials.

Preparation methods: Electrospinning can produce nanofibrous structures that mimic the natural extracellular matrix. These structures possess a high specific surface area and porosity, which are beneficial for cell attachment and nutrient exchange. Furthermore, 3D printing technology allows for precise control over the overall morphology and internal channel architecture of the membrane. Methods such as phase separation and solvent casting/particulate leaching are commonly employed to create sponge-like scaffolds with three-dimensionally interconnected macropores, providing space for cell infiltration and tissue vascularization.

Structural design: Modern membranes are shifting toward bilayer asymmetric or gradient functional configurations. The dense top layer serves as a physical barrier to prevent soft-tissue invasion. Conversely, the highly porous bottom layer facilitates the migration, proliferation, and ingrowth of osteoblasts and vascular endothelial cells. This directed architecture is fundamental to achieving guided regeneration.

Bio-functionalization: To act as an active inducer, several functionalization strategies are employed: 1) Biofactor Loading: Encapsulating growth factors (e.g., BMP-2) into microspheres or fibers for sustained, controlled release; 2) Inorganic Integration: Incorporating nHAp or bioglass to enhance osteogenic activity and bone-membrane integration; 3) Surface Modification: Grafting peptide sequences (e.g., RGD) to improve initial cell adhesion; 4) Immunomodulation: Engineering materials to polarize macrophages toward a pro-regenerative M2 phenotype, optimizing the local healing microenvironment.

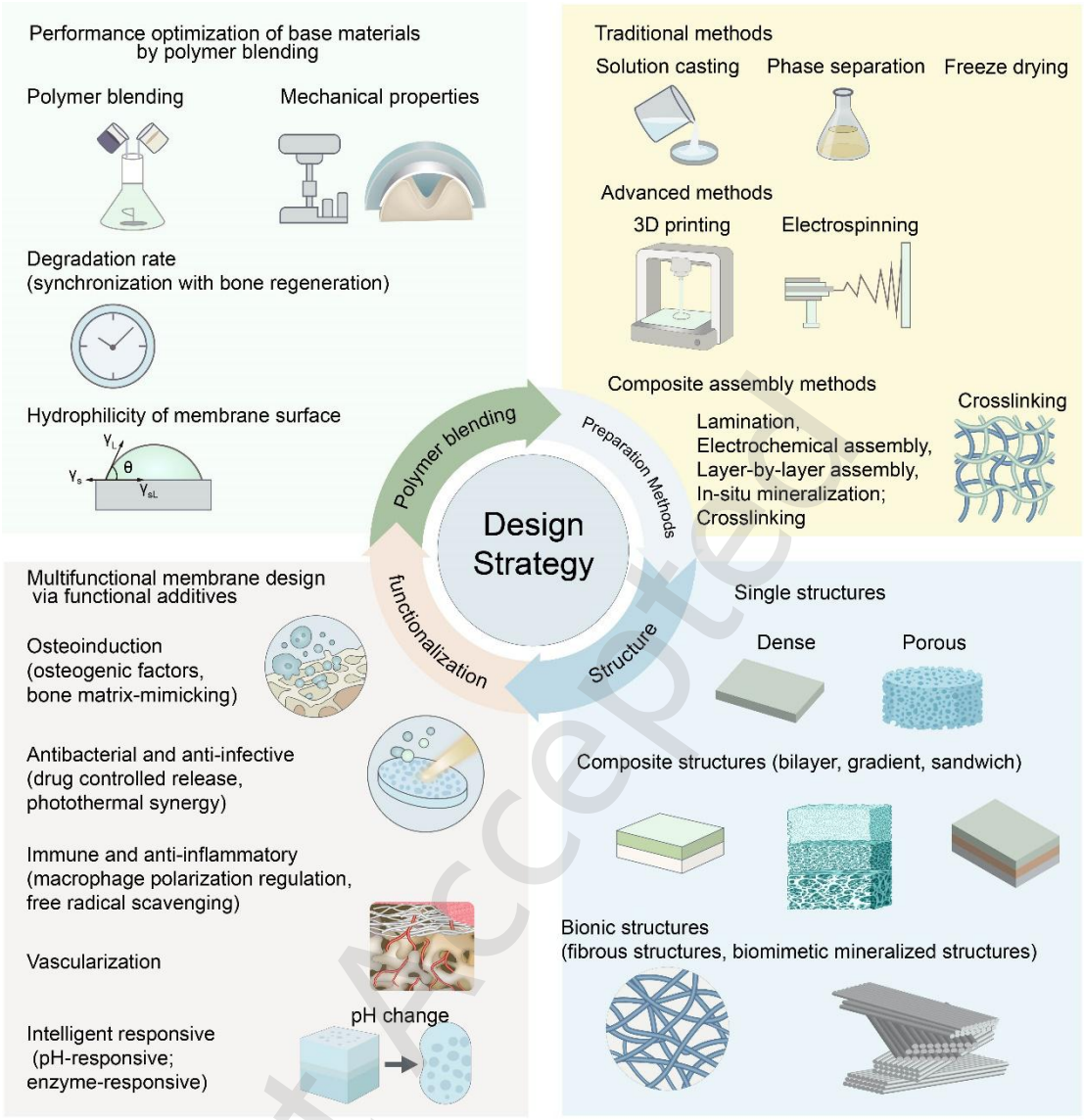

Figure 5 Design strategies for polymer GBR membranes.

3 Biodegradable metal GBR membranes

Biodegradable metals (BMs) are metal materials that degrade gradually in the body, elicit appropriate host responses by releasing corrosion products, and completely degrade after helping the host complete tissue repair without leaving any residue [165]. At present, several representative series of BMs have been developed, including magnesium (Mg)-based [166], zinc (Zn)-based [167], iron (Fe)-based [168], and molybdenum (Mo)-based [305]. BMs possess outstanding biodegradability, excellent mechanical strength, ductility, formability, osteogenic ability, anti-inflammatory properties, pro-angiogenic effects, neurogenic stimulation, and antimicrobial properties [169]. The primary

advantage of degradable metal implants is that they eliminate the need for secondary surgery while maintaining excellent mechanical properties [170]. Currently, research on GBR membranes of degradable metals primarily focuses on Mg-based and Zn-based metals [170, 171].

3.1 Mg and Mg alloys

Mg, an essential cation for human physiology, is highly valued for GBR membranes due to its excellent biocompatibility and biodegradability, which eliminates secondary removal surgeries [172-175]. Unlike traditional titanium alloys, Mg-based metals avoid stress-shielding effects because their elastic modulus (40—50 GPa) closely matches natural bone (10—30 GPa) [176-178]. Furthermore, released Mg^{2+} ions actively promote osteoblast proliferation and mineralization [179-181].

However, several challenges hinder clinical translation: Corrosion Control: Rapid degradation can lead to premature structural failure and hydrogen gas evolution [182, 183]. Microenvironment: Localized pH elevation (8.0—9.0) and Mg^{2+} overload (>50 mmol/L) may impair soft-tissue healing or cellular function. Mechanical Integrity: Stress corrosion and galvanic coupling with titanium fixation systems necessitate the development of compatible degradable Mg-based screws. Overcoming these barriers requires advances in compatible degradable Mg-based screws. [184, 185], surface modification [320-322], 3D printing [186, 187], and compatible fixation systems [188] to balance degradation kinetics with mechanical and biological responses.

Several studies on degradable Mg-based GBR membranes have been reported (as summarized in **Table 1**), with details provided below.

① Pure Mg

Frank Witte et al. developed a pure Mg GBR membrane (NOVA-Mag®, botiss biomaterials GmbH, Germany), the first of its kind to receive CE certification, with dimensions of 30 × 40 mm, a thickness of 140 μm (**Figure 6a**), and a purity of 99.95% [189-192]. The membrane was secured in vivo using biodegradable Mg screws fabricated from Mg alloy WZM211 and coated with magnesium fluoride (MgF_2) (**Figure 6b**) [193]. After 4 weeks of degradation, the Mg screws still exhibited superior mechanical performance compared to polymeric screws. In vivo studies confirmed that the Mg screws provided sufficient fixation during the critical early healing phase and were completely absorbed within 52 weeks (**Figure 6c**). This pure Mg barrier membrane was used to reconstruct the buccal or

palatal walls of severely compromised extraction sockets [194] and maxillary sinus floor elevation surgeries [195]. All clinical cases utilizing this Mg membrane demonstrated excellent bone regeneration (**Figure 6d**), with the newly formed bone presenting a thick cortical layer, but larger sample sizes and long-term studies are needed for further verification [194, 196]. The clinical advantages of the Mg membrane include: complete absorption without the need for removal; its synthetic origin, eliminating the need to harvest autogenous cortical bone from additional surgical sites; promotion of cortical bone formation; high mechanical strength capable of stabilizing the defect space; and ductility allowing contour adaptation to the defect morphology.

② Mg alloys

The properties of Mg alloys can be tailored through the addition of alloying elements. Altering microstructural characteristics can effectively decelerate the degradation of Mg alloys both in vitro and in vivo, reduce localized hydrogen evolution and pH elevation, and ultimately enhance their biocompatibility, making them suitable for use as GBR barrier membranes. Various novel high-performance Mg alloys, such as Mg-Zn, Mg-Ca, and Mg-Sr alloys, have been continuously developed for such applications [197, 198].

Mg-Zn alloy: Zn, an essential trace element, slows alloy degradation through a Zn oxide layer and eutectic phases, while released Zn^{2+} ions are harmlessly excreted [199]. Furthermore, Zn enhances the tensile strength and hardness of Mg-Zn alloys [200]. Heat treatment and surface fluoridation of a Mg-5Zn-0.5Zr alloy enhanced ductility and corrosion resistance, with early Mg^{2+} release promoting >80% new bone formation [201]. Mg-Zn-RE alloy membrane demonstrated biocompatibility and osteoinductive potential in rat cranial defects [202]. Adding yttrium can optimize the microstructure of Mg alloys, boosting strength and wear resistance. For example, adding 0.5wt.% Y element in Mg-6Zn-4Si Mg alloy increasing the tensile strength by 50%, the elongation by 65%, and reducing the wear rate under a 1N load by 50% [203]. Mg-Zn-Gd alloy has a yield strength (YS) of 150 MPa, an ultimate tensile strength (UTS) of 235 MPa, and an elongation of 22.5%, suitable for GBR membrane space maintenance [204].

Mg-Ca alloy: Calcium (Ca) is essential for bone healing, refines Mg alloy grains, and enhances strength, creep resistance, and corrosion resistance, even in small amounts [197, 205]. Alloy

composition critically influences performance. The Mg-0.8Ca-5Zn-1.5Ag (ZQ71) alloy demonstrated superior corrosion resistance and slower degradation than variants with higher or no Ag content. Its released ions stimulated significantly higher osteogenic activity and bone substitution, making it ideal for biodegradable grafts [206]. The Mg-0.2Ca-0.2La alloy exhibited a refined microstructure with excellent strength and ductility. Crucially, it maintained structural integrity under bending stress, required for adapting to alveolar contours, with a low corrosion rate (0.09 mm/year) and only 5.9% volume loss after 12 weeks in vivo, promoting significant bone growth [207, 208]. Addressing multifunctional needs, a novel Mg-Ca/Mg-Cu bilayer membrane was developed. This design integrates function: the Mg-Ca layer supports bone regeneration, while the Mg-Cu layer provides tailored antibacterial properties. It exhibited excellent mechanical stability (421.0 MPa bending yield strength), retained 86.4% volume after 21 days, and promoted osteogenesis via synergistic Mg^{2+}/Ca^{2+} release, with Cu^{2+} ions enhancing antibacterial effects [209] (**Figure 6e**). These advancements demonstrate that through precise alloying and structural design, Mg-Ca-based alloys can achieve the mechanical integrity, controlled degradation, biocompatibility, and bioactivity required for next-generation GBR membranes.

Mg-Sr alloy: A study evaluated Mg-1.5Sr alloy membranes for mandibular defect repair in dogs. Compared to collagen membranes, the Mg-Sr group showed significantly higher CBCT grayscale values and bone volume fraction at 12 weeks. Histology revealed thicker, more interwoven new bone, demonstrating that Mg-Sr alloy membranes effectively enhance high-quality bone regeneration [210].

Mg-Ag alloy: Mg-Ag alloys offer enhanced corrosion resistance, biocompatibility, and osteogenic activity. Mg-9Ag provides optimal mechanical properties (205.7 MPa tensile yield strength, 20.3% elongation). Despite a slightly increased corrosion rate, alloys demonstrate strong antibacterial efficacy against oral pathogens and support cell migration and osteogenic differentiation, making them promising for guided tissue regeneration (GTR) membranes [211].

Mg-Al alloy: A Mg-Al-Zn-Mn-Ag alloy membrane, in a rat skull defect model, exhibited excellent biocompatibility over 48 weeks, maintained structural integrity for 8 weeks, and degraded at a rate compatible with bone regeneration. By 48 weeks, defects were nearly fully covered by new bones without inflammation [212].

③ Coating modification

The rapid degradation rate of Mg in physiological environments remains a critical bottleneck limiting its clinical application. Surface modification techniques enable the construction of multifunctional coating systems (e.g., corrosion-resistant barriers and bioactive inductive layers), which allow for precise regulation of Mg's degradation kinetics while concurrently imparting enhanced biocompatibility.

1) MgF_2 coating

Fluorination treatment creates a protective composite layer (oxides and hydroxyfluorides (e.g., MgO, Mg $(OH)_2$, and $Mg(OH)_xF_{2-x}$)) on Mg surfaces, acting as a physical barrier against rapid corrosion and hydrogen bubble accumulation [213]. A Mg-5Zn-0.5Zr alloy treated with solution heat treatment and surface fluoridation demonstrated improved ductility and corrosion resistance, releasing appropriate Mg^{2+} concentrations to promote >80% new bone formation [201]. Similarly, HF-treated Mg fixation screws showed reduced gas formation, slower biodegradation, and enhanced osseointegration compared to untreated screws, inducing a macrophage layer rather than fibrous tissue response [188]. MgF_2-coated Mg-2Zn-0.46Y-0.5Nd GBR membranes with strategic hole designs were compared to BioGuide® membranes in beagles. At 3 months, the Mg group showed comparable new bone formation (45.44% vs. 43.49%) and vertical bone height, with complete membrane degradation and island-like new bone formation. Although rare earth elements accumulated in lymph nodes, no histopathological changes occurred, supporting fluorinated Mg alloys as promising GBR membrane materials [214].

2) Ca-P coating

Ca-P coatings significantly enhance the biocompatibility, bioactivity, and corrosion resistance of Mg-based implants [215, 216]. Wei Peng et al. [208] found Ca-P coatings improve Mg films' corrosion resistance in vivo and in vitro, reducing H_2 release, but their thinness and fast degradation fail to meet the 12-week clinical requirement. Shuang Wu et al. [217, 218] used PEO and HT to form a dense coating on pure Mg meshes, reducing degradation and increasing bone volume at skull defects. Lili Tan et al. [219] prepared Ca-P-coated Mg films for GBR; they degraded in 8 weeks (vs. 1 week for pure Mg), outperforming Ti films at 4 weeks but inferior at 8-12 weeks, requiring further degradation reduction.

Yujia Han et al. [220] fabricated a DCPD/MgF_2 Janus film with suitable degradability and selective osteogenic/soft tissue healing abilities (**Figure 6f**). Jiawen Si et al. [204] applied a Ca-P coating to Mg-2.0Zn-1.0Gd alloy, enhancing corrosion resistance, cytocompatibility, antibacterial activity, and promoting new bone formation in rabbit defects. Jun Gao et al. [221] fabricated a porous-yet-dense HA coating on $Mg_2ZnMnCaCe$ alloy via hydrothermal technology, improving hydrophilicity, corrosion resistance, and cell adhesion. These advances highlight Ca-P coatings as effective strategies to tailor Mg-based GBR membrane degradation and bioactivity.

3) PVD coating: Daniel Rothamel et al. [222] passivate Mg membranes for GBR/GTR via a method based on ion implantation combined with physical vapor deposition (PVD). Compared to pure Mg membranes, the PVD coating did not cause gas cavity formation while inducing fewer anti-inflammatory macrophages than both pure Mg membranes and collagen membranes.

④ Mg-Reinforced polymer composite GBR membranes

Biopolymer coatings enhance Mg alloy corrosion resistance in GBR membranes through two primary mechanisms: a physical barrier effect that prevents corrosive media contact, and the elimination of microgalvanic corrosion risk due to the absence of potential differences [223]. William R. Wagner et al. [358] developed an electrospun PLGA/Mg mesh/PLGA & DBM membrane. The Mg mesh improved flexural strength and modulus, promoting BMSC proliferation and osteogenic differentiation, with significantly enhanced bone repair at 12 weeks in rat calvarial defects. Yu Guo et al. [224] prepared a CS-Mg membrane by immersing Mg_3Gd alloy in chitosan solution, achieving comparable degradation rate, cell adhesion, and bone formation to commercial Heal-All membranes in rabbit defects. Mike Barbeck et al. [225] combined HF-treated Mg mesh with natural collagen membrane. Treated Mg showed higher cytocompatibility, prevented gas cavity formation, and degraded via monocyte phagocytosis over 12 weeks, unlike untreated Mg which triggered fibrous tissue reaction. Xin Du [226] and Hao Yang Zhang et al. [227] fabricated fluoride-coated AZ91 alloy-reinforced PLA composite membranes via hot pressing, achieving significantly higher mechanical properties lasting at least 3 weeks without cytotoxicity. Feilong Wang et al. [228] designed a sandwich-structured PLGA/Mg scaffold/PLGA-collagen membrane. The optimal PLGA-to-collagen ratio (100:10) demonstrated superior osteogenic performance with reduced strain, integrating

mechanical support, controlled degradation, and enhanced biocompatibility for GBR applications (**Figure 6g**).

⑤ 3D-printed Mg scaffolds for GBR

Mg 3D printing faces three core challenges: oxidation/combustion risk requiring inert environments, density defects from poor powder flowability and residual stress, and difficulty regulating degradation rates to match tissue repair cycles [229, 230]. Mg is compounded with polymers and ceramics, and composite scaffolds are prepared through low-temperature 3D printing (such as extrusion molding and inkjet printing) [231]. Yao Wang et al. [232] used selective laser melting to fabricate a titanium template, pressure-infiltrated molten Mg-1Zn-1Ca alloy, then etched away the titanium to obtain a porous Mg scaffold. The scaffold was negatively charged with NaOH treatment and dip-coated with collagen solution (pH=5), followed by dialysis, freeze-drying, and EDC/NHS cross-linking to create a collagen-coated (COL/Mg) composite scaffold. This composite maintains mechanical properties matching human bone while controlling Mg^{2+} release within the 2–10 mmol/L therapeutic window. It demonstrates significantly improved corrosion resistance and biocompatibility, promotes endothelial cell migration and osteoblast differentiation, and effectively enhances vascularized bone regeneration in rat skull defects without systemic adverse effects (**Figure 6h**).

Pure Mg

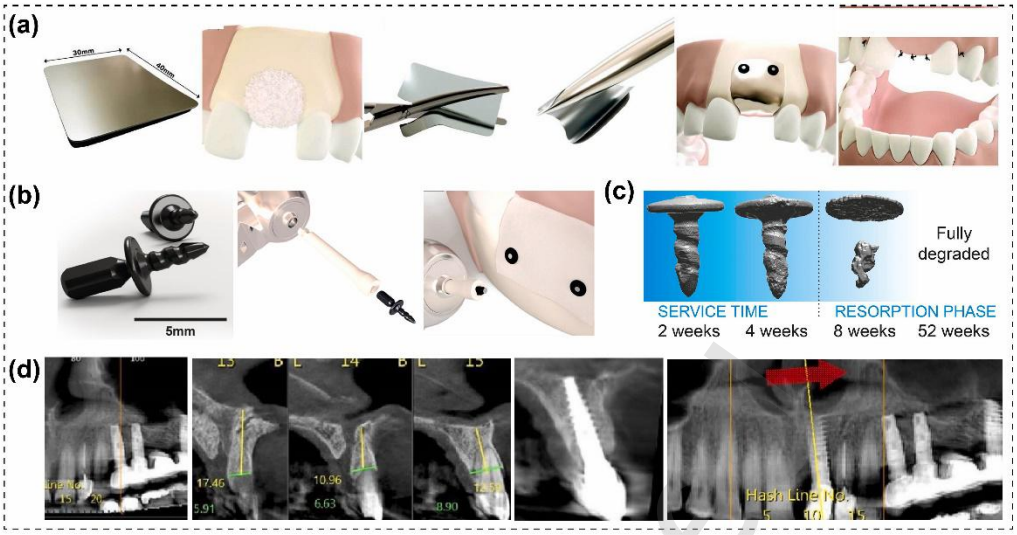

Mg-Ca/Mg-Cu alloy

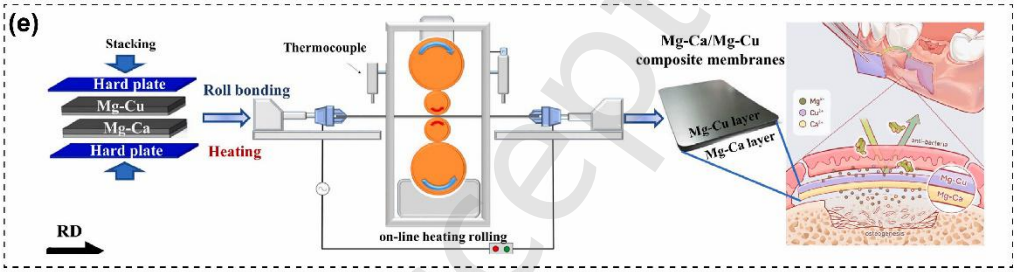

Inorganic coating

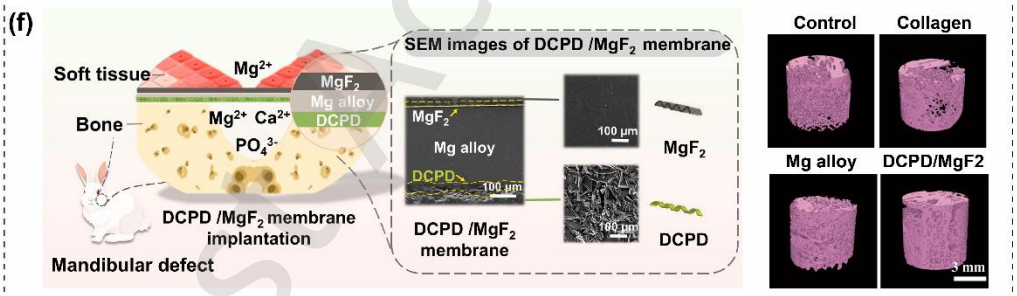

Mg-reinforced polymer composite membrane

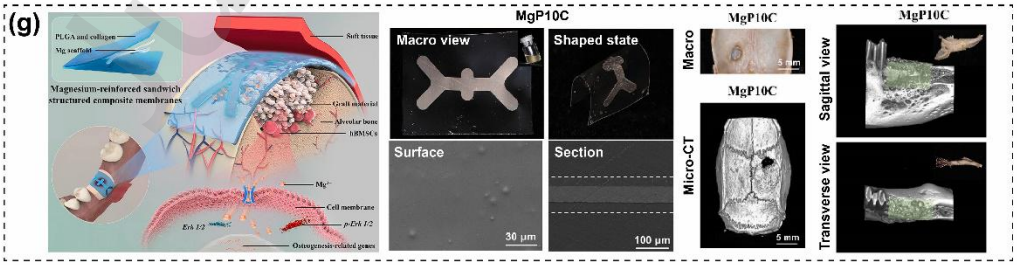

3D-Printed Mg scaffolds for GBR

Figure 6 Current research status of Mg-based alloys as a potential candidate material for GBR membranes. (a) pure Mg GBR barrier membranes (NOVA-Mag® , botiss biomaterials GmbH, Germany) and the implantation procedure (from left to right): physical view of the Mg membrane, filling the defect site with bone graft material, trimming the membrane to the desired shape using NOVA-Mag® scissors, bending the membrane to adapt to the contour of the defect, securing the membrane from both buccal and palatal/lingual aspects, and suturing the wound. Reproduced with permission from Ref. [189], © Elsevier 2022. (b) From left to right: Absorbable Mg fixation screw (NOVA-Mag® Fixation Screw, XS type, botiss biomaterials GmbH, Germany); installing the fixation screw to the NOVA-Mag® connector; once the screw is fully seated, its drive segment will fracture and detach, leaving a smooth, flat surface at the screw head. Reproduced with permission from Ref. [193], © Elsevier 2022. (c) 3D images of the Mg screw corroding after implantation into Yucatan minipigs after 2 weeks, 4 weeks, 8 weeks and 52 weeks [193], © Elsevier 2022. (d) The CBCT scan reveals that the buccal cortical bone plate has been restored following the application of the Mg membrane. Reproduced with permission from Ref. [194], © Elad, A. et al. 2023. (e) Schematic diagram illustrating the use of a Mg-Ca/Mg-Cu bilayer membrane. Reproduced with permission from Ref. [209], © Elsevier 2025. (f) Cross section and surface structure of DCPD/MgF_2 membrane of Mg-2Zn-0.5Nd-0.5Zr alloy, and the Micro-CT images of the bone of DCPD/MgF_2 coatings after 12 weeks. Reproduced with permission from Ref. [220], © Elsevier 2025. (g) Structural Diagram of MgP10C: inner-layer Mg scaffolds and bottom and top layer PLGA/collagen hybrid (top); macro view and shaped state of MgP10C. Reproduced with permission from Ref. [228], © Elsevier 2025. (h) Schematic illustration of fabrication of COL/Mg composite scaffolds. Reproduced with permission from Ref. [232], © American Chemical Society 2025.

Table 1 Research progress of Mg-based GBR barrier membranes

Raw materials	Author and year	Product Name (main materials)	Manufacturer / Preparation Method	Size/ Thickness	Animal / Clinical experiments	Performance features
Pure Mg	Akiva Elad, 2023 [233]	NovaMag® membrane/ Pure Mg (Purity: 99.95%) (CE certification)	Botiss biomaterials GmbH	30×40 mm /140 μm	Clinical patients aged between 60 and 68 years old	1. The maximum tensile stress is 183.0 ± 10.7 MPa. 2. 4 months post-surgery, good cortical bone regeneration. 3. Good healing of soft tissue. 4. High stability and good operability.
Mg-Zn Alloy	Da-Jun Lin, 2017 [234]	Mg-5Zn-0.5Zr	ECO-casting, heat treatment modification, HF-treatment	2×13 cm /0.4 mm	24 SD rats with calvarial defect models	1. Minimized stress corrosion and crevice corrosion. 2. New bone regeneration. 3. F coating had better long-term corrosion resistance.
	Mingyu Zhao, 2020[235]	Mg-Zn-RE (6 wt.% Zn and 0.90 wt.% Gd, 0.75 wt.% Y, 0.96 wt.% Ce and 0.08 wt.% La)	Melt casting	5×5 mm/110 μm	44 SD rats calvarial bone defect models	1. Mg matrix degraded first, then Zn dissolved and REs were released slowly 2. Good biocompatibility. 3. Enhanced bone formation.
Mg-Ca Alloy	Hewei Chen, 2021 [206]	Mg-0.8Ca, Mg-0.8Ca-5Zn-1.5Ag Mg-0.8Ca-5Zn-2.5Ag	Melt casting	2.5×4 mm/ 2 mm	15 SD rats femoral condyle defect models	1. ZQ71 exhibited the lowest degradation rate. 2. Good biocompatibility. 3. Antibacterial properties. 4. ZQ71 showed higher osteogenic activity and bone substitution rate than ZQ63 and ZQ.
	Kai Chen,	Mg-0.2Ca-0.2La	Melt-casting	8×11 mm/ 2	Cytocompatibility	1. Sufficient strength and adequate ductility.

	2022 [236]			mm	assay and cell migration	2. Higher SCC resistance. 3. Favorable HGF cellular response. 4. Good cytocompatibility.
	Wufei Ge 2022 [208]	Mg-0.2Ca-0.2La	Melt-casting	10×10 mm/ 1.5 mm	32 SD rats femoral condyle osseointegration models	1. Slow and uniform in vitro and vivo degradation. 2. Good osteogenesis capability. 3. No local or systemic adverse effect.
Mg-Ga and Mg-Cu alloy	Yanbo Shan 2024 [237]	Mg-Ca/Mg-Cu bilayer membrane	Melt-casting and online heating rolling process	10×10 mm/ 0.5 mm	30 SD rats cranial bone defect models	1. Good yield strength. 2. Outstanding volume stability. 3. Antibacterial properties. 4. Superior bone regeneration.
Mg-Ag Alloy	Sihui Ouyang 2024 [211]	Pure Mg Mg-5 wt% Ag Mg-9 wt% Ag	Melt-casting	10×10 mm/ 1mm	Cytotoxicity, migration, osteogenic differentiation	1. Superior tensile strength, flexural strength, plasticity, and acceptable corrosion. 2. Promote healing in periodontal tissue. 3. Antibacterial effects.
Mg-Sr alloy	Shanning Zhang, 2020 [210]	Mg-1.5 Sr alloy	Microarc oxidation	15×5mm/ 3.38mm	6 hybrid dogs mandible buccal fenestration bone defect models	1. Good osteogenic effect. 2. Degradation rate is not exactly matched with the regeneration process of bone tissue.
Ca-P coating	Shuang Wu, 2019 [238]	PEO/HT-treated Mg mesh/ Mg foils (99.9% purity)	Roll, plasma electrolytic oxidation, hydrothermal treatment	10×10mm (hole diameter of 0.4 mm)/ 0.4mm	Skull models of 16 SD rats	1. Decreased the biodegradation rate. 2. Improved bone regeneration in vivo.

	Wei Peng, 2019 [239]	Ca-P-coated Mg membrane	Roll and rapid solidification	8×8mm/ 50μm	Skull defect models of 9 New Zealand White rabbits	1. Lower corrosion rate. 2. More uniform corrosion. 3. Better bioactivity. 4. Could not meet the clinical service time (at least 12 weeks)
	Shuang Wu, 2021 [240]	Ca-P-Coated Mg Mesh	Roll and alkali-hydrothermal treatment	10×10mm (hole diameter of 0.4 mm)/ 0.1mm	Calvarial defect models of 8 SD rats	1. The corrosion rate and osteogenesis capability can be tailored. 2. Higher osteogenesis capability. 3. Low degradation.
	Jiawen Si, 2021 [204]	Ca-P-coated Mg-2.0Zn-1.0Gd alloy membrane	Melt and immerse	10×10mm / 0.6mm	Calvarial bone defects models of 48 New Zealand white rabbits	1. Excellent mechanical properties. 2. Good cytocompatibility. 3. Unsatisfying early gas formation.
	Jinying Du, 2022 [221]	HA-coated Mg-2Zn-Mn-Ca-Ce alloys	HAp coating	10×10 mm / 1mm	Cell proliferation-cytotoxicity, cell adhesion tests	1. Porous outer surface and compact inner layer. 2. Outstanding hydrophilicity. 3. Higher anticorrosion. 4. Good biocompatibility.
MgF2 coating	Da-Jun Lin, 2017 [234]	MgF2 coating Mg-5Zn-0.5Zr	ECO-casting techniques, heat treatment, HF-treatment	2×13 cm /0.4 mm	Skull models of 8 SD rats	1. Excellent corrosion resistance. 2. Lower bone regeneration ability of MgF_2 coating on Mg membrane.
	Zi-Yu Yan, 2022 [241]	Mg-2Zn-0.46Y-0.5Nd	HF-treatment	4×8 mm (hole	a mandibular second molar	1. Small holes for nutrition supply. 2. Good biocompatibility.

				diameters: 1.2 mm or 0.5 mm)/ 150-200 μm	distal bone defect in eight beagle dogs	3. Without subcutaneous emphysema or increasing infection risk. 4. Good osteogenic effect.
Mg-reinforced	Yujia Han, 2025 [220]	CaHPO4·2H2O (DCPD) / MgF_2 on Mg-1.98Zn-0.54Nd-0.59Zr	Chemical conversion, HF-treatment, chemical deposition	10×8 cm /0.3 mm	Mandibular defect models of 20 New Zealand White rabbits	1. The DCPD coating: enhanced osteogenic performance, 2. The MgF_2 coating: promoted fibroblast recruitment and adhesion.
	Yingqi Chen, 2018 [242]	Mg-PLGA@HA&DBM on AZ31 alloy	Electrospinning, electrospraying	15 × 10 mm/ 0.7-1 mm	Calvarial defect models of 25 SD rats	1. Flexural stress and modulus. 2. Stimulated the bone regeneration. 3. Combined beneficial effect in vitro and in vivo.
	Yu Guo, 2019 [224]	CS coating-Mg3Gd membrane	Dip-coating Mg with chitosan	10× 10 mm/ 1 mm	42 skull implant models in New Zealand White rabbits	1. Suitable degradation. 2. Good biocompatibility. 3. Promoted bone regeneration.
	Mike Barbeck, 2020 [243]	AZ31 Mg meshes and collagen membranes (Jason Membran, Botiss biomaterials GmbH)	HF-treatment and embedded in native collagen membranes	0.5×0.5 cm^2	18 skull implant models in New Zealand white rabbits	1. Outstanding volume stability. 2. Good cyto- and biocompatibility.
	Xin Du 2020 [244]	AZ31 Mg Alloy-Reinforced PLA-Integrated Membrane	HF-treatment and integration directly	30×5 mm/ 120 μm	Cell Proliferation Test	1. Appropriate degradation rate. 2. Better corrosion resistance. 3. Good cyto- and biocompatibility.

Polymer composite membrane	Hao Yang Zhang, 2020 [227]	Fluoride-coated AZ91 reinforced PLA membrane	HF-treatment and hot pressing	12 ×2 mm/ 0.15 mm	Cell viability	1. Superior mechanical properties. 2. Complete degradation. 3. Appropriate degradation rate and ion release. 4. Sustained cell viability.
	Feilong Wang 2025 [228]	Pure Mg-reinforced PLGA collagen hybrid sandwich membranes	Laser cutting technology and membrane applicator	8×16 mm/ 200 μm	Calvaria defect models of 20 SD rats and mandibular defect models of 10 SD rats	1. Good shaping properties. 2. The inner layer: excellent space maintenance. 3. The out-layer: regulated degradation rate and biocompatibility. 4. Good osteogenic effects.

3.2 Zn and Zn Alloys

Zn is an essential trace element crucial for nucleic acid metabolism and signal transduction, with a recommended daily intake of 8–11 mg for adults [245, 246]. Since 2011, Zn-based alloys have been proposed as biodegradable implant materials, with validated applications in orthopedics and cardiovascular fields [247]. Compared to Ti and Mg, Zn-based alloys offer distinct advantages for GBR membranes [248, 249]: they exhibit favorable mechanical properties and degrade without hydrogen gas release, eliminating subcutaneous emphysema risk associated with Mg [250, 251]. Released Zn^{2+} ions provide dual osteogenic and anti-resorptive effects, promoting osteoblast proliferation and matrix synthesis while inhibiting osteoclast differentiation via RANKL signaling [252]. With a standard electrode potential between Mg and Fe, Zn demonstrates moderate, tunable degradation without gas evolution [253]. Its Young's modulus (108 GPa) can be optimized through alloying to better match bone mechanics, while processed pure Zn exhibits 20-60% elongation for easy intraoperative shaping [254]. Zn also integrates anticoagulation properties with osteogenesis, enabling timed functional transition from early thrombus prevention to subsequent bone regeneration [255-257].

Major limitations and challenges of Zn as a GBR membrane material [249]: Zn ions have a narrow therapeutic window: concentrations below 60 μmol/L enhance cellular activity, while levels exceeding 140 μmol/L inhibit proliferation and may cause DNA damage [258]. Micro-galvanic corrosion in alloys can accelerate ion release, requiring controlled release strategies. Zn is also susceptible to stress corrosion cracking in physiological environments, with studies showing 13.6% strength reduction after 20 days in Hank's solution under strain. Additionally, static in vitro models may overestimate toxicity, as dynamic physiological conditions can mitigate adverse effects, necessitating long-term in vivo validation.

Optimization strategies include developing low-toxicity binary alloys (e.g., Zn-Mg/Ca/Li) to balance osteoinduction with safe ion release [259]; surface functionalization through micro/nano-structured coatings; and 3D printing for personalized pore structures [251]. Zn-based GBR membranes demonstrate significant potential for complex bone defect repair due to their osteogenic promotion, hydrogen-free degradation, and mechanical adaptability. Clinical translation requires overcoming challenges in controlled ion release, stress corrosion resistance, and precise toxicity modulation.

The current research status of Zn and Zn alloy-based GBR membranes is summarized as follows (**Table 2**):

① Pure Zn: Hui Guo et al.[260] evaluated pure Zn membranes with different pore sizes (non-porous, 300 μm, 1000 μm) against titanium controls in rat calvarial defects. The 300 μm pore membrane demonstrated osteogenic capacity comparable to non-porous titanium, establishing pure Zn as a promising GBR material with suitable degradation rate and mechanical properties amenable to alloying enhancement (**Figure 7a-c**). Kai Chen et al. [261] investigated pure Zn degradation in artificial saliva simulating membrane exposure scenarios. After 28 days, the degradation rate was approximately 31.42 mm/year, with corrosion products including zinc phosphate ($Zn_3(PO_4)_2$), calcium phosphate (CaP), and zinc oxide (ZnO). Pure zinc GBR membranes (50 μm thick, with pore sizes of 300/600 μm) still exhibit an ultimate tensile strength of more than 50 MPa after being soaked in simulated body fluid (SBF) for 45 days even following U- bending (significantly superior to commercial absorbable membranes), meeting the clinical application standards for GBR [262].

② Zn alloy

Zn-Cu alloy: Ping Li et al. [263] evaluated as-rolled Zn-xCu alloys (x=1,2,4 wt%) for craniomaxillofacial fixation. Zn-4Cu exhibited superior mechanical properties with uniform corrosion morphology and no significant cytotoxicity. Released Zn ions promoted osteoblast and periosteal cell proliferation while inhibiting oral multispecies biofilms. Wentai Zhang, et al [264] developed Zn-0.5Cu-xFe alloys via hot extrusion. Zn-0.5Cu-0.2Fe achieved optimal strength-ductility balance (202.3 MPa UTS, 41.2% elongation) with accelerated but uniform degradation, no cytotoxicity, and inhibited bacterial adhesion (**Figure 7d**).

Zn-Li alloy: Yu Zhang et al. [265] prepared 0.1 mm Zn-0.8Li-(Mg,Ag) alloys via casting and hot rolling. Zn-0.8Li-0.2Ag exhibited refined equiaxed grains (2.3 μm) with homogeneous $LiZn_4$ nanoprecipitates, achieving 97.9% elongation, superior corrosion resistance, and good biocompatibility. Ultrahigh pressure supersaturated solid solution treatment effectively eliminates the $LiZn_4$ phase in Zn-Li alloys, resulting in uniform degradation and significantly enhanced strength and formability [266]. The released Li^+ ions exhibit anti-inflammatory effects and promote bone healing, demonstrating great potential for application in biodegradable oral materials such as GBR membranes.

Zn-Fe/Zn-Mg alloy: Ying Liu et al. [267] fabricated Zn-0.5Fe membranes via powder sintering and rolling, achieving refined microstructure and reduced micro-galvanic corrosion. Xin Chu et al. [268]

developed Zn-0.5Fe-0.05Mg and Zn-0.5Mg-0.05Fe membranes. Tensile strengths reached 331.2 MPa and 352.2 MPa (vs. 88.9 MPa for pure Zn) with elongations of 25.8% and 20.2%. Corrosion rates were 0.180-0.210 mm/year with grade 0-1 cytotoxicity. After 12 weeks in vivo, BV/TV ratios reached 30.3% and 65.5%, demonstrating exceptional osteogenic potential. By adopting the accumulative roll bonding (ARB) method, ultrafine-grained Zn matrices reinforced by in-situ generated $MgZn_2$ and Mg_2Zn_{11} nanoparticles can be obtained by alternately stacking pure Zn sheets and Mg powder and repeating rolling cycles. This alloy exhibits an ultra-high tensile strength of approximately 560 MPa, a yield strength of about 540 MPa, and a uniform elongation of around 12%, which are far superior to most conventional Zn alloys. Meanwhile, the refined microstructure can reduce the degradation rate, and enhance biocompatibility, demonstrating great application potential in the field of high-strength GBR membranes [269].

Zn-Ti alloy: Xin Chu et al. [270] fabricated Zn-0.5Ti-0.5Fe and Zn-0.5Ti-0.5Mg membranes. Tensile strengths reached 145.3 MPa and 164.4 MPa (vs. 85.9 MPa for pure Zn) with elongations of 30.2% and 19.3%. Corrosion rates accelerated to 0.181-0.199 mm/year. After 12 weeks implantation, BV/TV ratios reached 30.3% and 65.5%, confirming strong GBR potential.

Zn-Ca alloy: A common challenge in the application of Zn alloys for implants is balancing antibacterial efficacy and biocompatibility. Xiangmin Li et al. [271] addressed the antibacterial-biocompatibility trade-off in Zn-Ca alloys via bottom circulating water-cooled casting and rolling, significantly refining $CaZn_{13}$ precipitates. The processed Zn-0.3Ca alloy achieved 49% elongation, the highest among Ca-containing Zn alloys, with superior antibacterial activity against E. coli and S. aureus, reduced cytotoxicity, improved degradation uniformity, and enhanced osteogenic induction.

In addition to the Zn alloys mentioned above, Zn alloys co-doped with bioactive elements like Ag and Se (Zn-4Ag-2Se alloy) through casting and hot rolling can endow the membranes with favorable mechanical properties, tunable degradation behavior, potent antibacterial activity, and even selective antitumor performance, which are highly beneficial for infection inhibition and postoperative safety in oral implantation [272].

③ Coating on Zn alloys

Wenjie Xu et al. [273] developed double-sided composite membranes (DSZM) by electrospinning PCL/chitosan nanofiber layers on pure Zn mesh. DSZM exhibited ~25.6 MPa UTS (6× Bio-Gide), low corrosion rate (17 μm/year), sustained Zn^{2+} release (~0.23 μg/mL/month), excellent

cytocompatibility, osteogenic promotion, and antibacterial activity against S. aureus, with superior performance in rat maxillary defects (**Figure 7e**). Kai Chen et al. [274] fabricated Mg/Cu-MOF coatings on pure Zn, creating an alkaline microenvironment with Zn^{2+}/Mg^{2+}/Cu^{2+} release promoting calcium phosphate deposition, osteogenesis, angiogenesis, and antibacterial effects (**Figure 7f**). Fanyu Yan et al. [275] constructed bilayered ss-HMC/Zn membranes integrating hierarchically mineralized collagen with Zn, providing mechanical barrier function and self-induced osteogenic microenvironment without supplements (**Figure 7g**). Hongyan Tang et al. [276] deposited Nb_2C MXene coatings on Zn via self-assembly, achieving controllable degradation, NIR-II photothermal response, >99% antibacterial efficacy, free radical scavenging, and immunomodulatory capacity (**Figure 7h**).

④ 3D-printed Zn meshes

Yanping Liu et al. [256] fabricated personalized porous curved pure Zn meshes via laser powder bed fusion, subsequently coating with chitosan/gelatin cryogel. This composite enabled nutrient transmission, prevented fibroblast infiltration, maintained structural integrity > 60 days, and achieved sustained Zn^{2+} release mitigating cytotoxicity while demonstrating osteogenic and anti-infective capabilities (**Figure 7 i, g**).

Table 2 Research progress of Zn-based GBR barrier membranes.

Raw materials	Author and year	Main materials	Manufacturer / Preparation Method	Size/ Thickness (mm)	Animal / Clinical experiments	Performance features
pure Zn	Hui Guo 2020 [277]	pure Zn membrane (Pure Zn foil (99.998% purity))	Laser cutting technology	10×20 mm/ 30 μm (pore diameter: 300 and 1000 μm)	Calvarial defect models of 40 SD rats	1. Laser cutting reduced the mechanical properties. 2. Suitable degradation rates. 3. Acceptable cytocompatibility and favorable osteogenic ability.
	Kai Chen 2021 [261]	Zn-based membranes (pure Zn bars (99.99 wt%))	Extruded pure Zn bars	thickness of 1.2 mm	Cytotoxicity test	1. The degradation rate: 31.42 μm / year. 2. The corrosion products: Zn3(PO4)2, Ca3(PO4)2, CaHPO4, Zn5(CO3)2(OH)6, and ZnO. 3. Acceptable cytocompatibility. 4. High antibacterial activity (Porphyromonas gingivalis).
	Ping Li 2019 [278]	Zn-4Cu alloy	Melt-casting and rolling	10×10 mm/ 1.8 mm	Cytotoxicity test	1. Enhanced the mechanical properties. 2. Uniform mode of corrosion. 3. No apparent cytotoxic effect. 4. Inhibited abundant biofilm formation of mixed oral bacteria.

Zn-Cu Alloy	Wentai Zhang 2021 [279]	Zn-0.5Cu-xFe (x = 0.1, 0.2 and 0.4 wt%) alloys	Melt-casting and extruded	10×10 mm/ 1.5 mm	Cytotoxicity test	1. Adding Fe reduces the elongation at fracture. 2. More uniform degradation behavior. 3. No cytotoxic effects.
Zn-Li Alloy	Yu Zhang 2019 [280]	Zn-0.8%Li-(Mg, Ag) alloys	Melt-casting and hot rolled with intermediate annealing	Thickness of 0.1 mm	Cytotoxicity tests and proliferation evaluation	1. Zn-Li-Mg alloy exhibited the highest yield strength and ultimate tensile strength, but a lower elongation than other alloys. 2. The corrosion rates were ranked as Zn-Li-Mg > Zn-Li > Zn-Li-Ag. 3. Good biocompatibility.
Zn-Fe Alloy	Ying Liu 2022 [281]	Zn-0.5Fe alloy membrane	Powder sintering, hot extruded and hot rolling	16×16 mm/ 0.1 mm	Cytotoxicity assays	1. More uniform fine microstructure. 2. Higher tensile strength. 3. Higher corrosion resistance. 4. Aadequate biocompatibility
	Xin Chu 2025 [268]	Zn-0.5Fe-0.05Mg and Zn-0.5Mg-0.05Fe alloy GBR membranes	Vacuum atomization process, reduction process Fe powders	20 mm/ 0.1 mm	8 skull implant models in New Zealand White rabbits	1. Refined the grain size of the alloy. 2. Improved mechanical properties. 3. Faster corrosion rate (Zn-based alloys). 4. Grade 0-1 cytotoxicity. 5. Promoted bone growth.
Zn-Ti Alloy	Xin Chu 2024	Zn-0.5Ti-0.5Fe and Zn-0.5Ti-0.5Mg alloy	Powder metallurgy, gas	20 mm/ 0.5 mm	New Zealand rabbit cranial	1. Favorable mechanical properties. 2. Good degradability and biocompatibility.

	[282]	GBR films	atomization, H_2 reduction, hydrogen embrittlement		parietal defect models	3. Zn-0.5Ti-0.5Mg had higher corrosion potential, corrosion current density and corrosion rate. 4. Superior new bone growth ability.
Zn-Ga Alloy	Xiang-Min Li 2024 [283]	BCWC-rolled alloy (Zn-0.3Ca)	Bottom circulating water-cooled casting (BCWC), hot/cold rolling	10×10 mm/ 0.1 mm	Cytotoxicity, osteogenic differentiation	1. Elongation is the highest among Zn-Ca alloys. 2. Corrosion uniformity. 3. Antibacterial activity (E. coli and S. aureus). 4. Good osteogenic differentiation ability.
Coating	Kai Chen 2024 [274]	Bimetallic Mg/Cu-MOF) coatings on pure Zn (99.99 wt %))	hydrothermal method	20 mm	18 subcutaneous Infection Model in SD rats	1. Regulate the degradation rate and water stability. 2. Promoted osteoblast differentiation. 3. Enhanced the vascularization of endothelial cells. 4. Superior antibacterial activity.
	Fanyu Yan 2025 [275]	Hierarchical mineralized collagen coated pure Zn membrane	Acid etching, micro polishing pre-treatments, self-assembly and biomimetic mineralization	10 × 20 mm/ 139 μm	Calvarial defect models of 40 SD rats	1. Barrier function and space maintenance capacity. 2. Relatively uniform degradation mode. 3. Promoted the migration and osteogenic differentiation of BMSCs.
	Hongyan Tang 2025 [276]	Nb_2C MXene coated-pure Zn (99.9%)	Drop coating and vacuum drying	Coating thickness: 1.3-3.5μm	Subcutaneous S. aureus infection model of 6 rats	1. Slow degradation rate with a reduction of 74%. 2. Antibacterial rate > 99% against E. coli and S. aureus; 3. Promoting soft tissue healing and bone regeneration; 4. Anti-inflammatory and antibacterial effects.

3D printing Zn GBR mesh	Yanping Liu 2025[12]	1A gas-atomized spherical pure Zn powder	Electrophoretic deposition, laser powder bed fusion additives	1 mm × 14 mm/ 20 × 20 × 20 mm	Cytocompatibility, osteogenic capability	1. A complex and manufacturable curved surface. 2. Unit cell integrity and uniform stress. 3. Efficient nutrient transfer. 4. Inhibiting 100 % fibroblasts infiltration. 5. Osteogenesis and anti-infection capacity in vitro. 6. Reduced the biodegradation rate.

Pure Zn

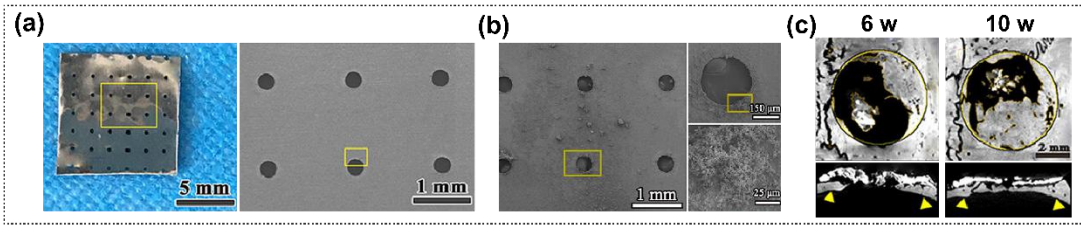

Zn-Cu alloy

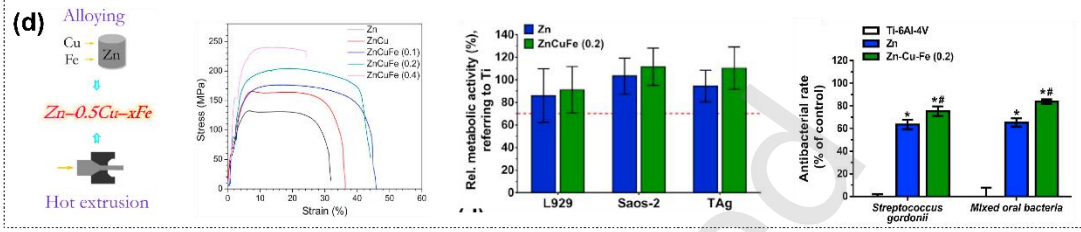

Coating on Zn alloys

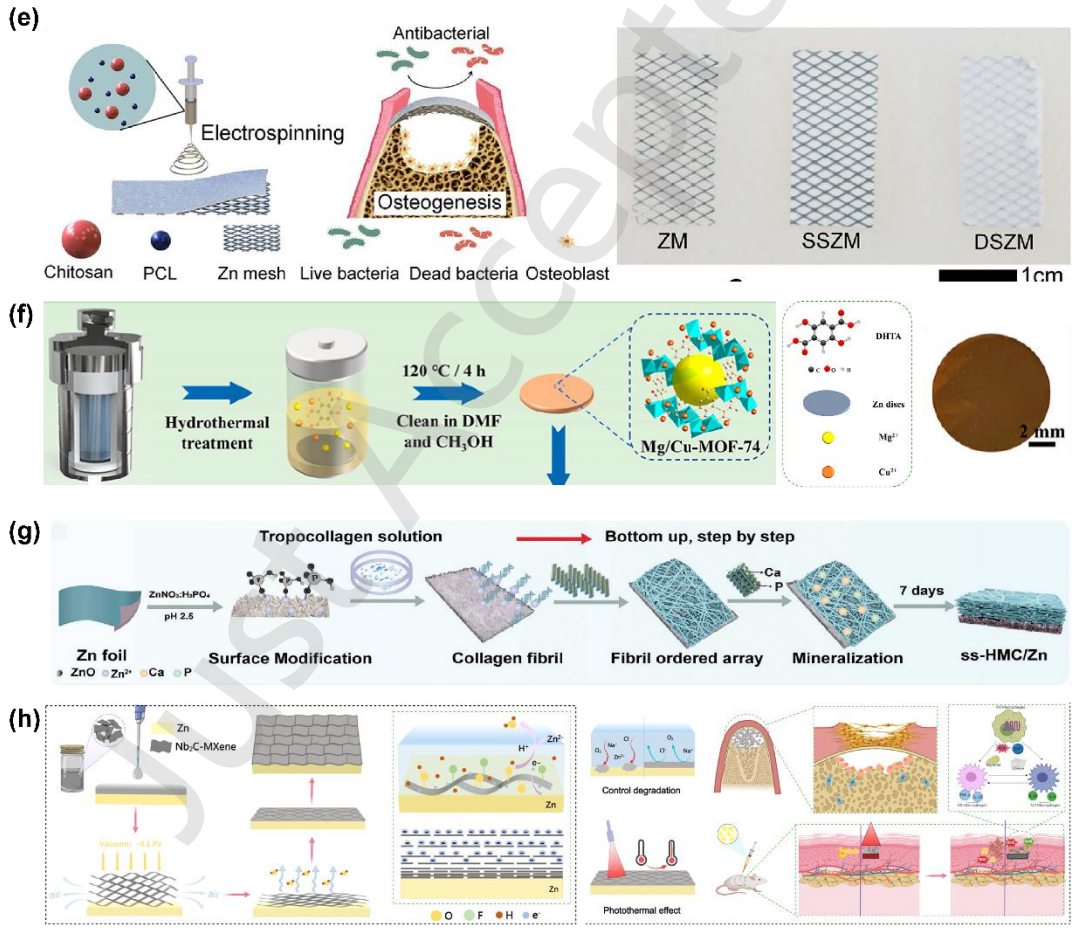

3D-printed Zn meshes

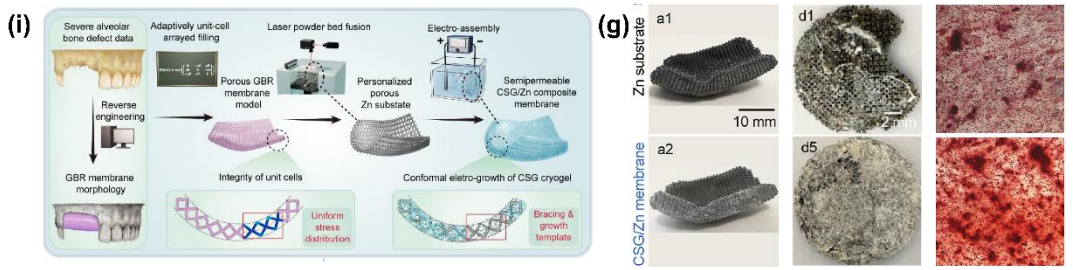

Figure 7 Current research status of Zn-based alloys as a potential candidate material for GBR membranes: (a) Macroscopic images of pure Zn membrane with 300 μm pores (left) and scanning electron microscope (SEM) graphs of the corresponding magnified areas of yellow rectangles in left (right). Reproduced with permission from Ref. [260], © Elsevier 2020. (b) Typical surface morphologies of Zn membrane with 300 μm pores after immersion in Hank's solution for 60 days. Reproduced with permission from Ref. [260], © Elsevier 2020. (c) Representative micro-CT images of pure Zn membrane with 300 μm after implantation for 6 and 10 weeks, respectively (New bone formation areas were circled by yellow lines, and the edges of bone defect area were marked with yellow arrowheads). Reproduced with permission from Ref. [260], © Elsevier 2020. (d) Schematic of strategy to fabricate hot-extruded Zn-0.5Cu-xFe alloys as GBR membranes; Mechanical performance of the hot-extruded Zn and Zn-based alloys; Relative cell metabolic activities of L929, Saos-2, and TAg cells after 24 h of incubation with sample extracts determined by CCK-8 assay; Antibacterial rates of pure Zn and ZnCuFe (0.2 wt%) alloy to both planktonic S. gordonii and mixed oral bacteria after 12 h of incubation. Reproduced with permission from Ref. [264], © Elsevier 2021. (e) Schematic illustration of bone-defect repair treated with GBR membrane, preparation process, and photographs for biodegradable Single Zn mesh membrane (ZM), Single-sided complex PCL-CS Zn mesh membrane (SSZM), and Double-sided complex PCL-CS Zn mesh membrane (DSZM). Reproduced with permission from Ref. [273], © Elsevier 2024. (f) Schematic diagram of synthesizing bimetallic Mg/Cu-MOF coatings on pure Zn discs. Reproduced with permission from Ref. [274], © American Chemical Society 2024. Digital photos of Mg/Cu-MOF-coated samples. Reproduced with permission from Ref. [274], © American Chemical Society 2024. (g) ss-HMC was coated on the Zn surface via a self-assembly strategy. Reproduced with permission from Ref. [275], © Wiley 2025. (h) Schematic illustration of MXene coating deposition on Zn substrate surface, and schematic diagram of MXene-coated Zn to control degradation for osteogenesis, soft tissue healing and antibacterial activity. Reproduced with permission from Ref. [276], © Elsevier 2025. (i) The personalized porous Zn substrate is designed using an adaptively unit-cell arrayed filling method to achieve a complex curved surface shape while ensuring the integrity of unit cells and uniform stress distribution. Subsequently, the Zn substrate is fabricated by laser powder bed fusion additive manufacturing and serves as both the bracing structure and template for conformal electro-growth of CSG cryogel to obtain the CSG/Zn composite membrane. Reproduced with permission from Ref. [284], © Elsevier

2025. (g) Digital photos of the personalized morphology of the 3D-printed Zn substrate and CSG/Zn composite membrane designed based on the shape of a patient's alveolar bone defect (left); Representative digital photos of the 3D-printed Zn substrate and CSG/Zn composite membrane immersed for 60 days (middle); Alizarin red staining of 3D-printed Zn substrate and CSG/Zn composite membrane at 21 days (right). Reproduced with permission from Ref. [284], © Elsevier 2025.

4 Novel GBR membranes

4.1 Advanced structural design

4.1.1 Asymmetric membranes

To address the distinct biological microenvironments of the soft tissue and bone defect sides, asymmetric GBR membranes utilize interface-specific designs [11, 285]. The soft tissue interface acts as a physical barrier against fibroblast migration while promoting tissue integration and antibacterial protection. Conversely, the bone interface features topographies and chemistries that facilitate protein adsorption and osteogenic differentiation [285]. Current asymmetric designs include: ① Structurally asymmetric membranes. Inspired by natural nacre, researchers fabricated bilayer membranes (dense nacre-like layer/porous layer) via self-assembly and ice-templating [286]. These exhibit superior mechanical properties and biocompatibility compared to Bio-Gide® (**Figure 8a**). ② Functionally asymmetric membranes**:** These multi-layers are loaded with different agents [285]. A Janus-type GBR membrane was constructed by a stepwise electrospinning technique [54, 287]: The inner layer was composed of random gelatin fibers loaded with HAP for osteogenesis; the outer layer consisted of aligned PCL nanofibers loaded with poly([2-(methacryloyloxy)ethyl]trimethylammonium chloride-co-2-aminoethyl methacrylate hydrochloride) (P(DMC-AMA)), resisting epithelial tissue invasion and bacterial infection (**Figure 8b**). ③ *Asymmetric laminated composite membranes:* Integrate membranes with different specific functions into a single membrane. For example, an antibacterial layer-osteoinductive layer-mechanical support layer composite membrane [11]. Preparation methods include solution casting, phase inversion, freeze-drying/cryogelation, gas foaming, electrospinning, and 3D or 4D printing [11, 285].

4.1.2 Bioinspired structural membranes

Bio-inspired GBR membranes emulate the multiscale features of natural tissues, such as pore gradients and surface topographies, to optimize cell migration and nutrient transport. ① Spider Silk-Inspired: Wenze Chen et al. [75] fabricated a double-layered silk fibroin membrane with cone-shaped microporous passageways (CSMP-DSF membrane) (**Figure 8c**) containing tapered microchannels within a smooth, dense layer, which guides rapid and directional liquid transport from the dense layer to the rough, loose layer, offering excellent mechanical strength and anti-bacterial adhesion comparable to Bio-Gide®. ② Nacre & Bouligand-Inspired: Shui Yuan et al. [288] integrated nacre-like "brick and mortar" discontinuities into a fiber-based Bouligand structure (**Figure 8d**). This nanocomposite (d-BLG) achieved a tensile strength of 12.43 MPa and superior toughness of 6.70±0.63 MJ/m^3, outperforming disordered or pure organic membranes. In rat calvarial models, the d-BLG structure demonstrated significantly higher new bone volume than commercial collagen membranes after 8 weeks.

4.1.3 Integrated barrier-scaffold membranes

Traditional GBR treatments combining membranes with bone grafts often fail in large defects due to graft displacement and insufficient mechanical support. Integrating GBR membranes with 3-D porous scaffolds offers a robust solution for reconstructing extensive soft and hard tissue deficiencies [289]. ① Multifunctional Nano-networks: Shuyi Wu et al. [83] developed a dual-layered system featuring a dense, N-halamine-functionalized BC layer to block fibroblasts and bacteria, paired with a loose CS-HAp micro-network. This loose layer conforms to bone defects, creating a pro-osteogenic microenvironment. ② Gradient Scaffolds: Li Yuan et al. [290] fused an electrospun PLGA/fish collagen membrane with a 3D-printed PLGA/nHAp scaffold. This biodegradable gradient structure effectively guided oral tissue regeneration in beagle dog models (**Figure 8e**). ③ Periosteum-Bone Mimicry: Inspired by the natural periosteum-bone complex, Jiye Zhang et al. [291] utilized personalized negative molds and phase separation to fabricate a hierarchical PLGA/BCL scaffold. Similarly, Mengqi Zhang et al. [291] designed a hierarchical structure where a dense surface prevents soft-tissue invasion, while a loose underside promotes protein adsorption. The internal macropores, synergized with loaded baicalein, further stimulate angiogenesis and osteogenesis (**Figure 8f**).

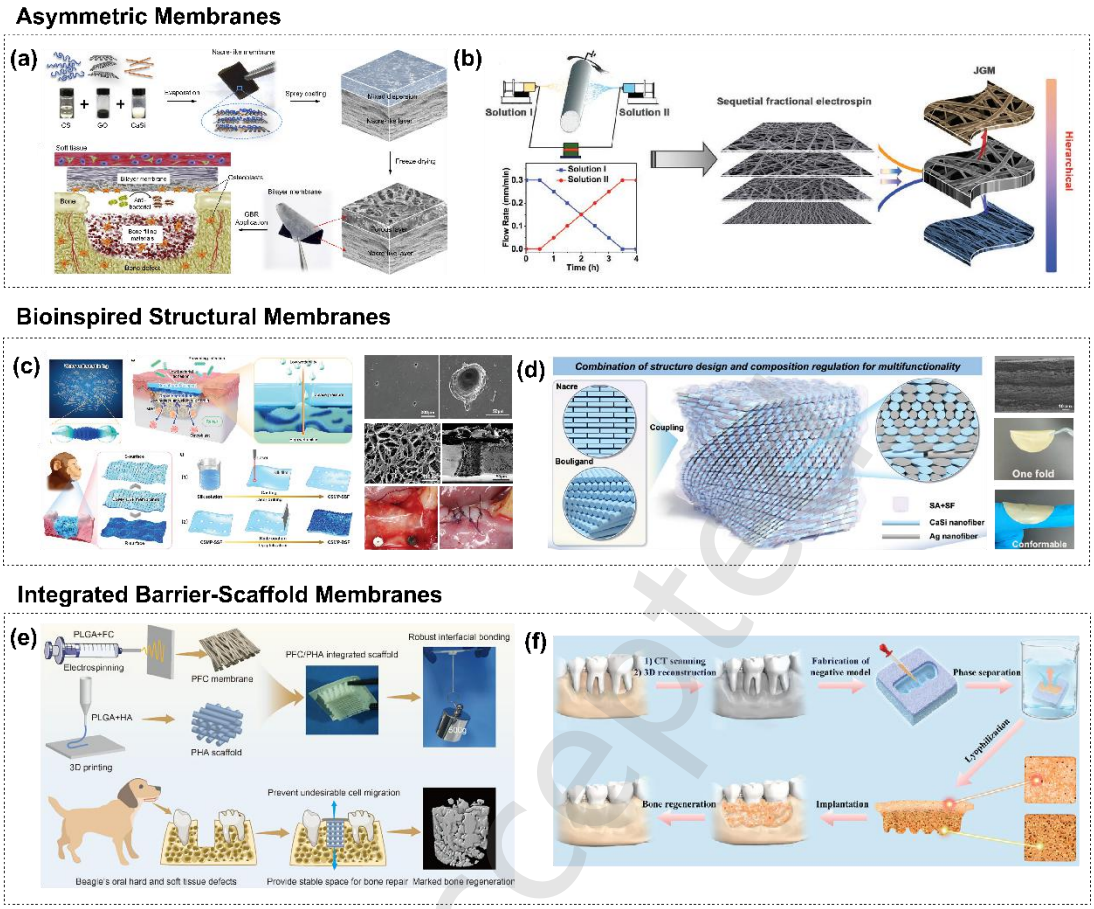

Figure 8 New-generation structural designs of GBR membranes: (a) The bilayer nanocomposite membrane consisting of a porous layer and a dense nacre-like layer. Reproduced with permission from Ref. [286], © Elsevier 2019. (b) Schematic of the sequential fractional electrospinning process of hierarchical Janus nanofibrous membrane: The inner layer is random gelatin (GEL) nanofibers loaded with HAp, and the outer layer is oriented polycaprolactone (PCL) nanofibers loaded with P (DMC-AMA), and genipin cross-linking is used to improve stability and mechanical properties. Reproduced with permission from Ref. [54], © Wiley 2021. (c) Double-Layered Silk Fibroin Membrane with Cone-Shaped Microporous Passageways (CSMP-DSF membrane): the smooth surface (S-surface) is oriented towards the soft tissue, and the rough surface (R-surface) faces the bone defect area; SEM images of the smooth surface (top), the rough surface (bottom), conical microporous channels (top) and a cross-section of CSMP-DSF membrane (bottom); after grafting the defects (alveolar bone defects in cynomolgus monkeys) with bone substitute material, the CSMP-DSF membrane was positioned over the defect site and secured with membrane screws (top), and the wound margins were then meticulously sutured (bottom). Reproduced with permission from Ref.

[75], © Wiley 2024. (d) Schematic illustration of bioinspired design of a multicomponent nacre-inspired discontinuous bouligand (d-BLG) membrane; Cross-sectional SEM image of the d-BLG membrane showing a corrugated pattern; Digital photographs of d-BLG membrane; shape conformable capabilities of d-BLG membrane. Reproduced with permission from Ref. [288], © Wiley 2025. (e) PFC/PHA integrated scaffold prepared by electrospinning and 3D printing, the integrated scaffold prevents undesirable cell migration and provides a stable space for bone repair. Reproduced with permission from Ref. [290], © Springer Nature 2024. (f) Schematic illustration of personalized fabrication and bone repair processes of PLGA/BCL-S with hierarchical porous structure. Reproduced with permission from Ref. [291], © Wiley 2024.

4.2 Smart responsive GBR membranes

Smart responsive GBR membranes represent a paradigm shift from static barriers to dynamic sensing-decision-execution systems. By integrating stimuli-responsive molecules (e.g., pH-sensitive MOFs) and nano-intelligent carriers (e.g., light-responsive liposomes) into GBR substrates, these adaptive scaffolds detect biochemical cues, such as inflammatory pH drops or thermal shifts, to trigger "on-demand" therapeutic release.

① Stimuli-responsive mechanisms.

Enzyme/infection-responsive: To minimize systemic toxicity, Min He et al. covalently grafted metronidazole (MNA) onto gelatin nanofibers via ester linkages, forming an insoluble prodrug (Pro-MNA). This bond remains stable under physiological conditions but specifically hydrolyzes in the presence of bacterial esterases, ensuring targeted, long-term antibacterial efficacy (**Figure 9a**) [292].

pH-responsive: Yiyuan Xie et al. developed a bilayer PCL/Col/ZIF-8 composite membrane (**Figure 9b**). This system utilizes the pH-dependent release of Zn ions from metal-organic frameworks (MOFs) to synergistically promote angiogenesis and bone regeneration [293].

Light-responsive: Electrospun PLLA membranes doped with black phosphorus (BP) and calcium peroxide (CPO) utilize NIR (808 nm) laser irradiation to induce photothermal effects, accelerating phosphorus release and osteogenesis [294]. Advanced scaffolds using AIE nanoparticles and BP nanosheets (AIE NPs@BP NSs@FSs) further modulate the immune microenvironment by promoting M2 macrophage polarization and eliminating biofilms under NIR-II irradiation (**Figure 9c**) [295].

② 4D printing and shape memory

4D printing advances GBR by creating scaffolds that evolve in shape or function over time in response to external stimuli (such as heat and light) [296-300]. However, existing 4D printed scaffolds have problems such as inappropriate deformation conditions (e.g., excessively high transformation temperature), inherent hydrophobicity, and lack of bone regeneration function [301]. Xiaodong Guo et al. [302] fabricated a dual-tunable scaffold using direct ink writing (DIW). By compounding a hard PLMC/nHA framework with a soft nHA@PDA/GelMA hydrogel, they achieved an ideal transition temperature (38.8°C) matching human physiology, and shape memory functionality (97% fixation, 90% recovery) triggered by NIR/thermal stimuli, and continuous release of pargyline (PGL) to drive osteogenic differentiation (**Figure 9d**).

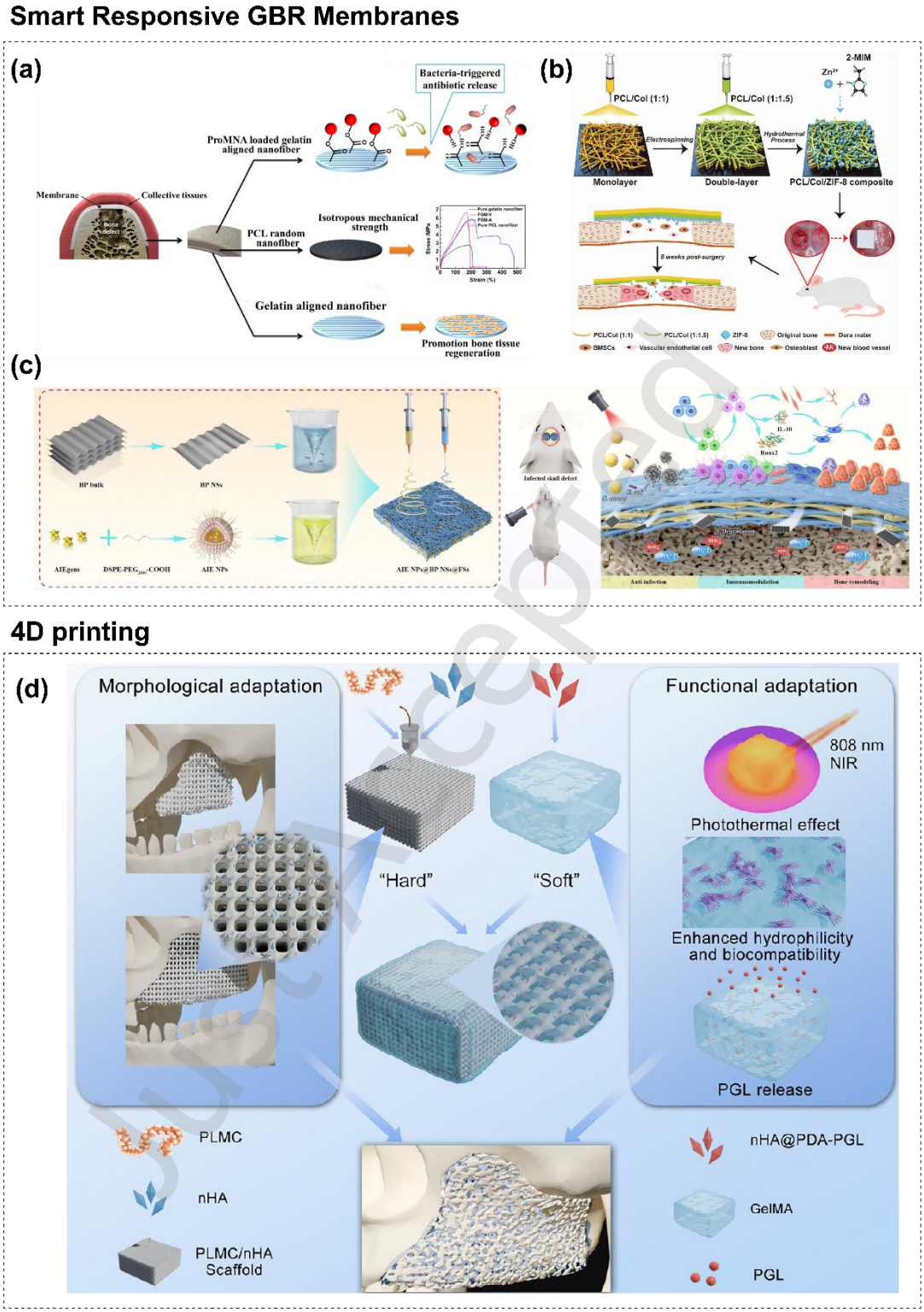

Figure 9 (a) Schematic illustration of the trilayer functional membranes (pro-MNA loaded gelatin aligned nanofiber/PCL random nanofiber/Gelatin aligned nanofiber) in displaying their functions for improving bone regeneration performance. Reproduced with permission from Ref. [292], © Elsevier 2020. (b) Fabrication process of the asymmetric bilayer PCL/Col/ZIF-8 composite

membrane: The membrane was prepared by electrospinning a PCL/Col polymer blend (mass ratios of 1:1 and 1:1.5), followed by the in situ hydrothermal growth of ZIF-8 crystals on one side of the bilayer structure. Reproduced with permission from Ref. [293], © Wiley 2021. (c) Schematic illustration of the fabrication and therapeutic mechanism of AIE NPs@BP NSs@FSs for treating infected cranial bone defects in rats. Reproduced with permission from Ref. [295], © Wiley 2025. (d) Schematic illustration of the concept of the morphology and function dual-adjustable 4D-printed scaffold composed of a hard 4D-printed shape-morphing framework and a soft functionalized hydrogel for the regenerative repair of complex bone defects in the oral and maxillofacial region. Reproduced with permission from Ref. [302], © Wiley 2025.

4.3 Electroactive GBR membrane

Biopiezoelectric materials generate localized currents in vivo, restoring the physiological electrical microenvironment to accelerate bone regeneration [303, 304]. Common matrices include PVDF, PLLA, and silk fibroin, often enhanced with piezoelectric fillers like barium titanate (BT) or boron nitride nanotubes (BNNTs).

Key research highlights include: ①Enhanced bioactivity: PVDF/PCL/HA nanofibrous scaffolds exhibit 20% higher piezoelectric performance than PCL, leading to a 12% increase in mineralization and alkaline phosphatase activity [305]. ② Rapid regeneration: BT/PLA composite membranes with optimized d_{33} coefficients (7.03 pC/N) have demonstrated near-complete closure of rat calvarial defects within 12 weeks, with bone density approaching normal tissue [306]. ③ Ultrasound-driven therapy: PGBT membranes under 100 mW/cm^2 ultrasound stimulation generate a 130 mV piezoelectric voltage, providing antibacterial effects and osteogenesis without additional poling [307]. Similarly, bilayer PLLA/PLLA-ZnO membranes leverage the synergy of piezoelectricity and Zn^{2+} release to achieve anti-inflammatory and regenerative goals (**Figure 10a**) [308]. The most reported piezoelectric GBR membranes are currently fabricated using electrospinning technology (**Figure 10b**), 3D printing and solution casting technique [309]. Future development requires optimizing signal precision, mechanical properties, and biocompatibility through interdisciplinary mechanistic studies.

4.4 Nanomaterial-based GBR membranes

Integrating advanced nanomaterials into GBR membranes offers transformative improvements in conductivity, mechanical strength, and bioactive delivery. ① MXenes: These 2D transition metal

carbides/nitrides offer exceptional electrical conductivity and hydrophilicity [310-312]. Sijie Wan et al. [313] fabricated densified MXene films with extraordinary tensile strength (755 MPa) and toughness (17.4 $MJ \cdot m^{-3}$), using roll-to-roll doctor-blading (**Figure 10c**). These films demonstrate superior electromagnetic shielding and photothermal conversion. Furthermore, combining MXene with BC significantly improves membrane flexibility, biocompatibility, and degradation kinetics [84]. ② Carbon-based nanomaterials: Graphene and carbon nanotubes (CNTs) are utilized primarily to reinforce polymer matrices and enhance cell adhesion [314, 315]. For example, single-walled carbon nanotubes (SWCNTs) dispersed in hyaluronic acid have been shown to selectively promote osteoblast proliferation (**Figure 10d**). While promising, these applications remain largely in the laboratory phase [315]. ③ Metal-Organic Frameworks (MOFs): MOFs provide high specific surface areas and tunable porosity, serving as ideal carriers for growth factors and antibacterial agents [316]. Their chemical versatility allows for smart responsiveness, such as pH-triggered drug release to combat postoperative infections. When hybridized with traditional materials like collagen or PLA, MOFs enhance membrane hydrophilicity and nutrient permeability, facilitating rapid integration with host bone tissue [293].

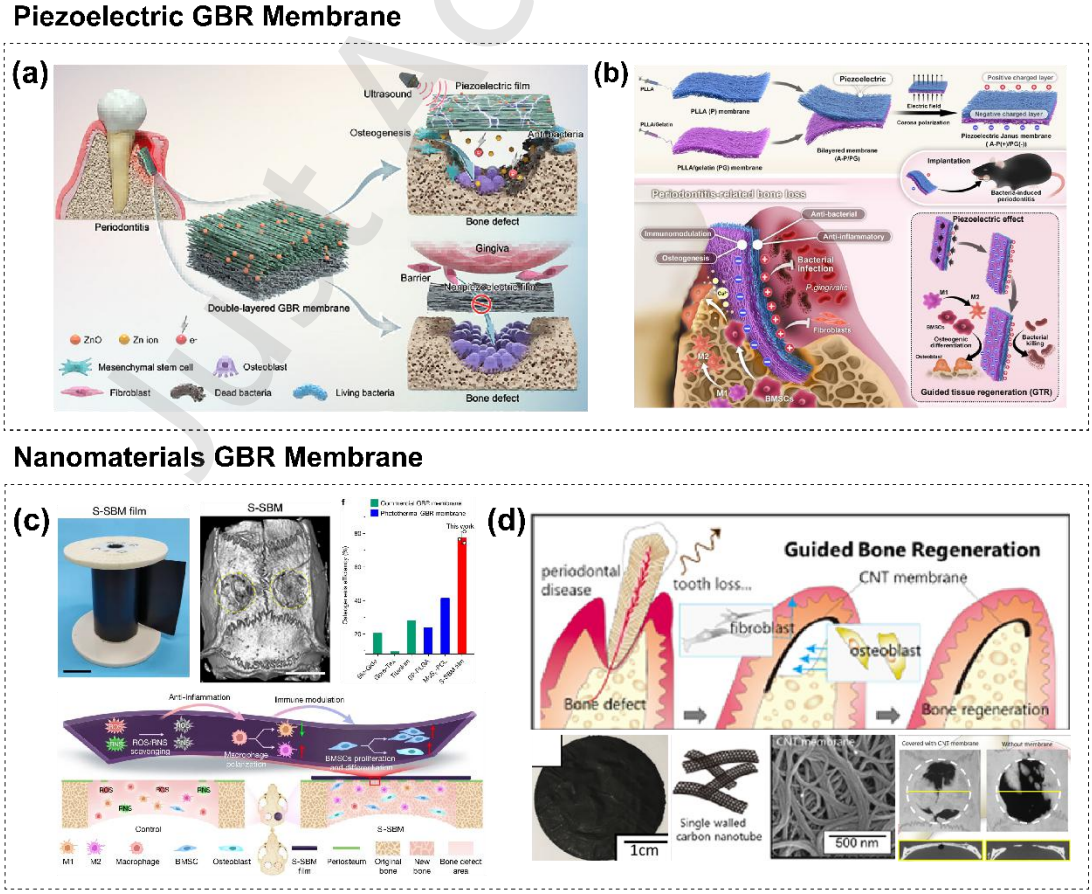

Figure 10 (a) Schematic diagram of the structure and applications of the double-layered piezoelectric PLLA-ZnO composite GBR membrane. Reproduced with permission from Ref. [308], © Wiley 2025. (b) Design and fabrication of a biodegradable piezoelectric Janus membrane for simultaneous antibacterial and bone regenerative therapy in periodontitis; Pure PLLA and PLLA/Gelatin (PG) membranes were fabricated using electrospinning. Reproduced with permission from Ref. [317], © American Chemical Society 2025. (c) Photograph of a roll of scalable sequentially bridged MXene (S-SBM) film with a width of 25 cm; The S-SBM membrane outperforms existing commercial and previously reported photothermal GBR membranes in osteogenic efficiency; 3D-reconstructed micro-CT images of whole rat calvarial bone in S-SBM group. Reproduced with permission from Ref. [313], © Springer Nature 2024. (d) Single-walled carbon nanotube membranes accelerate active osteogenesis in bone defect. Reproduced with permission from Ref. [315], © American Chemical Society 2022.

4.5 Functional additives for GBR membranes

To transition from passive barriers to bioactive scaffolds, functional materials are increasingly incorporated into GBR membrane matrices to achieve multi-target therapy (**Figure 11**).

① Bioactive Substances and Osteoinduction: Inorganic compounds, including HAp, β-TCP, and bioglass, are primary additives that stimulate osteogenic differentiation and regulate bone remodeling through ion release (e.g., Mg^{2+}, Zn^{2+}, Sr^{2+}) [318]. Due to their inherent brittleness, these are typically integrated with polymers (e.g., PLA, PCL) in three configurations [18, 150]: Composite Fillers: Blending particles into the matrix to enhance bioactivity and mechanical support. Surface Coatings: Depositing inorganic layers to improve bone-tissue integration. Asymmetric Bilayers: Utilizing a porous inorganic layer for bone ingrowth and a polymeric layer for soft-tissue exclusion. Beyond minerals, the loading of cytokines and growth factors (e.g., BMP-2, VEGF) provides direct signaling to accelerate regeneration. However, synchronizing the release kinetics and material degradation with the pace of new bone formation remains a significant technical hurdle.

② Advanced antibacterial strategies: GBR membranes utilize both chemical and physical strategies to realize antibacterial properties. Chemical Agents: Beyond traditional antibiotics, which risk inducing resistance, researchers are incorporating metal ions (Ag, Cu, Zn). These generate reactive oxygen species (ROS) to disrupt bacterial membranes while potentially promoting osteogenesis. However, their release must be strictly controlled to avoid cytotoxicity [319]. Physical

Therapies: Photodynamic Therapy (PDT) and Photothermal Therapy (PTT) utilize photosensitizers or materials like MoS_2 to eliminate bacteria via light-induced ROS or localized heat [320]. The challenge lies in balancing bacterial eradication with the thermal or oxidative tolerance of surrounding periodontal tissues.

③ Improving mechanical support: Natural and synthetic polymers often lack the compressive strength required to maintain space for bone growth. Performance is enhanced by incorporating inorganic reinforcing particles or employing advanced fabrication techniques like 3D printing, electrospinning, and cross-linking to tailor porosity and stiffness. BMs (e.g., Mg, Zn) offer superior mechanical support, though their rapid degradation requires precise tuning to match the regenerative timeline.

④ Anti-inflammatory and synergistic modulation: Loading substances that modulate inflammatory factors, such as non-steroidal anti-inflammatory drugs (NSAIDs, e.g., ibuprofen, piroxicam), into the membrane can inhibit cyclooxygenase activity. This prevents the conversion of arachidonic acid into prostaglandins, which are detrimental to periodontal regeneration, thereby reducing the inflammatory response [321]. An electrospun poly(lactic-co-carbonate) (PDT) composite nanofibrous membrane incorporating MXene and β-TCP via in situ doping, synergistically enhancing bone regeneration through combined electrical stimulation and osteoinductive activity [322].

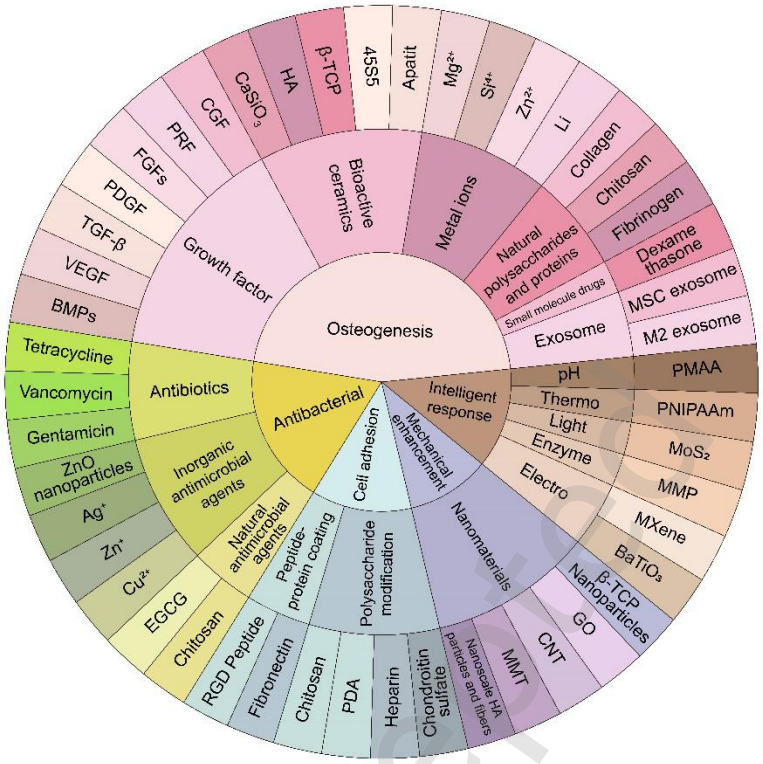

Figure 11 Supplemental additives commonly used to improve the performance of GBR membranes.

5 Prospects and challenges

5.1 Key future research directions

The evolution of GBR membranes is undergoing a paradigm shift toward intelligent integrated systems, synergizing advanced materials science with digital health to achieve multifunctional, personalized, and autonomous regenerative platforms (**Figure 12)**.

① Multifunctional composite membranes: Integrating multiple technologies enables biomimetic structures (electrospun nanofibers mimicking ECM, biomimetically mineralized membranes) and combinations of diverse biomaterials to achieve synergistic antibacterial, anti-inflammatory, pro-angiogenic, and osteoinductive effects [323, 324]. For instance, copper-loaded polydopamine-coated Zn membranes, and MSCs or exosomes-loaded membranes.

② Smart responsive membranes: To synchronize therapy with biological healing, smart responsive membranes utilize pH- or enzyme-sensitive triggers to release therapeutic agents, such as lysozyme for infection control or PLGA-encapsulated BMP-2 for sustained osteogenesis [325, 326].

③ Personalized design: Leveraging patient CT data and 3D printing, membranes can now be customized to fit complex bone defects precisely, reducing surgical adjustment time [327]. 3D-

printed Ti mesh is in preclinical stages, and the printing of BMs (Mg, Zn) and polymers represents a nascent but vital frontier.

④ Precision medicine: GBR membranes can be tailored according to patient-specific genetic profiles (e.g., vitamin D receptor gene polymorphisms) or metabolic states (e.g., pro-inflammatory microenvironments in diabetic patients). For instance, high Mg^{2+} release coatings can compensate for low osteogenic activity, while antioxidant-functionalized membranes can mitigate the pro-inflammatory microenvironments found in diabetic patients, advancing toward a one-patient-one-membrane strategy.

⑤ Green manufacturing: Environmentally friendly biodegradable materials, via biosynthetic processes or natural polymer modification, enable fully degradable membranes (e.g., BC-based), reducing the environmental impact of non-resorbable materials.

⑥ Sensor-integrated membrane: Although wearable devices have been applied in rehabilitation management, issues with patient compliance often hinder the effectiveness of real-time monitoring. The integration of wearable sensors (e.g., pressure sensors, biomarker detectors) [328, 329] into GBR membranes enables real-time monitoring of bone regeneration progress and early warning of postoperative complications, thereby improving therapeutic outcomes, extending implant longevity, and opening new avenues for the development of next-generation GBR membranes.

⑦ AI is revolutionizing GBR by optimizing the entire development-to-clinical chain. (a) Machine learning enables high-throughput screening of material compositions, predicting how parameters like pore size and degradation rates influence osteoblast adhesion [330]. Neural networks can simulate in vivo degradation kinetics under mechanical loading, ensuring biocompatibility by preventing premature membrane failure or inflammatory responses. (b) Deep learning algorithms provide non-invasive efficacy assessments by analyzing CBCT/MRI data to quantify new bone volume and density [331]. With > 90% concordance with histological findings, these models replace invasive biopsies. Furthermore, AI identifies early imaging signals of complications, such as edema or abnormal vascularity, to establish predictive risk models [332, 333]. (c) AI utilizes patient CT data to construct 3D models for one-patient-one-membrane precision, optimizing scaffold geometry for complex defects. When integrated with wearable sensors, machine learning enables dynamic feedback, regulating the release of bioactive agents (e.g., BMP-2) based on real-time inflammatory markers [329].

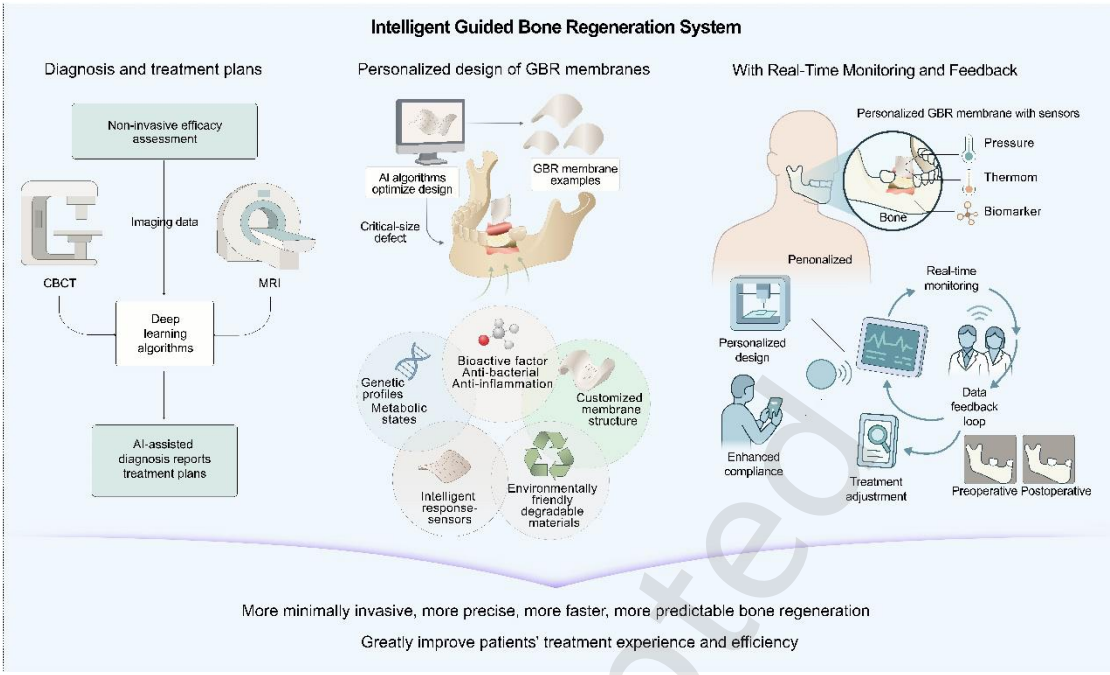

Figure 12 Future development of GBR membranes toward intelligent integrated systems.

5.2 Major challenges

Despite rapid advancements, GBR membranes face multifaceted hurdles in clinical translation and material performance (**Figure 13**).

① Optimization of material properties: A primary challenge lies in balancing competing characteristics: high mechanical strength and barrier function often compromise the porosity required for nutrient transport. Furthermore, achieving precise bioactivity regulation remains difficult; growth factors must be released at specific dosages and timelines to promote osteogenesis without triggering adverse immune responses. Additionally, matching degradation kinetics to individual bone healing rates is complex, as healing capacity varies significantly based on patient systemic health and the specific defect site.

② Advancements in manufacturing technologies: While 3D printing enables personalized scaffolds, printing complex curved surfaces often results in uneven stress distribution or mechanical failure. High-resolution printing of micro-pores also frequently suffers from blockage, hindering scalability. Similarly, nanotechnology integration faces hurdles in achieving uniform nanoparticle dispersion and ensuring the long-term toxicological safety of nano-enhanced matrices. Mass-producing these complex, gradient, or multilayered architectures at a low cost remains a significant technical barrier.

③ Expansion of clinical applications: The interaction between GBR membranes and combination therapies, such as immediate implant placement or orthodontic loading, warrants further study to ensure membranes do not impede osseointegration or soft-tissue healing. Furthermore, current membranes often struggle with high-difficulty cases, including severe bone deficiencies caused by periodontitis or systemic comorbidities like diabetes and osteoporosis, which fundamentally alter the local regenerative microenvironment.

④ Safety and long-term efficacy evaluation: The introduction of novel materials (e.g., carbon nanomaterials, biodegradable Mg, or Zn alloys) necessitates rigorous validation. Beyond acute cytotoxicity, research must address the long-term systemic impact of degradation byproducts. There is currently a critical lack of longitudinal data (spanning decades) regarding the performance of smart or composite membranes in diverse populations. Understanding late-stage biological responses and long-term bone volume maintenance is essential for establishing these technologies as the gold standard in regenerative medicine.

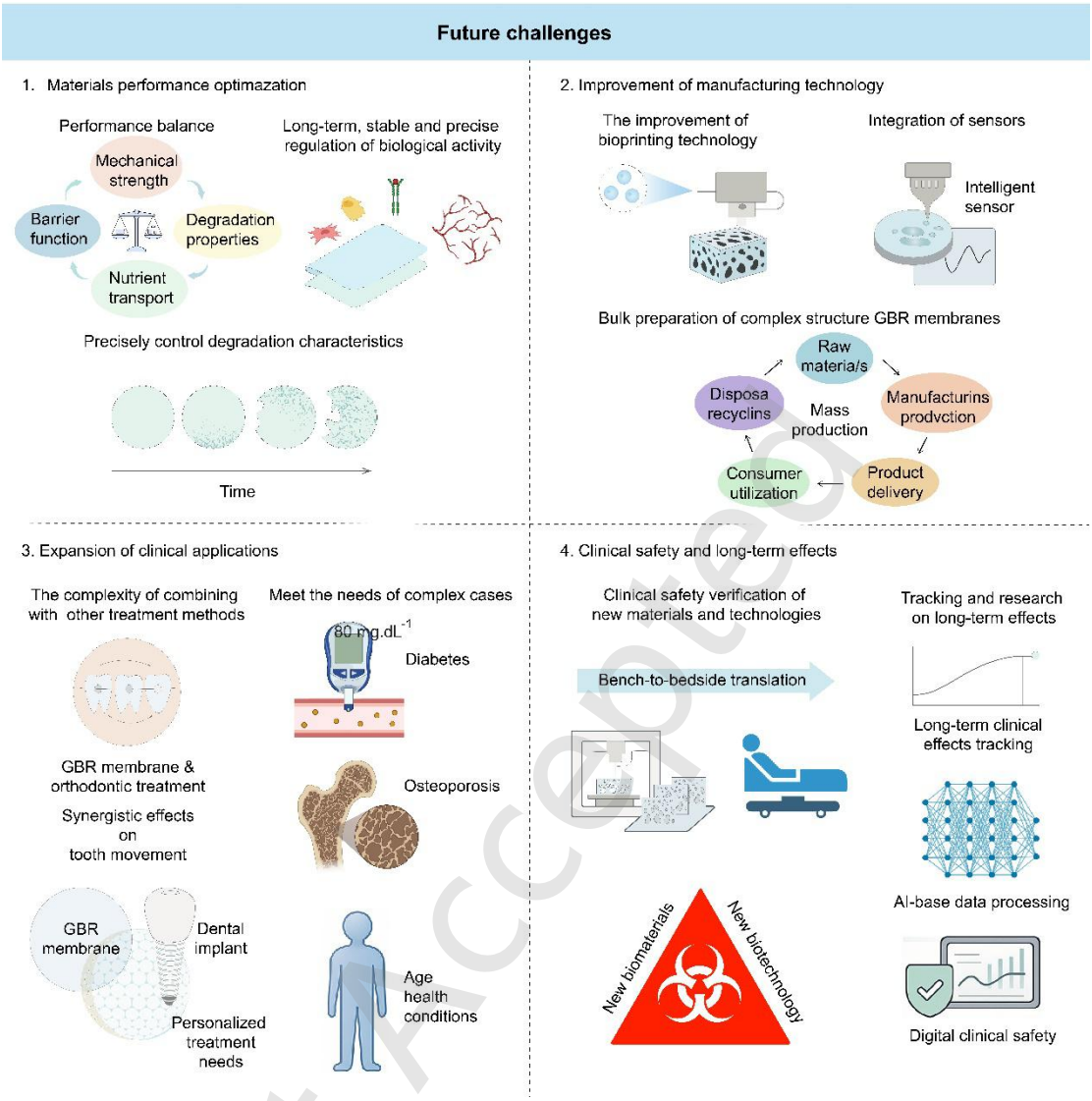

Figure 13 The challenges that GBR membranes will face in the future.

6 Conclusions

GBR membranes are transitioning from passive physical barriers to active, intelligent therapeutic platforms. While natural and synthetic polymers remain clinical staples due to their biocompatibility and tunable degradation, BMs (Mg, Zn) are emerging as superior alternatives, offering excellent space maintenance without the need for secondary surgery. Future advancements lie in fourth-generation intelligent membranes that integrate flexible sensors and AI for real-time postoperative monitoring and treatment. Despite challenges in balancing mechanical strength with degradation kinetics, mass production, and clinical safety, these interdisciplinary innovations pave the way for personalized, predictable, and precise bone tissue engineering.

Data availability

Not applicable.

Acknowledgements

The authors acknowledge funding from National Key Research and Development Project (2023YFC2416800), Medicine-Engineering Interdisciplinary Project of Shanghai Xuhui District Dental Center (No. SHXYFYG202305), Shanghai Pujiang Program (No. 23PJ1400500), Donghua University Young Teachers Scientific Research Startup Fund Project (No. 117-07-0053014).

Declaration of competing interest

All the contributing author(s) report(s) no conflict of interests in this work.

Author contribution statement

J. H. N., T. T. C. and X. N. Z. conceived the review's theme and framework and designed the review's structural content. J. H. N., Z. Z. and W. H. W supervised the review writing process. J. H. N., X. G., C. X. W., N. Z. W., and J. L. collected most of the literature materials, and performed data analysis. X. Y. G. and L. Z. provided technical expertise in relevant fields and assisted in revising the review. T. T. C and X. N. Z provided funding acquisition. All authors participated in the review discussions and examined and revised the final manuscript. All the authors have approved the final manuscript.

Informed consent

Not applicable.

Ethics statement

Not applicable.

Use of AI statement

None.

References

[1] Hong, D. G. K.; Oh, J.-H. Recent advances in dental implants. *Maxillofacial plastic and reconstructive surgery* **2017**; *39*, 1–10.

[2] Silva, R. C., Agrelli, A., Andrade, A. N., Mendes-Marques, C. L., Arruda, I. R., Santos, L. R., Vasconcelos, N. F.,Machado, G. Titanium dental implants: an overview of applied nanobiotechnology to improve biocompatibility and prevent infections. *Materials* **2022**; *15*(9), 3150.

[3] Rupp, F., Liang, L., Geis-Gerstorfer, J., Scheideler, L.,Hüttig, F. Surface characteristics of dental implants: A review. *Dental materials* **2018**; *34*(1), 40–57.

[4] Aghaloo, T. L.; Moy, P. K. Which hard tissue augmentation techniques are the most successful in furnishing bony support for implant placement? *International Journal of Oral & Maxillofacial Implants* **2007**; *22*(7)

[5] Mcallister, B. S.; Haghighat, K. Bone augmentation techniques. *Journal of periodontology* **2007**; *78*(3), 377–396.

[6] Elgali, I., Omar, O., Dahlin, C.,Thomsen, P. Guided bone regeneration: materials and biological mechanisms revisited. *European journal of oral sciences* **2017**; *125*(5), 315–337.

[7] Wang, B., Feng, C., Liu, Y., Mi, F.,Dong, J. Recent advances in biofunctional guided bone regeneration materials for repairing defective alveolar and maxillofacial bone: A review. *Japanese Dental Science Review* **2022**; *58*, 233–248.

[8] Retzepi, M.; Donos, N. Guided bone regeneration: biological principle and therapeutic applications. *Clinical oral implants research* **2010**; *21*(6), 567–576.

[9] Omar, O., Elgali, I., Dahlin, C.,Thomsen, P. Barrier membranes: More than the barrier effect? *Journal of Clinical Periodontology* **2019**; *46*, 103–123.

[10] Mizraji, G., Davidzohn, A., Gursoy, M., Gursoy, U. K., Shapira, L.,Wilensky, A. Membrane barriers for guided bone regeneration: An overview of available biomaterials. *Periodontology 2000* **2023**; *93*(1), 56–76.

[11] Bee, S. L.; Hamid, Z. a. A. Asymmetric resorbable ‐ based dental barrier membrane for periodontal guided tissue regeneration and guided bone regeneration: A review. *Journal of Biomedical Materials Research Part B: Applied Biomaterials* **2022**; *110*(9), 2157–2182.

[12] Ren, Y., Fan, L., Alkildani, S., Liu, L., Emmert, S., Najman, S., Rimashevskiy, D., Schnettler, R., Jung, O.,Xiong, X. Barrier membranes for guided bone regeneration (GBR): a focus on recent advances in collagen membranes. *International journal of molecular sciences* **2022**; *23*(23), 14987.

[13] Kim, K., Su, Y., Kucine, A. J., Cheng, K.,Zhu, D. Guided bone regeneration using barrier membrane in dental applications. *ACS Biomaterials Science & Engineering* **2023**; *9*(10), 5457–5478.

[14] Filipowska, J., Tomaszewski, K. A., Niedźwiedzki, Ł., Walocha, J. A.,Niedźwiedzki, T. The role of vasculature in bone development, regeneration and proper systemic functioning. *Angiogenesis* **2017**; *20*, 291–302.

[15] Garcia, J., Dodge, A., Luepke, P., Wang, H. L., Kapila, Y.,Lin, G. H. Effect of membrane exposure on guided bone regeneration: A systematic review and meta ‐ analysis. *Clinical oral implants research* **2018**; *29*(3), 328–338.

[16] Fontana, F., Maschera, E., Rocchietta, I.,Simion, M. Clinical classification of complications in guided bone regeneration procedures by means of a nonresorbable membrane. *International Journal of Periodontics and Restorative Dentistry* **2011**; *31*(3), 265.

[17] Tay, J. R. H., Lu, X. J., Lai, W. M. C.,Fu, J.-H. Clinical and histological sequelae of surgical complications in horizontal guided bone regeneration: a systematic review and proposal for management. *International journal of implant dentistry* **2020**; *6*(1), 76.

[18] Yang, Z., Wu, C., Shi, H., Luo, X., Sun, H., Wang, Q.,Zhang, D. Advances in barrier membranes for guided bone regeneration techniques. *Frontiers in bioengineering and biotechnology* **2022**; *10*, 921576.

[19] Stoecklin-Wasmer, C., Rutjes, A., Da Costa, B., Salvi, G., Jüni, P.,Sculean, A. Absorbable collagen membranes for periodontal regeneration: a systematic review. *Journal of dental research* **2013**; *92*(9), 773–781.

[20] Soldatos, N. K., Stylianou, P., Koidou, V. P., Angelov, N., Yukna, R.,Romanos, G. E. Limitations and options using resorbable versus nonresorbable membranes for successful guided bone regeneration. *Quintessence International* **2017**; *48*(2)

[21] Nair, L. S.; Laurencin, C. T. Biodegradable polymers as biomaterials. *Progress in polymer science* **2007**; *32*(8-9), 762–798.

[22] Gao, Y., Wang, S., Shi, B., Wang, Y., Chen, Y., Wang, X., Lee, E.-S.,Jiang, H.-B. Advances in modification methods based on biodegradable membranes in guided bone/tissue regeneration: a review. *Polymers* **2022**; *14*(5), 871.

[23] Abtahi, S., Chen, X., Shahabi, S.,Nasiri, N. Resorbable membranes for guided bone regeneration: critical features, potentials, and limitations. *ACS Materials Au* **2023**; *3*(5), 394–417.

[24] Bhatia, S., *Natural polymers vs synthetic polymer*, in *Natural polymer drug delivery systems: nanoparticles, plants, and algae*. 2016, Springer. p. 95–118.

[25] Dang, J. M.; Leong, K. W. Natural polymers for gene delivery and tissue engineering. *Advanced drug delivery reviews* **2006**; *58*(4), 487–499.

[26] Guo, L., Liang, Z., Yang, L., Du, W., Yu, T., Tang, H., Li, C.,Qiu, H. The role of natural polymers in bone tissue engineering. *Journal of Controlled Release* **2021**; *338*, 571–582.

[27] Bunyaratavej, P.; Wang, H. L. Collagen membranes: a review. *Journal of periodontology* **2001**; *72*(2), 215–229.

[28] Sbricoli, L., Guazzo, R., Annunziata, M., Gobbato, L., Bressan, E.,Nastri, L. Selection of collagen membranes for bone regeneration: A literature review. *Materials* **2020**; *13*(3), 786.

[29] Schlegel, A., Möhler, H., Busch, F.,Mehl, A. Preclinical and clinical studies of a collagen membrane (Bio-Gide®). *Biomaterials* **1997**; *18*(7), 535–538.

[30] Baek, S.-H., Yang, B.-E., Park, S.-Y., On, S.-W., Ahn, K.-M.,Byun, S.-H. Efficacy of Cross-Linked Collagen Membranes for Bone Regeneration: In Vitro and Clinical Studies. *Bioengineering* **2025**; *12*(8), 876.

[31] Bouguezzi, A., Debibi, A., Chokri, A., Sioud, S., Hentati, H.,Selmi, J. Cross-linked versus natural collagen membrane for guided bone regeneration? A literature review. *American Journal of Medical and Biological Research* **2020**; *8*(1), 12–16.

[32] Wu, W., Li, B., Liu, Y., Wang, X.,Tang, L. Effect of multilaminate small intestinal submucosa as a barrier membrane on bone formation in a rabbit mandible defect model. *BioMed Research International* **2018**; *2018*(1), 3270293.

[33] Allan, B., Ruan, R., Landao-Bassonga, E., Gillman, N., Wang, T., Gao, J., Ruan, Y., Xu, Y., Lee, C.,Goonewardene, M. Collagen membrane for guided bone regeneration in dental and orthopedic applications. *Tissue Engineering Part A* **2021**; *27*(5-6), 372–381.

[34] Jiménez García, J., Berghezan, S., Caramês, J. M. M., Dard, M.,Marques, D. Effect of cross‐linked vs non‐cross‐linked collagen membranes on bone: a systematic review. *Journal of Periodontal Research* **2017**; *52*(6), 955–964.

[35] Adamiak, K.; Sionkowska, A. Current methods of collagen cross-linking. *International Journal of Biological Macromolecules* **2020**; *161*, 550–560.

[36] Gu, L., Shan, T., Ma, Y.-X., Tay, F. R.,Niu, L. Novel biomedical applications of crosslinked collagen. *Trends in biotechnology* **2019**; *37*(5), 464–491.

[37] Yang, F., Yang, D., Tu, J., Zheng, Q., Cai, L.,Wang, L. Strontium enhances osteogenic differentiation of mesenchymal stem cells and in vivo bone formation by activating Wnt/catenin signaling. *Stem cells* **2011**; *29*(6), 981–991.

[38] Mao, L., Xia, L., Chang, J., Liu, J., Jiang, L., Wu, C.,Fang, B. The synergistic effects of Sr and Si bioactive ions on osteogenesis, osteoclastogenesis and angiogenesis for osteoporotic bone regeneration. *Acta biomaterialia* **2017**; *61*, 217–232.

[39] Saha, S., Costa, R. C., Silva, M. C., Fonseca-Santos, J. M., Chen, L., Phakatkar, A. H., Bhatia, H., Faverani, L. P., Barão, V. A.,Shokuhfar, T. Collagen membrane functionalized with magnesium oxide via room-temperature atomic layer deposition promotes osteopromotive and antimicrobial properties. *Bioactive materials* **2023**; *30*, 46–61.

[40] Peng, F., Zhang, X., Wang, Y., Zhao, R., Cao, Z., Chen, S., Ruan, Y., Wu, J., Song, T.,Qiu, Z. Guided bone regeneration in long-bone defect with a bilayer mineralized collagen membrane. *Collagen and Leather* **2023**; *5*(1), 36.

[41] Li, M., Cheng, G., Xiao, S., Jiang, B., Guo, S.,Ding, Y. Biomimetic Mineralized Hydroxyapatite–Fish-Scale Collagen/Chitosan Nanofibrous Membranes Promote Osteogenesis for Periodontal Tissue Regeneration. *ACS Biomaterials Science & Engineering* **2024**; *10*(8), 5108–5121.

[42] Zhao, Y., Sun, W., Wu, X., Gao, X., Song, F., Duan, B., Lu, A., Yang, H.,Huang, C. Janus membrane with intrafibrillarly strontium-apatite-mineralized collagen for guided bone regeneration. *ACS nano* **2024**; *18*(9), 7204–7222.

[43] Chu, C., Liu, L., Wang, Y., Wei, S., Wang, Y., Man, Y.,Qu, Y. Macrophage phenotype in the epigallocatechin‐3‐gallate (EGCG)‐modified collagen determines foreign body reaction. *Journal of Tissue Engineering and Regenerative Medicine* **2018**; *12*(6), 1499–1507.

[44] Chu, C., Wang, Y., Wang, Y., Yang, R., Liu, L., Rung, S., Xiang, L., Wu, Y., Du, S.,Man, Y. Evaluation of epigallocatechin-3-gallate (EGCG) modified collagen in guided bone regeneration (GBR) surgery and modulation of macrophage phenotype. *Materials Science and Engineering: C* **2019**; *99*, 73–82.

[45] Chu, C., Rung, S., Yang, R., Man, Y.,Qu, Y. Application of EGCG modified EDC/NHS cross-linked extracellular matrix to promote macrophage adhesion. *bioRxiv* **2020**, 2020.2010. 2003.325068.

[46] Rung, S., Zhao, X., Chu, C., Yang, R., Qu, Y.,Man, Y. Application of epigallocatechin-3-gallate (EGCG) modified 1-ethyl-3-(3-dimethylaminopropylcarbodiimide hydrochloride/N-hydroxy-succinimide (EDC/NHS) cross-linked collagen membrane to promote macrophage adhesion. *Materials* **2021**; *14*(16), 4660.

[47] Takallu, S., Mirzaei, E., Zakeri Bazmandeh, A., Ghaderi Jafarbeigloo, H. R.,Khorshidi, H. Addressing antimicrobial properties in guided tissue/bone regeneration membrane: enhancing effectiveness in periodontitis treatment. *ACS Infectious Diseases* **2024**; *10*(3), 779–807.

[48] Chen, E., Wang, T., Sun, Z., Gu, Z., Xiao, S.,Ding, Y. Polyphenols-based intelligent oral barrier membranes for periodontal bone defect reconstruction. *Regenerative biomaterials* **2024**; *11*, rbae058.

[49] Yang, D., Xu, Z., Huang, D., Luo, Q., Zhang, C., Guo, J., Tan, L., Ge, L., Mu, C.,Li, D. Immunomodulatory multifunctional janus collagen-based membrane for advanced bone regeneration. *Nature Communications* **2025**; *16*(1), 4264.

[50] Gómez-Guillén, M., Giménez, B., López-Caballero, M. A.,Montero, M. Functional and bioactive properties of collagen and gelatin from alternative sources: A review. *Food hydrocolloids* **2011**; *25*(8), 1813–1827.

[51] Alipal, J., Pu'ad, N. M., Lee, T., Nayan, N., Sahari, N., Basri, H., Idris, M.,Abdullah, H. A review of gelatin: Properties, sources, process, applications, and commercialisation. *Materials Today: Proceedings* **2021**; *42*, 240–250.

[52] Hu, X., He, Y., Tong, Y., Sun, N., Ma, G., Liu, H.,Kou, N. Fabrication and characterization of a multi-functional GBR membrane of gelatin-chitosan for osteogenesis and angiogenesis. *International journal of biological macromolecules* **2024**; *266*, 130978.

[53] Chang, K.-H., Wei, J.-J., Lan, G.-Y., Lin, Y.-K., Lin, Y.-T., Chen, T.-C.,Yu, J. Minimally Invasive, High Transmittance, Adhesive and Antioxidative Hydrogel Complex for Treatments of Both Optic Neuropathy and Retinopathy. *Advanced healthcare materials*, e2501583.

[54] Wang, Q., Feng, Y., He, M., Zhao, W., Qiu, L.,Zhao, C. A hierarchical janus nanofibrous membrane combining direct osteogenesis and osteoimmunomodulatory functions for advanced bone regeneration. *Advanced Functional Materials* **2021**; *31*(8), 2008906.

[55] Jin, M., Hou, Y.,Kang, F. Polydopamine-Coated Copper-Doped Mesoporous Silica/Gelatin–Waterborne Polyurethane Composite: A Multifunctional GBR Membrane Bone Defect Repair. *Journal of Functional Biomaterials* **2025**; *16*(4), 122.

[56] Kim, M. H., Chalisserry, E. P., Mondal, S., Oh, J.,Nam, S. Y. Silicon-substituted hydroxyapatite reinforced 3D printed gelatin membrane for guided bone regeneration. *Materials Letters* **2021**; *304*, 130670.

[57] Han, Q., Zhao, D., Wang, X., Shang, M., Zhou, W., Li, Q.,Song, H. Composite barrier membrane for bone regeneration: advancing biomaterial strategies in defect repair. *RSC advances* **2025**; *15*(2), 1290–1299.

[58] Kamaci, Ö., Yücel, N., Köten, H., Bulus, E.,Bulus, G. A Review polylactic acid and gelatin biomaterial GBR (Guided Bone Regeneration) and multilayer GBR membranes. *Politeknik Dergisi* **2023**, 1–1.

[59] Yuan, S., Chen, Q., Guo, M., Xu, Y., Wang, W.,Li, Z. Fabrication of Bioresorbable Barrier Membranes from Gelatin/Poly (4‐Hydroxybutyrate)(P4HB). *Macromolecular Bioscience* **2024**; *24*(8), 2400036.

[60] Qin, X., Pan, H., Yang, K., Xie, W., Yang, G.,Wang, J. Biodegradable and biocompatible alginate/gelatin/MXene composite membrane with efficient osteogenic activity and its application in guided bone regeneration. *Journal of Biomaterials Science, Polymer Edition* **2023**; *34*(13), 1843–1857.

[61] Jin, M., Hou, Y.,Kang, F. Polydopamine-Coated Copper-Doped Mesoporous Silica/Gelatin–Waterborne Polyurethane Composite: A Multifunctional GBR Membrane for Bone Defect Repair. *Journal of Functional Biomaterials* **2025**; *16*(4), 122.

[62] Kim, Y., Zharkinbekov, Z., Raziyeva, K., Tabyldiyeva, L., Berikova, K., Zhumagul, D., Temirkhanova, K.,Saparov, A. Chitosan-based biomaterials for tissue regeneration. *Pharmaceutics* **2023**; *15*(3), 807.

[63] Dash, M., Chiellini, F., Ottenbrite, R. M.,Chiellini, E. Chitosan—A versatile semi-synthetic polymer in biomedical applications. *Progress in polymer science* **2011**; *36*(8), 981–1014.

[64] Bee, S.-L.; Hamid, Z. a. A. Chitosan-based dental barrier membrane for periodontal guided tissue regeneration and guided bone regeneration: A review. *International Journal of Biological Macromolecules* **2025**, 139504.

[65] Xu, C., Lei, C., Meng, L., Wang, C.,Song, Y. Chitosan as a barrier membrane material in periodontal tissue regeneration. *Journal of Biomedical Materials Research Part B: Applied Biomaterials* **2012**; *100*(5), 1435–1443.

[66] Xiaojie, X., Jinbing, C., Yiling, C., Jingjing, S., Yuan, L., Yu, P., Hao, Y.,Hui, C. A photo-thermal dual crosslinked chitosan-based hydrogel membrane for guided bone regeneration. *International Journal of Biological Macromolecules* **2025**; *296*, 139712.

[67] Gümüşderelioğlu, M., Sunal, E., Tolga Demirtaş, T.,Kiremitçi, A. S. Chitosan-based double-faced barrier membrane coated with functional nanostructures and loaded with BMP-6. *Journal of Materials Science: Materials in Medicine* **2020**; *31*(1), 4.

[68] Bhardwaj, N.; Kundu, S. C. Silk fibroin protein and chitosan polyelectrolyte complex porous scaffolds for tissue engineering applications. *Carbohydrate polymers* **2011**; *85*(2), 325–333.

[69] Cai, Y., Guo, J., Chen, C., Yao, C., Chung, S.-M., Yao, J., Lee, I.-S.,Kong, X. Silk fibroin membrane used for guided bone tissue regeneration. *Materials Science and Engineering: C* **2017**; *70*, 148–154.

[70] Ho, T.-C., Chang, C.-C., Chan, H.-P., Chung, T.-W., Shu, C.-W., Chuang, K.-P., Duh, T.-H., Yang, M.-H.,Tyan, Y.-C. Hydrogels: properties and applications in biomedicine. *Molecules* **2022**; *27*(9), 2902.

[71] Dong, S., An, S., Saiding, Q., Chen, Q., Liu, B., Kong, N., Chen, W.,Tao, W. Therapeutic Hydrogels: Properties and Biomedical Applications. *Chemical Reviews* **2025**; *125*(18), 8835–8920.

[72] Xu, J., Xia, Y., Song, H., Wang, L., Zhang, X., Lian, J., Zhang, Y., Li, X., Li, Y.,Kang, J. Electrospun the oriented silk fibroin/bioactive glass@ silk fibroin/polycaprolactone composite bi-layered membranes for guided bone regeneration. *Colloids and Surfaces A: Physicochemical and Engineering Aspects* **2023**; *676*, 132224.

[73] Atila, D., Gurses, S.,Tezcaner, A. Self-composite silk fibroin membranes for guided bone regeneration: 1 material 3 architectures with intrinsic integrity. *Materials Today Communications* **2024**; *39*, 109215.

[74] Xiang, J., Li, Y., Ren, M., He, P., Liu, F., Jing, Z., Li, Y., Zhang, H., Ji, P.,Yang, S. Sandwich-like nanocomposite electrospun silk fibroin membrane to promote osteogenesis and antibacterial activities. *Applied Materials Today* **2022**; *26*, 101273.

[75] Chen, W., Liu, K., Liao, X., Wu, J., Chen, L., Yang, Z., Wang, X., Liao, Y., Fu, G.,Yang, X. Harmonizing thickness and permeability in bone tissue engineering: A novel silk fibroin membrane inspired by spider silk dynamics. *Advanced Materials* **2024**; *36*(13), 2310697.

[76] Wu, M., Han, Z., Liu, W., Yao, J., Zhao, B., Shao, Z.,Chen, X. Silk-based hybrid microfibrous mats as guided bone regeneration membranes. *Journal of Materials Chemistry B* **2021**; *9*(8), 2025–2032.

[77] Li, B., Chen, Y., He, J., Shu, Y., Yang, H., Liu, J., Zhang, C., Xiao, W., Liu, Z.,Liao, X. Silk fibroin/methacrylated gelatine/hydroxyapatite biomimetic nanofibrous membranes for guided bone regeneration. *International Journal of Biological Macromolecules* **2024**; *263*, 130380.

[78] Wang, Y., Yang, Z., Chen, X., Jiang, X.,Fu, G. Silk fibroin hydrogel membranes prepared by a sequential cross-linking strategy for guided bone regeneration. *Journal of the Mechanical Behavior of Biomedical Materials* **2023**; *147*, 106133.

[79] Chen, L., Yu, L., Qi, L., Eichhorn, S. J., Isogai, A., Lizundia, E., Zhu, J.,Chen, C. Cellulose nanocomposites by supramolecular chemistry engineering. *Nature Reviews Materials* **2025**, 1–22.

[80] Saska, S., Pigossi, S. C., Oliveira, G. J., Teixeira, L. N., Capela, M. V., Gonçalves, A., De Oliveira, P. T., Messaddeq, Y., Ribeiro, S. J.,Gaspar, A. M. M. Biopolymer-based membranes associated with osteogenic growth peptide for guided bone regeneration. *Biomedical Materials* **2018**; *13*(3), 035009.

[81] Luz, E. P. C. G., Das Chagas, B. S., De Almeida, N. T., De Fátima Borges, M., Andrade, F. K., Muniz, C. R., Castro-Silva, I. I., Teixeira, E. H., Popat, K.,De Freitas Rosa, M. Resorbable bacterial cellulose membranes with strontium release for guided bone regeneration. *Materials Science and Engineering: C* **2020**; *116*, 111175.

[82] Kraisuriyawong, P., Kornsuthisopon, C., Pavasant, P., Rattanapisit, K., Phoolcharoen, W.,Hoven, V. P. Functionalizable bacterial cellulose composite membrane for guided tissue regeneration. *International Journal of Biological Macromolecules* **2024**; *268*, 131655.

[83] Wu, S., Luo, S., Cen, Z., Li, Q., Li, L., Li, W., Huang, Z., He, W., Liang, G.,Wu, D. All-in-one porous membrane enables full protection in guided bone regeneration. *Nature Communications* **2024**; *15*(1), 119.

[84] Zhou, H., Zhao, Y., Zha, X., Zhang, Z., Zhang, L., Wu, Y., Ren, R., Zhao, Z., Yang, W.,Zhao, L. A Janus, robust, biodegradable bacterial cellulose/Ti3C2Tx MXene bilayer membranes for guided bone regeneration. *Biomaterials Advances* **2024**; *161*, 213892.

[85] Yang, J.-S., Xie, Y.-J.,He, W. Research progress on chemical modification of alginate: A review. *Carbohydrate polymers* **2011**; *84*(1), 33–39.

[86] Hurtado, A., Aljabali, A. A., Mishra, V., Tambuwala, M. M.,Serrano-Aroca, Á. Alginate: Enhancement strategies for advanced applications. *International Journal of Molecular Sciences* **2022**; *23*(9), 4486.

[87] Joo, G., Park, M., Park, S.-S., Tripathi, G.,Lee, B.-T. Tailored alginate/PCL-gelatin-β-TCP membrane for guided bone regeneration. *Biomedical Materials* **2022**; *17*(4), 045011.

[88] Xie, J., Cao, Q.,Zheng, X. Preparation and antibacterial properties of ceftazidime-loaded polycaprolactone coating/nano-lithium magnesium silicate-doped bioactive glass three-dimensional scaffolds. *Materials and Technology* **2025**; *59*(3), 383–390–383–390.

[89] Kishen, A., Cecil, A.,Chitra, S. Fabrication of hydroxyapatite reinforced polymeric hydrogel membrane for regeneration. *The Saudi Dental Journal* **2023**; *35*(6), 678–683.

[90] Assadi, Z., Rezvanian, P., Gounani, Z., Ejeian, F., Zarrabi, A.,Masaeli, E. Multilayered nanocomposite membrane orchestrating targeted dual release strategies for enhanced guided bone regeneration. *Chemical Engineering Journal* **2024**; *484*, 149237.

[91] Qin, X., Lei, S., Yang, K., Xie, W.,Wang, J. Green synthetic sodium alginate-glycerol-MXene nanocomposite membrane with excellent flexibility and mineralization ability for guided bone regeneration. *Journal of the Mechanical Behavior of Biomedical Materials* **2024**; *150*, 106336.

[92] Zarrintaj, P., Manouchehri, S., Ahmadi, Z., Saeb, M. R., Urbanska, A. M., Kaplan, D. L.,Mozafari, M. Agarose-based biomaterials for tissue engineering. *Carbohydrate polymers* **2018**; *187*, 66–84.

[93] Salati, M. A., Khazai, J., Tahmuri, A. M., Samadi, A., Taghizadeh, A., Taghizadeh, M., Zarrintaj, P., Ramsey, J. D., Habibzadeh, S.,Seidi, F. Agarose-based biomaterials: opportunities and challenges in cartilage tissue engineering. *Polymers* **2020**; *12*(5), 1150.

[94] Peña, C., Castillo, T., García, A., Millán, M.,Segura, D. Biotechnological strategies to improve production of microbial poly‐(3‐hydroxybutyrate): a review of recent research work. *Microbial biotechnology* **2014**; *7*(4), 278–293.

[95] Sadi, R. K., Fechine, G. J.,Demarquette, N. R. Photodegradation of poly (3-hydroxybutyrate). *Polymer Degradation and Stability* **2010**; *95*(12), 2318–2327.

[96] Suwantong, O., Waleetorncheepsawat, S., Sanchavanakit, N., Pavasant, P., Cheepsunthorn, P., Bunaprasert, T.,Supaphol, P. In vitro biocompatibility of electrospun poly (3-hydroxybutyrate) and poly (3-hydroxybutyrate-co-3-hydroxyvalerate) fiber mats. *International Journal of Biological Macromolecules* **2007**; *40*(3), 217–223.

[97] Ramier, J., Bouderlique, T., Stoilova, O., Manolova, N., Rashkov, I., Langlois, V., Renard, E., Albanese, P.,Grande, D. Biocomposite scaffolds based on electrospun poly (3-hydroxybutyrate) nanofibers and electrosprayed hydroxyapatite nanoparticles for bone tissue engineering applications. *Materials Science and Engineering: C* **2014**; *38*, 161–169.

[98] Salvatore, L., Carofiglio, V. E., Stufano, P., Bonfrate, V., Calò, E., Scarlino, S., Nitti, P., Centrone, D., Cascione, M.,Leporatti, S. Potential of electrospun poly (3‐hydroxybutyrate)/collagen blends for tissue engineering applications. *Journal of healthcare engineering* **2018**; *2018*(1), 6573947.

[99] Shumilova, A., Myltygashev, M., Kirichenko, A., Nikolaeva, E., Volova, T.,Shishatskaya, E. Porous 3D implants of degradable poly‐3‐hydroxybutyrate used to enhance regeneration of rat cranial defect. *Journal of Biomedical Materials Research Part A* **2017**; *105*(2), 566–577.

[100] Sanhueza, C., Pavéz, M., Hermosilla, J., Rocha, S., Valdivia-Gandur, I., Manzanares, M.-C., Beltrán, V.,Acevedo, F. Poly-3-hydroxybutyrate-silver nanoparticles membranes as advanced antibiofilm strategies for combatting peri-implantitis. *International Journal of Biological Macromolecules* **2024**; *269*, 131974.

[101] Abatangelo, G., Vindigni, V., Avruscio, G., Pandis, L.,Brun, P. Hyaluronic acid: redefining its role. *Cells* **2020**; *9*(7), 1743.

[102] E Silva, E. C., Omonte, S. V., Martins, A. G. V., De Castro, H. H. O., Gomes, H. E., Zenóbio, É. G., De Oliveira, P. a. D., Horta, M. C. R.,Souza, P. E. A. Hyaluronic acid on collagen membranes: An experimental study in rats. *Archives of Oral Biology* **2017**; *73*, 214–222.

[103] Özan, F., Şençimen, M., Gülses, A.,Ayna, M., *Guided bone regeneration technique using hyaluronic acid in oral implantology*, in *A Textbook of Advanced Oral and Maxillofacial Surgery Volume 3*. 2016, IntechOpen.

[104] Park, J. K., Yeom, J., Oh, E. J., Reddy, M., Kim, J. Y., Cho, D.-W., Lim, H. P., Kim, N. S., Park, S. W.,Shin, H.-I. Guided bone regeneration by poly (lactic-co-glycolic acid) grafted hyaluronic acid bi-layer films for periodontal barrier applications. *Acta Biomaterialia* **2009**; *5*(9), 3394–3403.

[105] Ayanoğlu, S., Esenyel, C. Z., Adanır, O., Dedeoğlu, S., Imren, Y.,Esen, T. Effects of hyaluronic acid (Hyalonect) on callus formation in rabbits. *Acta Orthop Traumatol Turc* **2015**; *49*(3), 319–325.

[106] Chang, K.-C., Lin, D.-J., Wu, Y.-R., Chang, C.-W., Chen, C.-H., Ko, C.-L.,Chen, W.-C. Characterization of genipin-crosslinked gelatin/hyaluronic acid-based hydrogel membranes and loaded with hinokitiol: In vitro evaluation of antibacterial activity and biocompatibility. *Materials Science and Engineering: C* **2019**; *105*, 110074.

[107] Cheah, C. W., Al-Namnam, N. M., Lau, M. N., Lim, G. S., Raman, R., Fairbairn, P.,Ngeow, W. C. Synthetic material for bone, periodontal, and dental tissue regeneration: where are we now, and where are we heading next? *Materials* **2021**; *14*(20), 6123.

[108] Mir, M., Ali, M. N., Barakullah, A., Gulzar, A., Arshad, M., Fatima, S.,Asad, M. Synthetic polymeric biomaterials for wound healing: a review. *Progress in biomaterials* **2018**; *7*(1), 1–21.

[109] Sionkowska, A. Current research on the blends of natural and synthetic polymers as new biomaterials. *Progress in polymer science* **2011**; *36*(9), 1254–1276.

[110] Sheikh, Z., Hamdan, N., Ikeda, Y., Grynpas, M., Ganss, B.,Glogauer, M. Natural graft tissues and synthetic biomaterials for periodontal and alveolar bone reconstructive applications: a review. *Biomaterials research* **2017**; *21*(1), 9.

[111] Taib, N.-a. a. B., Rahman, M. R., Huda, D., Kuok, K. K., Hamdan, S., Bakri, M. K. B., Julaihi, M. R. M. B.,Khan, A. A review on poly lactic acid (PLA) as a biodegradable polymer. *Polymer Bulletin* **2023**; *80*(2), 1179–1213.

[112] Capuana, E., Lopresti, F., Ceraulo, M.,La Carrubba, V. Poly-l-lactic acid (PLLA)-based biomaterials for regenerative medicine: a review on processing and applications. *Polymers* **2022**; *14*(6), 1153.

[113] Zhu, H., Feng, X., Zhang, H., Guo, Y., Zhang, J.,Chen, J. Structural characteristics and properties of silk fibroin/poly (lactic acid) blend films. *Journal of Biomaterials Science, Polymer Edition* **2009**; *20*(9), 1259–1274.

[114] Bergström, J. S.; Hayman, D. An overview of mechanical properties and material modeling of polylactide (PLA) for medical applications. *Annals of biomedical engineering* **2016**; *44*(2), 330–340.

[115] More, N., Avhad, M., Utekar, S.,More, A. Polylactic acid (PLA) membrane—significance, synthesis, and applications: a review. *Polymer bulletin* **2023**; *80*(2), 1117–1153.

[116] Zhu, Y., Zhang, X., Chang, G., Deng, S.,Chan, H. F. Bioactive glass in tissue regeneration: Unveiling recent advances in regenerative strategies and applications. *Advanced Materials* **2025**; *37*(2), 2312964.

[117] Liu, S., Yang, H., Zhang, L., Bianco, A., Ma, B.,Ge, S. Multifunctional barrier membranes promote bone regeneration by scavenging H2O2, generating O2, eliminating inflammation, and regulating immune response. *Colloids and Surfaces B: Biointerfaces* **2023**; *222*, 113147.

[118] Zhang, Y., Chen, Y., Ding, T., Zhang, Y., Yang, D., Zhao, Y., Liu, J., Ma, B., Bianco, A.,Ge, S. Janus porous polylactic acid membranes with versatile metal–phenolic interface for biomimetic periodontal bone regeneration. *NPJ Regenerative medicine* **2023**; *8*(1), 28.

[119] Shakeri, H., Nazarpak, M. H., Imani, R.,Tayebi, L. Poly (l-lactic acid)-based modified nanofibrous membrane with dual drug release capability for GBR application. *International journal of biological macromolecules* **2023**; *231*, 123201.

[120] Rota, I., Bertolo, D.,Gastaldi, D. Printing fidelity assessment and micro-mechanical characterization of FDM-printed PLA/HA composite for maxillofacial and oral applications. *Journal of the Mechanical Behavior of Biomedical Materials* **2025**; *168*, 106987.

[121] Zhang, H. Y., Jiang, H. B., Ryu, J.-H., Kang, H., Kim, K.-M.,Kwon, J.-S. Comparing properties of variable pore-sized 3D-printed PLA membrane with conventional PLA membrane for guided bone/tissue regeneration. *Materials* **2019**; *12*(10), 1718.

[122] Petposri, S., Thuaksuban, N., Buranadham, S., Suwanrat, T., Punyodom, W.,Supphaprasitt, W. Physical characteristics and biocompatibility of 3D-printed polylactic-co-glycolic acid membranes used for guided bone regeneration. *Journal of Functional Biomaterials* **2023**; *14*(5), 275.

[123] Wang, J., Chen, W., Huang, M., Zhong, Z., Wang, P.,Wu, R. Comparative analysis of gelatin/polylactic acid and commercial pla membranes for guided bone regeneration: a randomized clinical trial. *Medical science monitor: international medical journal of experimental and clinical research* **2025**; *31*, e944713.

[124] Gentile, P., Chiono, V., Carmagnola, I.,Hatton, P. V. An overview of poly (lactic-co-glycolic) acid (PLGA)-based biomaterials for bone tissue engineering. *International journal of molecular sciences* **2014**; *15*(3), 3640–3659.

[125] Martins, C., Sousa, F., Araújo, F.,Sarmento, B. Functionalizing PLGA and PLGA derivatives for drug delivery and tissue regeneration applications. *Advanced healthcare materials* **2018**; *7*(1), 1701035.

[126] Jin, S., Xia, X., Huang, J., Yuan, C., Zuo, Y., Li, Y.,Li, J. Recent advances in PLGA-based biomaterials for bone tissue regeneration. *Acta biomaterialia* **2021**; *127*, 56–79.

[127] Wang, Y., Zhang, X., Zhang, S., Yang, G., Li, Y., Mao, Y., Yang, L., Chen, J.,Wang, J. Development of a rapid-shaping and user-friendly membrane with long-lasting space maintenance for guided bone regeneration. *Journal of Materials Chemistry B* **2024**; *12*(6), 1495–1511.

[128] Dos Santos, V. I., Merlini, C., Aragones, Á., Cesca, K.,Fredel, M. C. In vitro evaluation of bilayer membranes of PLGA/hydroxyapatite/β-tricalcium phosphate for guided bone regeneration. *Materials Science and Engineering: C* **2020**; *112*, 110849.

[129] Guo, T., Holzberg, T. R., Lim, C. G., Gao, F., Gargava, A., Trachtenberg, J. E., Mikos, A. G.,Fisher, J. P. 3D printing PLGA: a quantitative examination of the effects of polymer composition and printing parameters on print resolution. *Biofabrication* **2017**; *9*(2), 024101.

[130] Woodruff, M. A.; Hutmacher, D. W. The return of a forgotten polymer—Polycaprolactone in the 21st century. *Progress in polymer science* **2010**; *35*(10), 1217–1256.

[131] Labet, M.; Thielemans, W. Synthesis of polycaprolactone: a review. *Chemical society reviews* **2009**; *38*(12), 3484–3504.

[132] Malikmammadov, E., Tanir, T. E., Kiziltay, A., Hasirci, V.,Hasirci, N. PCL and PCL-based materials in biomedical applications. *Journal of Biomaterials science, Polymer edition* **2018**; *29*(7-9), 863–893.

[133] Moura, N. K. D., Siqueira, I. A., Machado, J. P. D. B., Kido, H. W., Avanzi, I. R., Rennó, A. C. M., Trichês, E. D. S.,Passador, F. R. Production and characterization of porous polymeric membranes of PLA/PCL blends with the addition of hydroxyapatite. *Journal of Composites Science* **2019**; *3*(2), 45.

[134] Shu, Z., Zhang, C., Yan, L., Lei, H., Peng, C., Liu, S., Fan, L.,Chu, Y. Antibacterial and osteoconductive polycaprolactone/polylactic acid/nano-hydroxyapatite/Cu@ ZIF-8 GBR membrane with asymmetric porous structure. *International Journal of Biological Macromolecules* **2023**; *224*, 1040–1051.

[135] Kumar, A., Mir, M., Aldulijan, I., Mahajan, A., Anwar, A., Leon, C. H., Terracciano, A., Zhao, X., Su, T. L.,Kalyon, D. M. Load‐bearing biodegradable PCL‐PGA‐beta TCP scaffolds for bone tissue regeneration. *Journal of Biomedical Materials Research Part B: Applied Biomaterials* **2021**; *109*(2), 193–200.

[136] Wang, W., Huang, B., Byun, J. J.,Bártolo, P. Assessment of PCL/carbon material scaffolds for bone regeneration. *Journal of the mechanical behavior of biomedical materials* **2019**; *93*, 52–60.

[137] Castro, A. G., Diba, M., Kersten, M., Jansen, J. A., Van Den Beucken, J. J.,Yang, F. Development of a PCL-silica nanoparticles composite membrane for guided bone regeneration. *Materials Science and Engineering: C* **2018**; *85*, 154–161.

[138] Xue, J., He, M., Liu, H., Niu, Y., Crawford, A., Coates, P. D., Chen, D., Shi, R.,Zhang, L. Drug loaded homogeneous electrospun PCL/gelatin hybrid nanofiber structures for anti-infective tissue regeneration membranes. *Biomaterials* **2014**; *35*(34), 9395–9405.

[139] Janmohammadi, M.; Nourbakhsh, M. Electrospun polycaprolactone scaffolds for tissue engineering: a review. *International Journal of Polymeric Materials and Polymeric Biomaterials* **2019**; *68*(9), 527–539.

[140] Arif, Z. U., Khalid, M. Y., Noroozi, R., Sadeghianmaryan, A., Jalalvand, M.,Hossain, M. Recent advances in 3D-printed polylactide and polycaprolactone-based biomaterials for tissue engineering applications. *International journal of biological macromolecules* **2022**; *218*, 930–968.

[141] Liu, Y., Du, L., Song, J., Zhang, M., Du, S., Long, W., Song, W., Chang, X.,Li, Z. A 3D printed magnesium ammonium phosphate/polycaprolactone composite membrane for Guided bone regeneration. *Materials & Design* **2024**; *239*, 112733.

[142] Budak, K., Sogut, O.,Aydemir Sezer, U. A review on synthesis and biomedical applications of polyglycolic acid. *Journal of polymer research* **2020**; *27*(8), 208.

[143] Low, Y. J., Andriyana, A., Ang, B. C.,Zainal Abidin, N. I. Bioresorbable and degradable behaviors of PGA: Current state and future prospects. *Polymer Engineering & Science* **2020**; *60*(11), 2657–2675.

[144] Gentile, P., Chiono, V., Tonda‐Turo, C., Ferreira, A. M.,Ciardelli, G. Polymeric membranes for guided bone regeneration. *Biotechnology journal* **2011**; *6*(10), 1187–1197.

[145] Shuai, C., Yang, W., Feng, P., Peng, S.,Pan, H. Accelerated degradation of HAP/PLLA bone scaffold by PGA blending facilitates bioactivity and osteoconductivity. *Bioactive Materials* **2021**; *6*(2), 490–502.

[146] Kim, B. N., Ko, Y.-G., Yeo, T., Kim, E. J., Kwon, O. K.,Kwon, O. H. Guided regeneration of rabbit calvarial defects using silk fibroin nanofiber–poly (glycolic acid) hybrid scaffolds. *ACS Biomaterials Science & Engineering* **2019**; *5*(10), 5266–5272.

[147] Özdemir, J. H., Cinfer, Ş. P.,Hazar, A. B. Y., *Poly (ethylene glycol) based biomaterials*, in *Handbook of Polymers in Medicine*. 2023, Elsevier. p. 219–242.

[148] Shahdad, S., Gamble, E., Matani, J., Zhang, L.,Gambôa, A. Randomized clinical trial comparing PEG‐based synthetic to porcine‐derived collagen membrane in the preservation of alveolar bone following tooth extraction in anterior maxilla. *Clinical Oral Implants Research* **2020**; *31*(10), 1010–1024.

[149] Thoma, D. S., Halg, G. A., Dard, M. M., Seibl, R., Hammerle, C. H.,Jung, R. E. Evaluation of a new biodegradable membrane to prevent gingival ingrowth into mandibular bone defects in minipigs. *Clinical Oral Implants Research* **2009**; *20*(1), 7–16.

[150] Dehnavi, S. S., Mehdikhani, M., Rafienia, M.,Bonakdar, S. Preparation and in vitro evaluation of polycaprolactone/PEG/bioactive glass nanopowders nanocomposite membranes for GTR/GBR applications. *Materials Science and Engineering: C* **2018**; *90*, 236–247.

[151] Pan, P., Wang, J., Wang, X., Yu, X., Chen, T., Jiang, C.,Liu, W. Barrier membrane with Janus function and structure for guided bone regeneration. *ACS Applied Materials & Interfaces* **2024**; *16*(36), 47178–47191.

[152] Türkkan, S., Pazarçeviren, A. E., Keskin, D., Machin, N. E., Duygulu, Ö.,Tezcaner, A. Nanosized CaP-silk fibroin-PCL-PEG-PCL/PCL based bilayer membranes for guided bone regeneration. *Materials Science and Engineering: C* **2017**; *80*, 484–493.

[153] Sun, H., Luan, J.,Dong, S. Hydrogels promote periodontal regeneration. *Frontiers in Bioengineering and Biotechnology* **2024**; *12*, 1411494.

[154] Humber, C. C., Sándor, G., Davis, J. M., Peel, S. A., Brkovic, B. M., Kim, Y. D., Holmes, H. I.,Clokie, C. M. Bone healing with an in situ–formed bioresorbable polyethylene glycol hydrogel membrane in rabbit calvarial defects. *Oral Surgery, Oral Medicine, Oral Pathology, Oral Radiology, and Endodontology* **2010**; *109*(3), 372–384.

[155] Sun, S., Cui, Y., Yuan, B., Dou, M., Wang, G., Xu, H., Wang, J., Yin, W., Wu, D.,Peng, C. Drug delivery systems based on polyethylene glycol hydrogels for enhanced bone regeneration. *Frontiers in bioengineering and biotechnology* **2023**; *11*, 1117647.

[156] Jung, R. E., Mihatovic, I., Cordaro, L., Windisch, P., Friedmann, A., Blanco Carrion, J., Sanz Sanchez, I., Hallman, M., Quirynen, M.,Hammerle, C. H. Comparison of a polyethylene glycol membrane and a collagen membrane for the treatment of bone dehiscence defects at bone level implants—A prospective, randomized, controlled, multicenter clinical trial. *Clinical oral implants research* **2020**; *31*(11), 1105–1115.

[157] Mathews, M. M. Polydioxanone: applications in surgery and tissue engineering. *Synthetic Polymers in Drug and Biotherapeutics Delivery* **2025**, 315–334.

[158] Martins, J. A., Lach, A. A., Morris, H. L., Carr, A. J.,Mouthuy, P.-A. Polydioxanone implants: a systematic review on safety and performance in patients. *Journal of biomaterials applications* **2020**; *34*(7), 902–916.

[159] Saska, S., Pilatti, L., Silva, E. S. D. S., Nagasawa, M. A., Câmara, D., Lizier, N., Finger, E., Dyszkiewicz Konwińska, M., Kempisty, B.,Tunchel, S. Polydioxanone-based membranes for bone regeneration. *Polymers* **2021**; *13*(11), 1685.

[160] Boland, E. D., Coleman, B. D., Barnes, C. P., Simpson, D. G., Wnek, G. E.,Bowlin, G. L. Electrospinning polydioxanone for biomedical applications. *Acta biomaterialia* **2005**; *1*(1), 115–123.

[161] Abdo, V. L., Shibli, J. A., Costa, R. C., Rossy Borges, M. H., Wong, A., Sotomayor, M. D., Bertolini, M., Figueiredo, L. C., Barão, V. A.,Rangel, E. C. Tackling Microbial Contamination in Polydioxanone-Based

Membranes for Regenerative Therapy: Bioengineering an Antibiotic-Loaded Platform. *ACS Applied Bio Materials* **2025**; *8*(5), 4119–4131.

[162] Quirino, L. C., De Azambuja Carvalho, P. H., Neto, R. T. A., Comachio, C. A., Monteiro, N. G., Ervolino-Silva, A. C., Okamoto, R.,Pereira-Filho, V. A. Polydioxanone membrane compared with collagen membrane for bone regeneration. *Polymers* **2023**; *15*(4), 868.

[163] Shim, J.-H., Won, J.-Y., Sung, S.-J., Lim, D.-H., Yun, W.-S., Jeon, Y.-C.,Huh, J.-B. Comparative efficacies of a 3D-printed PCL/PLGA/β-TCP membrane and a titanium membrane for guided bone regeneration in beagle dogs. *Polymers* **2015**; *7*(10), 2061–2077.

[164] Shuai, C., Yang, W., Feng, P., Peng, S.,Pan, H., *Accelerated degradation of HAP/PLLA bone scaffold by PGA blending facilitates bioactivity and osteoconductivity, Bioact. Mater. 6 (2021) 490–502*.

[165] Zheng, Y. F., Gu, X. N.,Witte, F. Biodegradable metals. *Materials Science and Engineering: R: Reports* **2014**; *77*, 1–34.

[166] Witte, F. The history of biodegradable magnesium implants: a review. *Acta biomaterialia* **2010**; *6*(5), 1680–1692.

[167] Yang, H., Jia, B., Zhang, Z., Qu, X., Li, G., Lin, W., Zhu, D., Dai, K.,Zheng, Y. Alloying design of biodegradable zinc as promising bone implants for load-bearing applications. *Nature communications* **2020**; *11*(1), 401.

[168] Lin, W.-J., Zhang, D.-Y., Zhang, G., Sun, H.-T., Qi, H.-P., Chen, L.-P., Liu, Z.-Q., Gao, R.-L.,Zheng, W. Design and characterization of a novel biocorrodible iron-based drug-eluting coronary scaffold. *Materials & Design* **2016**; *91*, 72–79.

[169] Liu, Y., Zheng, Y., Chen, X. H., Yang, J. A., Pan, H., Chen, D., Wang, L., Zhang, J., Zhu, D.,Wu, S. Fundamental theory of biodegradable metals—definition, criteria, and design. *Advanced Functional Materials* **2019**; *29*(18), 1805402.

[170] Chen, K., Zhao, L., Sun, J., Gu, X., Huang, C., Su, H.,Fan, Y. Utilizing biodegradable alloys as guided bone regeneration (GBR) membrane: Feasibility and challenges. *Science China Materials* **2022**; *65*(10), 2627–2646.

[171] Chen, K., Zhao, L., Huang, C., Yin, X., Zhang, X., Li, P., Gu, X.,Fan, Y. Recent Advances in the Development of Magnesium-Based Alloy Guided Bone Regeneration (GBR) Membrane. *Metals* **2022**; *12*(12), 2074.

[172] Zoroddu, M. A., Aaseth, J., Crisponi, G., Medici, S., Peana, M.,Nurchi, V. M. The essential metals for humans: a brief overview. *Journal of inorganic biochemistry* **2019**; *195*, 120–129.

[173] Jomova, K., Makova, M., Alomar, S. Y., Alwasel, S. H., Nepovimova, E., Kuca, K., Rhodes, C. J.,Valko, M. Essential metals in health and disease. *Chemico-biological interactions* **2022**; *367*, 110173.

[174] Xie, J., Zhang, T., Jiang, J., Xue, W., Wang, W., Ni, J., Zhang, X.,Liu, X. Advances in magnesium-based implants for biomedical applications: A comprehensive review and future perspectives. *Journal of Magnesium and Alloys* **2025**; *13*(7), 2978–3003.

[175] Wang, W., Zhang, X.,Liu, X. Surface nanostructuring and functionalisation of magnesium-based biomaterials: Challenges and prospects. *Journal of Magnesium and Alloys* **2025**; *13*(7), 2927–2929.

[176] Zhang, Y., Xu, J., Ruan, Y. C., Yu, M. K., O'laughlin, M., Wise, H., Chen, D., Tian, L., Shi, D.,Wang, J. Implant-derived magnesium induces local neuronal production of CGRP to improve bone-fracture healing in rats. *Nature medicine* **2016**; *22*(10), 1160–1169.

[177] Wang, J. L., Xu, J. K., Hopkins, C., Chow, D. H. K.,Qin, L. Biodegradable magnesium‐based implants in orthopedics—a general review and perspectives. *Advanced science* **2020**; *7*(8), 1902443.

[178] Zhao, D., Witte, F., Lu, F., Wang, J., Li, J.,Qin, L. Current status on clinical applications of magnesium-based orthopaedic implants: A review from clinical translational perspective. *Biomaterials* **2017**; *112*, 287–302.

[179] Chaya, A., Yoshizawa, S., Verdelis, K., Myers, N., Costello, B. J., Chou, D.-T., Pal, S., Maiti, S., Kumta, P. N.,Sfeir, C. In vivo study of magnesium plate and screw degradation and bone fracture healing. *Acta biomaterialia* **2015**; *18*, 262–269.

[180] Antoniac, I., Miculescu, M., Mănescu, V., Stere, A., Quan, P. H., Păltânea, G., Robu, A.,Earar, K. Magnesium-based alloys used in orthopedic surgery. *Materials* **2022**; *15*(3), 1148.

[181] Hung, C. H., Kwok, Y. C., Yip, J., Wong, H. H.,Leung, Y. Y. Bioabsorbable Magnesium-Based Materials Potential and Safety in Bone Surgery: A Systematic Review. *Craniomaxillofacial Trauma & Reconstruction* **2025**; *18*(2), 24.

[182] Zeng, Z., Salehi, M., Kopp, A., Xu, S., Esmaily, M.,Birbilis, N. Recent progress and perspectives in additive manufacturing of magnesium alloys. *Journal of Magnesium and Alloys* **2022**; *10*(6), 1511–1541.

[183] Allavikutty, R., Gupta, P., Santra, T. S.,Rengaswamy, J. Additive manufacturing of Mg alloys for biomedical applications: Current status and challenges. *Current Opinion in Biomedical Engineering* **2021**; *18*, 100276.

[184] Zhang, J., Zhai, B., Gao, J., Li, Z., Zheng, Y., Ma, M., Li, Y., Zhang, K., Guo, Y.,Shi, X. Plain metallic biomaterials: opportunities and challenges. *Regenerative Biomaterials* **2023**; *10*, rbac093.

[185] Yang, L., Li, X.,Lu, K. Making materials plain: Concept, principle and applications. *Acta Metall Sin* **2017**; *53*(11), 1413–1417.

[186] Dong, Q., Zhang, M., Zhou, X., Shao, Y., Li, J., Wang, L., Chu, C., Xue, F., Yao, Q.,Bai, J. 3D-printed Mg-incorporated PCL-based scaffolds: A promising approach for bone healing. *Materials Science and Engineering: C* **2021**; *129*, 112372.

[187] Chua, K., Khan, I., Malhotra, R.,Zhu, D. Additive manufacturing and 3D printing of metallic biomaterials. *Engineered Regeneration* **2021**; *2*, 288–299.

[188] Jung, O., Hesse, B., Stojanovic, S., Seim, C., Weitkamp, T., Batinic, M., Goerke, O., Kačarević, Ž. P., Rider, P.,Najman, S. Biocompatibility analyses of HF-passivated magnesium screws for guided bone regeneration (GBR). *International journal of molecular sciences* **2021**; *22*(22), 12567.

[189] Rider, P., Kačarević, Ž. P., Elad, A., Tadic, D., Rothamel, D., Sauer, G., Bornert, F., Windisch, P., Hangyási, D. B.,Molnar, B. Biodegradable magnesium barrier membrane used for guided bone regeneration in dental surgery. *Bioactive materials* **2022**; *14*, 152–168.

[190] Amberg, R., Elad, A., Rothamel, D., Fienitz, T., Szakacs, G., Heilmann, S.,Witte, F. Design of a migration assay for human gingival fibroblasts on biodegradable magnesium surfaces. *Acta biomaterialia* **2018**; *79*, 158–167.

[191] Amberg, R., Elad, A., Beuer, F., Vogt, C., Bode, J.,Witte, F. Effect of physical cues of altered extract media from biodegradable magnesium implants on human gingival fibroblasts. *Acta Biomaterialia* **2019**; *98*, 186–195.

[192] Rider, P., Kačarević, Ž. P., Elad, A., Rothamel, D., Sauer, G., Bornert, F., Windisch, P., Hangyási, D., Molnar, B.,Hesse, B. Analysis of a pure magnesium membrane degradation process and its functionality when used in a guided bone regeneration model in beagle dogs. *Materials* **2022**; *15*(9), 3106.

[193] Kačarević, Ž. P., Rider, P., Elad, A., Tadic, D., Rothamel, D., Sauer, G., Bornert, F., Windisch, P., Hangyási, D. B.,Molnar, B. Biodegradable magnesium fixation screw for barrier membranes used in guided bone regeneration. *Bioactive materials* **2022**; *14*, 15–30.

[194] Elad, A., Rider, P., Rogge, S., Witte, F., Tadić, D., Kačarević, Ž. P.,Steigmann, L. Application of biodegradable magnesium membrane shield technique for immediate dentoalveolar bone regeneration. *Biomedicines* **2023**; *11*(3), 744.

[195] Elad, A., Pul, L., Rider, P., Rogge, S., Witte, F., Tadić, D., Mijiritsky, E., Kačarević, Ž. P.,Steigmann, L. Resorbable magnesium metal membrane for sinus lift procedures: a case series. *BMC Oral Health* **2023**; *23*(1), 1006.

[196] Hangyasi, D. B., Körtvélyessy, G., Blašković, M., Rider, P., Rogge, S., Siber, S., Kačarević, Ž. P.,Čandrlić, M. Regeneration of intrabony defects using a novel magnesium membrane. *Medicina* **2023**; *59*(11), 2018.

[197] Li, Z., Gu, X., Lou, S.,Zheng, Y. The development of binary Mg–Ca alloys for use as biodegradable materials within bone. *Biomaterials* **2008**; *29*(10), 1329–1344.

[198] Gu, X., Zheng, Y., Cheng, Y., Zhong, S.,Xi, T. In vitro corrosion and biocompatibility of binary magnesium alloys. *Biomaterials* **2009**; *30*(4), 484–498.

[199] Zhang, S., Zhang, X., Zhao, C., Li, J., Song, Y., Xie, C., Tao, H., Zhang, Y., He, Y.,Jiang, Y. Research on an Mg–Zn alloy as a degradable biomaterial. *Acta biomaterialia* **2010**; *6*(2), 626–640.

[200] Cai, S., Lei, T., Li, N.,Feng, F. Effects of Zn on microstructure, mechanical properties and corrosion behavior of Mg–Zn alloys. *Materials Science and Engineering: C* **2012**; *32*(8), 2570–2577.

[201] Lin, D.-J., Hung, F.-Y., Lee, H.-P.,Yeh, M.-L. Development of a novel degradation-controlled magnesium-based regeneration membrane for future guided bone regeneration (GBR) therapy. *Metals* **2017**; *7*(11), 481.

[202] Zhao, M., Liu, G., Li, Y., Yu, X., Yuan, S., Nie, Z., Wang, J., Han, J., Tan, C.,Guo, C. Degradation behavior, transport mechanism and osteogenic activity of Mg–Zn–RE alloy membranes in critical-sized rat calvarial defects. *Coatings* **2020**; *10*(5), 496.

[203] Cong, M., Zhang, Y., Zhang, Y., Liu, X., Lu, Y.,Li, X. Tensile properties and wear resistance of Mg alloy containing high Si as implant materials. *Journal of Renewable Materials* **2023**; *11*(4), 1977.

[204] Si, J., Shen, H., Miao, H., Tian, Y., Huang, H., Shi, J., Yuan, G.,Shen, G. In vitro and in vivo evaluations of Mg-Zn-Gd alloy membrane on guided bone regeneration for rabbit calvarial defect. *Journal of Magnesium and Alloys* **2021**; *9*(1), 281–291.

[205] Bai, L., Song, P.,Su, J. Bioactive elements manipulate bone regeneration. *Biomaterials Translational* **2023**; *4*(4), 248.

[206] Chen, H., Yuan, B., Zhao, R., Yang, X., Xiao, Z., Aurora, A., Iulia, B. A., Zhu, X., Iulian, A. V.,Zhang, X. Evaluation on the corrosion resistance, antibacterial property and osteogenic activity of biodegradable Mg-Ca and Mg-Ca-Zn-Ag alloys. *Journal of Magnesium and Alloys* **2022**; *10*(12), 3380–3396.

[207] Chen, K., Zhao, Y., Liu, C., Li, Q., Bai, Y., Li, P., Wang, C., Gu, X.,Fan, Y. Novel Mg-Ca-La alloys for guided bone regeneration: Mechanical performance, stress corrosion behavior and biocompatibility. *Materials Today Communications* **2022**; *32*, 103949.

[208] Ge, W., Chen, K., Tang, H., Arken, X., Zhang, X., Gu, X.,Zhu, C. Degradability and in vivo biocompatibility of micro-alloyed Mg-Ca-La alloys as orthopedic implants. *Materials Letters* **2022**; *310*, 131510.

[209] Shan, Y., Qiao, B., Ouyang, S., Du, C., Zhao, L., Wang, G., Ye, J., Xiong, Y., Wei, Y.,Song, J. Biodegradable Mg-Ca/Mg-Cu bilayer membranes with enhanced mechanical, osteogenesis and antibacterial performances for GBR applications. *Journal of Magnesium and Alloys* **2025**; *13*(2), 792–809.

[210] Zhang, S., Sun, X., Kang, C., Yang, M., Zhao, Y.,Wang, C. Study on repairing canine mandibular defect with porous Mg–Sr alloy combined with Mg–Sr alloy membrane. *Regenerative biomaterials* **2020**; *7*(3), 331–336.

[211] Ouyang, S., Wu, X., Meng, L., Jing, X., Qiao, L., She, J., Zheng, K., Chen, X.,Pan, F. More than the barrier effect: biodegradable Mg-Ag alloy membranes for guided bone/tissue regeneration. *Journal of Magnesium and Alloys* **2024**; *12*(11), 4454–4467.

[212] Chen, L., Yan, Z., Qiu, T., Zhu, J., Liu, G., Han, J.,Guo, C. Long-Term Temporospatial Complementary Relationship between Degradation and Bone Regeneration of Mg–Al Alloy. *ACS Applied Bio Materials* **2023**; *6*(11), 4703–4713.

[213] Quan, P. H., Antoniac, I., Miculescu, F., Antoniac, A., Robu, A., Biţa, A.-I., Miculescu, M., Saceleanu, A., Bodog, A. D.,Saceleanu, V. Fluoride treatment and in vitro corrosion behavior of Mg-Nd-Y-Zn-Zr alloys type. *Materials* **2022**; *15*(2), 566.

[214] Yan, Z.-Y., Zhu, J.-H., Liu, G.-Q., Liu, Z.-C., Guo, C.-B., Cui, N.-H.,Han, J.-M. Feasibility and Efficacy of a Degradable Magnesium‐Alloy GBR Membrane for Bone Augmentation in a Distal Bone‐Defect Model in Beagle Dogs. *Bioinorganic Chemistry and Applications* **2022**; *2022*(1), 4941635.

[215] Song, Y., Zhang, S., Li, J., Zhao, C.,Zhang, X. Electrodeposition of Ca–P coatings on biodegradable Mg alloy: in vitro biomineralization behavior. *Acta Biomaterialia* **2010**; *6*(5), 1736–1742.

[216] Xu, L., Pan, F., Yu, G., Yang, L., Zhang, E.,Yang, K. In vitro and in vivo evaluation of the surface bioactivity of a calcium phosphate coated magnesium alloy. *Biomaterials* **2009**; *30*(8), 1512–1523.

[217] Wu, S., Jang, Y.-S., Kim, Y.-K., Kim, S.-Y., Ko, S.-O.,Lee, M.-H. Surface modification of pure magnesium mesh for guided bone regeneration: In vivo evaluation of rat calvarial defect. *Materials* **2019**; *12*(17), 2684.

[218] Wu, S., Jang, Y.-S.,Lee, M.-H. Enhancement of bone regeneration on calcium-phosphate-coated magnesium mesh: using the rat calvarial model. *Frontiers in Bioengineering and Biotechnology* **2021**; *9*, 652334.

[219] Peng, W., Chen, J.-X., Shan, X.-F., Wang, Y.-C., He, F., Wang, X.-J., Tan, L.-L.,Yang, K. Mg-based absorbable membrane for guided bone regeneration (GBR): a pilot study. *Rare Metals* **2019**; *38*, 577–587.

[220] Han, Y., Wang, X., Wei, P., Zhang, D., Gao, M., Yu, Z., Wang, Q., Tan, L.,Tian, Y. Biodegradable Magnesium alloy Janus membrane with surface-selective osteoinduction and soft tissue healing properties in guided bone regeneration. *Acta Biomaterialia* **2025**; *195*, 582–598.

[221] Du, J., Wang, G., Song, D., Jiang, J., Jiang, H.,Gao, J. In-vitro degradation behavior and biocompatibility of superhydrophilic hydroxyapatite coating on Mg–2Zn–Mn–Ca–Ce alloy. *Journal of Materials Research and Technology* **2022**; *17*, 2742–2754.

[222] Steigmann, L., Jung, O., Kieferle, W., Stojanovic, S., Proehl, A., Görke, O., Emmert, S., Najman, S., Barbeck, M.,Rothamel, D. Biocompatibility and immune response of a newly developed volume-stable magnesium-based barrier membrane in combination with a PVD coating for guided bone regeneration (GBR). *Biomedicines* **2020**; *8*(12), 636.

[223] Li, L.-Y., Cui, L.-Y., Zeng, R.-C., Li, S.-Q., Chen, X.-B., Zheng, Y.,Kannan, M. B. Advances in functionalized polymer coatings on biodegradable magnesium alloys–A review. *Acta Biomaterialia* **2018**; *79*, 23–36.

[224] Guo, Y., Yu, Y., Han, L., Ma, S., Zhao, J., Chen, H., Yang, Z., Zhang, F., Xia, Y.,Zhou, Y. Biocompatibility and osteogenic activity of guided bone regeneration membrane based on chitosan-coated magnesium alloy. *Materials Science and Engineering: C* **2019**; *100*, 226–235.

[225] Barbeck, M., Kühnel, L., Witte, F., Pissarek, J., Precht, C., Xiong, X., Krastev, R., Wegner, N., Walther, F.,Jung, O. Degradation, bone regeneration and tissue response of an innovative volume stable magnesium-supported GBR/GTR barrier membrane. *International Journal of Molecular Sciences* **2020**; *21*(9), 3098.

[226] Du, X., Song, Y., Xuan, X., Chen, S., Wu, X., Jiang, H. B., Lee, E.-S.,Wang, X. Characterization of a Bioresorbable Magnesium‐Reinforced PLA‐Integrated GTR/GBR Membrane as Dental Applications. *Scanning* **2020**; *2020*(1), 6743195.

[227] Zhang, H. Y., Jiang, H. B., Kim, J.-E., Zhang, S., Kim, K.-M.,Kwon, J.-S. Bioresorbable magnesium-reinforced PLA membrane for guided bone/tissue regeneration. *Journal of the Mechanical Behavior of Biomedical Materials* **2020**; *112*, 104061.

[228] Wang, F., He, Y., Xiang, D., Liu, X., Yang, F., Hou, Y., Wu, W., Xia, D., Xu, Y.,Liu, Y. Magnesium-reinforced sandwich structured composite membranes promote osteogenesis. *Journal of Magnesium and Alloys* **2025**; *13*(4), 1561–1578.

[229] Ni, J., Ling, H., Zhang, S., Wang, Z., Peng, Z., Benyshek, C., Zan, R., Miri, A., Li, Z.,Zhang, X. Three-dimensional printing of metals for biomedical applications. *Materials Today Bio* **2019**; *3*, 100024.

[230] Karunakaran, R., Ortgies, S., Tamayol, A., Bobaru, F.,Sealy, M. P. Additive manufacturing of magnesium alloys. *Bioactive materials* **2020**; *5*(1), 44–54.

[231] Lai, Y., Li, Y., Cao, H., Long, J., Wang, X., Li, L., Li, C., Jia, Q., Teng, B.,Tang, T. Osteogenic magnesium incorporated into PLGA/TCP porous scaffold by 3D printing for repairing challenging bone defect. *Biomaterials* **2019**; *197*, 207–219.

[232] Wang, Y., Wang, Y., Yu, L., Hua, Y., Wang, N., Shi, E., Li, C., Chen, M.,Han, J. Collagen-Coated 3D-Printed Magnesium Alloy Scaffold with Controlled Mg2+ Release for Enhanced Repair of Critical-Sized Bone Defects. *ACS Applied Materials & Interfaces* **2025**;

[233] Elad, A., Rider, P., Rogge, S., Witte, F., Tadić, D., Kačarević, Ž. P.,Steigmann, L. *Application of Biodegradable Magnesium Membrane Shield Technique for Immediate Dentoalveolar Bone Regeneration*. Biomedicines, 2023. **11**, DOI: 10.3390/biomedicines11030744.

[234] Lin, D.-J., Hung, F.-Y., Lee, H.-P.,Yeh, M.-L. *Development of a Novel Degradation-Controlled Magnesium-Based Regeneration Membrane for Future Guided Bone Regeneration (GBR) Therapy*. Metals, 2017. **7**, DOI: 10.3390/met7110481.

[235] Zhao, M., Liu, G., Li, Y., Yu, X., Yuan, S., Nie, Z., Wang, J., Han, J., Tan, C.,Guo, C. *Degradation Behavior, Transport Mechanism and Osteogenic Activity of Mg–Zn–RE Alloy Membranes in Critical-Sized Rat Calvarial Defects*. Coatings, 2020. **10**, DOI: 10.3390/coatings10050496.

[236] Chen, K., Zhao, Y., Liu, C. L., Li, Q., Bai, Y. J., Li, P., Wang, C., Gu, X. N.,Fan, Y. B. Novel Mg-Ca-La alloys for guided bone regeneration: Mechanical performance, stress corrosion behavior and biocompatibility. *MATERIALS TODAY COMMUNICATIONS* **2022**; *32*

[237] Shan, Y., Qiao, B., Ouyang, S., Du, C., Zhao, L., Wang, G., Ye, J., Xiong, Y., Wei, Y., Song, J., She, J., Peng, J., Chen, X., Pan, F.,Wen, N. Biodegradable Mg-Ca/Mg-Cu bilayer membranes with enhanced mechanical, osteogenesis and antibacterial performances for GBR applications. *Journal of Magnesium and Alloys* **2025**; *13*(2), 792–809.

[238] Wu, S., Jang, Y.-S., Kim, Y.-K., Kim, S.-Y., Ko, S.-O.,Lee, M.-H. *Surface Modification of Pure Magnesium Mesh for Guided Bone Regeneration: In Vivo Evaluation of Rat Calvarial Defect*. Materials, 2019. **12**, DOI: 10.3390/ma12172684.

[239] Peng, W., Chen, J.-X., Shan, X.-F., Wang, Y.-C., He, F., Wang, X.-J., Tan, L.-L.,Yang, K. Mg-based absorbable membrane for guided bone regeneration (GBR): a pilot study. *Rare Metals* **2019**; *38*(6), 577–587.

[240] Wu, S., Jang, Y.-S.,Lee, M.-H. Enhancement of Bone Regeneration on Calcium-Phosphate-Coated Magnesium Mesh: Using the Rat Calvarial Model. *Frontiers in Bioengineering and Biotechnology* **2021**; *Volume 9 - 2021*

[241] Yan, Z.-Y., Zhu, J.-H., Liu, G.-Q., Liu, Z.-C., Guo, C.-B., Cui, N.-H.,Han, J.-M. Feasibility and Efficacy of a Degradable Magnesium-Alloy GBR Membrane for Bone Augmentation in a Distal Bone-Defect Model in Beagle Dogs. *Bioinorganic Chemistry and Applications* **2022**; *2022*(1), 4941635.

[242] Chen, Y., Ye, S.-H., Sato, H., Zhu, Y., Shanov, V., Tiasha, T., D'amore, A., Luketich, S., Wan, G.,Wagner, W. R. Hybrid scaffolds of Mg alloy mesh reinforced polymer/extracellular matrix composite for critical-sized calvarial defect reconstruction. *Journal of Tissue Engineering and Regenerative Medicine* **2018**; *12*(6), 1374–1388.

[243] Barbeck, M., Kühnel, L., Witte, F., Pissarek, J., Precht, C., Xiong, X., Krastev, R., Wegner, N., Walther, F.,Jung, O. *Degradation, Bone Regeneration and Tissue Response of an Innovative Volume Stable Magnesium-Supported GBR/GTR Barrier Membrane*. International Journal of Molecular Sciences, 2020. **21**, DOI: 10.3390/ijms21093098.

[244] Du, X., Song, Y., Xuan, X., Chen, S., Wu, X., Jiang, H. B., Lee, E.-S.,Wang, X. Characterization of a Bioresorbable Magnesium-Reinforced PLA-Integrated GTR/GBR Membrane as Dental Applications. *Scanning* **2020**; *2020*(1), 6743195.

[245] Seo, H.-J., Cho, Y.-E., Kim, T., Shin, H.-I.,Kwun, I.-S. Zinc may increase bone formation through stimulating cell proliferation, alkaline phosphatase activity and collagen synthesis in osteoblastic MC3T3-E1 cells. *Nutrition research and practice* **2010**; *4*(5), 356–361.

[246] Su, Y., Cockerill, I., Wang, Y., Qin, Y.-X., Chang, L., Zheng, Y.,Zhu, D. Zinc-based biomaterials for regeneration and therapy. *Trends in biotechnology* **2019**; *37*(4), 428–441.

[247] Vojtěch, D., Kubásek, J., Šerák, J.,Novák, P. Mechanical and corrosion properties of newly developed biodegradable Zn-based alloys for bone fixation. *Acta biomaterialia* **2011**; *7*(9), 3515–3522.

[248] Zhu, D., Cockerill, I., Su, Y., Zhang, Z., Fu, J., Lee, K.-W., Ma, J., Okpokwasili, C., Tang, L.,Zheng, Y. Mechanical strength, biodegradation, and in vitro and in vivo biocompatibility of Zn biomaterials. *ACS applied materials & interfaces* **2019**; *11*(7), 6809–6819.

[249] Yang, H., Huang, H., Li, S., Qin, Y., Wen, P., Qu, X., Jia, B.,Zheng, Y. Biodegradable zinc-based metallic materials: Mechanisms, properties, and applications. *Progress in Materials Science* **2025**, 101584.

[250] Huang, L., Lu, Y., Chen, K., Guan, Q., Huang, C., Qin, Y., Zhang, L., Wang, Z., Zheng, Y.,Huang, Y. Bridging Research and Application: Zn‐Based Alloys as Next‐Generation Biodegradable Orthopedic Implants. *Advanced Materials* **2026**; *38*(4), e13733.

[251] Chen, K., Li, P., Guan, Q., Gu, X., Zhao, L., Huang, L., Huang, C., Qin, Y., Yu, C.,Zhang, T. Biodegradable Zinc‐Based Alloys for Guided Bone Regeneration Membranes: Feasibility, Current Status, and Future Prospects. *Advanced Science* **2025**; *12*(40), e06513.

[252] Wen, X., Wang, J., Pei, X.,Zhang, X. Zinc-based biomaterials for bone repair and regeneration: mechanism and applications. *Journal of Materials Chemistry B* **2023**; *11*(48), 11405–11425.

[253] Wang, X., Li, X., Fan, H.,Ma, L. Solid electrolyte interface in Zn-based battery systems. *Nano-Micro Letters* **2022**; *14*(1), 205.

[254] Bednarczyk, W., Wątroba, M., Kawałko, J.,Bała, P. Can zinc alloys be strengthened by grain refinement? A critical evaluation of the processing of low-alloyed binary zinc alloys using ECAP. *Materials Science and Engineering: A* **2019**; *748*, 357–366.

[255] Li, S., Yang, H., Qu, X., Qin, Y., Liu, A., Bao, G., Huang, H., Sun, C., Dai, J.,Tan, J. Multiscale architecture design of 3D printed biodegradable Zn-based porous scaffolds for immunomodulatory osteogenesis. *Nature Communications* **2024**; *15*(1), 3131.

[256] Liu, Y., Li, Y., Dong, Z., Wang, Y., Han, C., Liao, Z., Li, Y., Huang, H., Mou, J.,Mi, J. Additive manufacturing of personalized, semipermeable and biodegradable polymer/metal composite membrane for guided bone regeneration. *Materials Today* **2025**;

[257] Huang, L., Lu, Y., Chen, K., Guan, Q., Huang, C., Qin, Y., Zhang, L., Wang, Z., Zheng, Y.,Huang, Y. Bridging Research and Application: Zn‐Based Alloys as Next‐Generation Biodegradable Orthopedic Implants. *Advanced Materials* **2025**, e13733.

[258] Chen, K., Lu, Y., Tang, H., Gao, Y., Zhao, F., Gu, X.,Fan, Y. Effect of strain on degradation behaviors of WE43, Fe and Zn wires. *Acta Biomaterialia* **2020**; *113*, 627–645.

[259] Li, H., Xie, X., Zheng, Y. F., Cong, Y., Zhou, F., Qiu, K., Wang, X., Chen, S., Huang, L.,Tian, L. Development of biodegradable Zn-1X binary alloys with nutrient alloying elements Mg, Ca and Sr. *Scientific reports* **2015**; *5*(1), 10719.

[260] Guo, H., Xia, D., Zheng, Y., Zhu, Y., Liu, Y.,Zhou, Y. A pure zinc membrane with degradability and osteogenesis promotion for guided bone regeneration: In vitro and in vivo studies. *Acta biomaterialia* **2020**; *106*, 396–409.

[261] Chen, K., Zhou, G., Li, Q., Tang, H., Wang, S., Li, P., Gu, X.,Fan, Y. In vitro degradation, biocompatibility and antibacterial properties of pure zinc: assessing the potential of Zn as a guided bone regeneration membrane. *Journal of Materials Chemistry B* **2021**; *9*(25), 5114–5127.

[262] Chen, K., Gu, X., Zhang, N., Zhao, L., Huang, C., Qin, Y., Cheng, Y., Zheng, Y.,Fan, Y. Corrosion behavior and mechanical integrity of Zn-based guided bone generation (GBR) membrane subjected to U-bending deformation. *Corrosion Science* **2024**; *236*, 112272.

[263] Li, P., Zhang, W., Dai, J., Xepapadeas, A. B., Schweizer, E., Alexander, D., Scheideler, L., Zhou, C., Zhang, H.,Wan, G. Investigation of zinc‐ copper alloys as potential materials for craniomaxillofacial osteosynthesis implants. *Materials Science and Engineering: C* **2019**; *103*, 109826.

[264] Zhang, W., Li, P., Shen, G., Mo, X., Zhou, C., Alexander, D., Rupp, F., Geis-Gerstorfer, J., Zhang, H.,Wan, G. Appropriately adapted properties of hot-extruded Zn–0.5 Cu–xFe alloys aimed for biodegradable guided bone regeneration membrane application. *Bioactive materials* **2021**; *6*(4), 975–989.

[265] Zhang, Y., Yan, Y., Xu, X., Lu, Y., Chen, L., Li, D., Dai, Y., Kang, Y.,Yu, K. Investigation on the microstructure, mechanical properties, in vitro degradation behavior and biocompatibility of newly developed Zn-0.8% Li-(Mg, Ag) alloys for guided bone regeneration. *Materials Science and Engineering: C* **2019**; *99*, 1021–1034.

[266] Li, W.-Y., Dai, Y.-L., Cai, W.-H., Lin, S.-H., Guo, L., Zhang, D.-C., Li, Y.,Wen, C. Ultrahigh strength and uniform corrosion in Zn-Li alloys through ultrahigh pressure supersaturated solid solution treatment for biodegradable orthopedic applications. *Rare Metals* **2024**; *43*(10), 5284–5304.

[267] Liu, Y., Fu, Z., Chu, X., Lu, Y., Zhang, J., Huang, J., Liu, Y., Yan, Y.,Yu, K. Fabrication and characterization of A Zn-0.5 Fe alloy membrane by powder metallurgy route for guided bone regeneration. *Materials Research Express* **2022**; *9*(6), 065401.

[268] Chu, X., Dai, Y., Fu, Z., Wang, J., Song, J., Dong, Z., Tang, Z., Yan, Y.,Yu, K. Mechanical properties, biodegradation behavior and biocompatibility of novel Zn-based alloy membranes prepared by powder metallurgy for guided bone regeneration. *Materials Today Communications* **2025**; *42*, 111367.

[269] Lin, J., Chen, Y., Dai, Y., Zhang, X., Zhang, D., Li, Y.,Wen, C. Mechanical properties, degradation action, and biocompatibility of in situ nanoparticle-reinforced MgxZny/Zn composite prepared via roll bonding. *Acta Biomaterialia* **2025**; *194*, 514–529.

[270] Chu, X., Fu, Z., Liu, Y., Dai, Y., Wang, J., Song, J., Dong, Z., Yan, Y.,Yu, K. Mechanical Properties, Microstructure, Degradation Behavior, and Biocompatibility of Zn-0.5 Ti-0.5 Fe and Zn-0.5 Ti-0.5 Mg Guided Bone Regeneration Barrier Membranes Prepared Using a Powder Metallurgy Method. *ACS Biomaterials Science & Engineering* **2024**; *10*(10), 6520–6532.

[271] Li, X.-M., Shi, Z.-Z., Tuoliken, A., Gou, W., Li, C.-H.,Wang, L.-N. Highly plastic Zn-0.3 Ca alloy for guided bone regeneration membrane: Breaking the trade-off between antibacterial ability and biocompatibility. *Bioactive Materials* **2024**; *42*, 550–572.

[272] Zhang, M., Li, F., Dai, Y.-L., Lin, J.-G., Zhang, X.-K., Zhang, D.-C., Li, Y.,Wen, C. A potent antibacterial and antitumor Zn–4Ag–2Se alloy for biodegradable orthopedic applications: M. Zhang et al. *Rare Metals* **2025**; *44*(10), 7615–7633.

[273] Xu, W., Gao, X., Zhang, M., Jiang, Z., Xu, X., Huang, L., Yao, H., Zhang, Y., Tong, X.,Li, Y. Electrospun polycaprolactone-chitosan nanofibers on a zinc mesh as biodegradable guided bone-regeneration membranes with enhanced mechanical, antibacterial, and osteogenic properties for alveolar bone-repair applications. *Acta Biomaterialia* **2024**; *187*, 434–450.

[274] Chen, K., Wang, Y., Tang, H., Niu, X., Yang, H., Bai, Y., Gu, X.,Zheng, Y. Fabrication of a nanoscale magnesium/copper metal–organic framework on Zn-based guided bone generation membranes for enhancing osteogenesis, angiogenesis, and bacteriostasis properties. *ACS Applied Materials & Interfaces* **2024**; *16*(5), 5648–5665.

[275] Yan, F., Yu, M., He, Y., Wang, F., Yang, F., Zhao, X., Zheng, Y., Liu, Y., Xia, D.,Liu, Y. Hierarchical mineralized collagen coated Zn membrane to tailor cell microenvironment for guided bone regeneration. *Advanced Functional Materials* **2025**; *35*(7), 2412695.

[276] Tang, H., Zhang, Y., Chen, Y., Wang, J., Huang, C., Yang, H., Wang, Q., Bai, Y., Li, P.,Gu, X. Fabrication of Nb2C MXene coated zinc for improved degradation, antibacterial activity, and osteogenesis for guided bone regeneration applications. *Journal of Materials Science & Technology* **2025**; *237*, 201–218.

[277] Guo, H., Xia, D. D., Zheng, Y. F., Zhu, Y., Liu, Y. S.,Zhou, Y. S. A pure zinc membrane with degradability and osteogenesis promotion for guided bone regeneration: In vitro and in vivo studies. *ACTA BIOMATERIALIA* **2020**; *106*, 396–409.

[278] Li, P., Zhang, W., Dai, J., Xepapadeas, A. B., Schweizer, E., Alexander, D., Scheideler, L., Zhou, C., Zhang, H., Wan, G.,Geis-Gerstorfer, J. Investigation of zinc‐ copper alloys as potential materials for craniomaxillofacial osteosynthesis implants. *Materials Science and Engineering: C* **2019**; *103*, 109826.

[279] Zhang, W., Li, P., Shen, G., Mo, X., Zhou, C., Alexander, D., Rupp, F., Geis-Gerstorfer, J., Zhang, H.,Wan, G. Appropriately adapted properties of hot-extruded Zn–0.5Cu–xFe alloys aimed for biodegradable guided bone regeneration membrane application. *Bioactive Materials* **2021**; *6*(4), 975–989.

[280] Zhang, Y., Yan, Y., Xu, X., Lu, Y., Chen, L., Li, D., Dai, Y., Kang, Y.,Yu, K. Investigation on the microstructure, mechanical properties, in vitro degradation behavior and biocompatibility of newly developed Zn-0.8%Li-(Mg, Ag) alloys for guided bone regeneration. *Materials Science and Engineering: C* **2019**; *99*, 1021–1034.

[281] Liu, Y., Fu, Z., Chu, X., Lu, Y., Zhang, J., Huang, J., Liu, Y., Yan, Y.,Yu, K. Fabrication and characterization of A Zn-0.5Fe alloy membrane by powder metallurgy route for guided bone regeneration. *Materials Research Express* **2022**; *9*(6), 065401.

[282] Chu, X., Fu, Z., Liu, Y., Dai, Y., Wang, J., Song, J., Dong, Z., Yan, Y.,Yu, K. Mechanical Properties, Microstructure, Degradation Behavior, and Biocompatibility of Zn-0.5Ti-0.5Fe and Zn-0.5Ti-0.5Mg Guided Bone Regeneration Barrier Membranes Prepared Using a Powder Metallurgy Method. *ACS Biomaterials Science & Engineering* **2024**; *10*(10), 6520–6532.

[283] Li, X.-M., Shi, Z.-Z., Tuoliken, A., Gou, W., Li, C.-H.,Wang, L.-N. Highly plastic Zn-0.3Ca alloy for guided bone regeneration membrane: Breaking the trade-off between antibacterial ability and biocompatibility. *Bioactive Materials* **2024**; *42*, 550–572.

[284] Liu, Y., Li, Y., Dong, Z., Wang, Y., Han, C., Liao, Z., Li, Y., Huang, H., Mou, J.,Mi, J. Additive manufacturing of personalized, semipermeable and biodegradable polymer/metal composite membrane for guided bone regeneration. *Materials Today* **2025**; *83*, 181–197.

[285] Zhang, J. Y., Zhang, X. Z., Feng, Z. Y., Jiang, Y. L., Fan, M. H., Han, C., Song, Y. T., Zou, C. Y., Liu, Y.,Nie, R. The Solver of Conflicting Needs: Research Advances in Janus Membranes for Tissue Engineering. *Advanced Functional Materials* **2025**, 2507418.

[286] Zhang, K.-R., Gao, H.-L., Pan, X.-F., Zhou, P., Xing, X., Xu, R., Pan, Z., Wang, S., Zhu, Y.,Hu, B. Multifunctional bilayer nanocomposite guided bone regeneration membrane. *Matter* **2019**; *1*(3), 770–781.

[287] Si, Y., Shi, Shuo, Zhi, Chuanwei, Lei, Leqi, Hu, Jinlian, Yang, Luming. Janus Electrospun Membranes. *Advanced Materials* **2025**; *2507498*, 1–37.

[288] Yuan, S., Feng, Y., Wang, H., Chen, S. M., Li, J. H., Zhu, Y. B., Yu, S. H.,Wang, Z. Sword and Board in One: A Bioinspired Nanocomposite Membrane for Guided Bone Regeneration. *Advanced Materials* **2025**, 2504577.

[289] Wei, Y., Wang, Z., Han, J., Jiang, X., Lei, L., Yang, X., Sun, W., Gou, Z.,Chen, L. Modularized bioceramic scaffold/hydrogel membrane hierarchical architecture beneficial for periodontal tissue regeneration in dogs. *Biomaterials Research* **2022**; *26*(1), 68.

[290] Yuan, L., Yuan, C., Wei, J., Jin, S., Zuo, Y., Li, Y., Liang, X.,Li, J. Electrospinning/3D printing-integrated porous scaffold guides oral tissue regeneration in beagles. *Bio-Design and Manufacturing* **2024**; *7*(6), 1000–1017.

[291] Zhang, M., Huang, Z., Wang, X., Liu, X., He, W., Li, Y., Wu, D.,Wu, S. Personalized PLGA/BCL Scaffold with Hierarchical Porous Structure Resembling Periosteum‐Bone Complex Enables Efficient Repair of Bone Defect. *Advanced Science* **2024**; *11*(35), 2401589.

[292] He, M., Wang, Q., Xie, L., Wu, H., Zhao, W.,Tian, W. Hierarchically multi-functionalized graded membrane with enhanced bone regeneration and self-defensive antibacterial characteristics for guided bone regeneration. *Chemical Engineering Journal* **2020**; *398*, 125542.

[293] Xue, Y., Zhu, Z., Zhang, X., Chen, J., Yang, X., Gao, X., Zhang, S., Luo, F., Wang, J.,Zhao, W. Accelerated bone regeneration by MOF modified multifunctional membranes through enhancement of osteogenic and angiogenic performance. *Advanced Healthcare Materials* **2021**; *10*(6), 2001369.

[294] Li, C., Geng, X., Chu, D., Li, J., Zhang, J., Jin, L.,Li, Z. NIR-responsive composite nanofibers provide oxygen and mineral elements to promote osteogenesis. *Materials & Design* **2022**; *224*, 111285.

[295] Yang, Q., Lou, S., Zhang, Y., Fang, Z., Xing, C., Wang, W., Han, M., Wang, Z., Tang, B. Z.,Zhang, M. NIR‐II Responsive Multifunctional Scaffold Enabling "Kill‐Modulation‐Build" Synergistic Therapy for Infectious Bone Defects. *Advanced Science* **2025**, e08948.

[296] Kalogeropoulou, M., Díaz-Payno, P. J., Mirzaali, M. J., Van Osch, G. J., Fratila-Apachitei, L. E.,Zadpoor, A. A. 4D printed shape-shifting biomaterials for tissue engineering and regenerative medicine applications. *Biofabrication* **2024**; *16*(2), 022002.

[297] Chen, X., Han, S., Wu, W., Wu, Z., Yuan, Y., Wu, J.,Liu, C. Harnessing 4D printing bioscaffolds for advanced orthopedics. *Small* **2022**; *18*(36), 2106824.

[298] Ding, A., Tang, F.,Alsberg, E. 4D printing: A comprehensive review of technologies, materials, stimuli, design, and emerging applications. *Chemical Reviews* **2025**; *125*(7), 3663–3771.

[299] Champeau, M., Heinze, D. A., Viana, T. N., De Souza, E. R., Chinellato, A. C.,Titotto, S. 4D printing of hydrogels: a review. *Advanced Functional Materials* **2020**; *30*(31), 1910606.

[300] Sydney Gladman, A., Matsumoto, E. A., Nuzzo, R. G., Mahadevan, L.,Lewis, J. A. Biomimetic 4D printing. *Nature materials* **2016**; *15*(4), 413–418.

[301] Alanazi, B. N., Ahmed, H. A., Alharbi, N. S., Ebrahim, N. A.,Soliman, S. M. Exploring 4D printing of smart materials for regenerative medicine applications. *RSC advances* **2025**; *15*(39), 32155–32171.

[302] Guo, X., Yi, J., Wan, Z., Wang, X., Yuan, Z., Cheung, W., Bai, X., Fu, Y., Zhai, M.,Lv, L. Morphology and Function Dual‐Adjustable Biomimetic 4D‐Printed Scaffold for the Regenerative Restoration of Complex Bone Defects. *Advanced Functional Materials* **2025**, 2509961.

[303] Ghosh, S., Qiao, W., Yang, Z., Orrego, S.,Neelakantan, P. Engineering dental tissues using biomaterials with piezoelectric effect: current progress and future perspectives. *Journal of Functional Biomaterials* **2022**; *14*(1), 8.

[304] Donate, R., Paz, R., Moriche, R., Sayagués, M. J., Alemán-Domínguez, M. E.,Monzón, M. An overview of polymeric composite scaffolds with piezoelectric properties for improved bone regeneration. *Materials & Design* **2023**; *231*, 112085.

[305] Akbari, N., Khorshidi, S.,Karkhaneh, A. Effect of piezoelectricity of nanocomposite electrospun scaffold on cell behavior in bone tissue engineering. *Iranian Polymer Journal* **2022**; *31*(8), 919–930.

[306] Dai, X., Yao, X., Zhang, W., Cui, H., Ren, Y., Deng, J.,Zhang, X. The osteogenic role of barium titanate/polylactic acid piezoelectric composite membranes as guiding membranes for bone tissue regeneration. *International journal of nanomedicine* **2022**; *17*, 4339.

[307] Zhu, K., Li, R., Yin, S., Yang, F., Sun, Y., Xing, Y., Yang, Y., Xu, W.,Yu, Y. A novel ultrasound-driven piezoelectric GBR membrane dispersed with boron nitride nanotubes promotes bone regeneration and anti-bacterial properties. *Materials Today Bio* **2025**; *30*, 101418.

[308] Cheng, J., Wu, L., Fu, H., Hu, L., Wang, W., Heng, B. C., Zhang, X., Liu, O., Deng, X.,Liu, Y. Biodegradable piezoelectric janus membrane with enhanced antibacterial and osteoinductive properties for periodontitis therapy. *Advanced Healthcare Materials* **2025**; *14*(12), 2500543.

[309] Lai, C., Cheng, M., Ning, C., He, Y., Zhou, Z., Yin, Z., Zhu, P., Xu, Y., Yu, P.,Xu, S. Janus electro-microenvironment membrane with surface-selective osteogenesis/gingival healing ability for guided bone regeneration. *Materials Today Bio* **2022**; *17*, 100491.

[310] Li, X., Huang, Z., Shuck, C. E., Liang, G., Gogotsi, Y.,Zhi, C. MXene chemistry, electrochemistry and energy storage applications. *Nature Reviews Chemistry* **2022**; *6*(6), 389–404.

[311] Babar, Z. U. D., Iannotti, V., Rosati, G., Zaheer, A., Velotta, R., Della Ventura, B., Álvarez-Diduk, R.,Merkoçi, A. MXenes in healthcare: synthesis, fundamentals and applications. *Chemical Society Reviews* **2025**;

[312] Kang, M. S., Jang, H. J., Jo, H. J., Raja, I. S.,Han, D.-W. MXene and Xene: promising frontier beyond graphene in tissue engineering and regenerative medicine. *Nanoscale Horizons* **2024**; *9*(1), 93–117.

[313] Wan, S., Chen, Y., Huang, C., Huang, Z., Liang, C., Deng, X.,Cheng, Q. Scalable ultrastrong MXene films with superior osteogenesis. *Nature* **2024**; *634*(8036), 1103–1110.

[314] Kinloch, I. A., Suhr, J., Lou, J., Young, R. J.,Ajayan, P. M. Composites with carbon nanotubes and graphene: An outlook. *Science* **2018**; *362*(6414), 547–553.

[315] Xu, Y., Hirata, E., Iizumi, Y., Ushijima, N., Kubota, K., Kimura, S., Maeda, Y., Okazaki, T.,Yokoyama, A. Single-walled carbon nanotube membranes accelerate active osteogenesis in bone defects: potential of guided bone regeneration membranes. *ACS biomaterials science & engineering* **2022**; *8*(4), 1667–1675.

[316] Valizadeh Harzand, F., Mousavi Nejad, S. N., Babapoor, A., Mousavi, S. M., Hashemi, S. A., Gholami, A., Chiang, W.-H., Buonomenna, M. G.,Lai, C. W. Recent advances in metal-organic framework (MOF) asymmetric membranes/composites for biomedical applications. *Symmetry* **2023**; *15*(2), 403.

[317] Li, K., Song, J., Lu, Y., Zhang, D., Wang, Y., Wang, X., Tang, Y., Yu, Y., Zhang, X.,Yang, X. Biodegradable Piezoelectric Janus Membrane Enabling Dual Antibacterial and Osteogenic Functions for Periodontitis Therapy. *ACS Applied Materials & Interfaces* **2025**; *17*(16), 23707–23721.

[318] Al-Bishari, A. M., Liu, T., Zhuang, J., Zhang, Q., Chen, J., Wang, Y., Liu, C., Gao, P., Liu, J.,Lu, L. Triple-layered multi-functional membrane for synergistic enhancement of guided bone regeneration. *Materials & Design* **2024**; *239*, 112816.

[319] Chen, S., Wu, Z., Huang, Z., Liang, C.,Lee, S. J. Implantable dental barrier membranes as regenerative medicine in dentistry: a comprehensive review. *Tissue Engineering and Regenerative Medicine* **2025**, 1–23.

[320] Ma, K., Liao, C., Huang, L., Liang, R., Zhao, J., Zheng, L.,Su, W. Electrospun PCL/MoS2 nanofiber membranes combined with NIR‐triggered photothermal therapy to accelerate bone regeneration. *Small* **2021**; *17*(51), 2104747.

[321] Liu, X., Zhang, W., Wang, Y., Chen, Y., Xie, J., Su, J.,Huang, C. One-step treatment of periodontitis based on a core-shell micelle-in-nanofiber membrane with time-programmed drug release. *Journal of Controlled Release* **2020**; *320*, 201–213.

[322] Zhang, S., Huang, L., Bian, M., Xiao, L., Zhou, D., Tao, Z., Zhao, Z., Zhang, J., Jiang, L. B.,Li, Y. Multifunctional bone regeneration membrane with flexibility, electrical stimulation activity and osteoinductive activity. *Small* **2024**; *20*(47), 2405311.

[323] Mu, Y., Ma, S., Wei, P., Wang, Y., Jing, W., Zhao, Y., Zhang, L., Wu, J., Zhao, B.,Deng, J. Multifunctional modification of SIS membrane with chimeric peptides to promote its antibacterial, osteogenic, and healing‐promoting abilities for applying to GBR. *Advanced Functional Materials* **2021**; *31*(31), 2101452.

[324] Yang, D., Xu, Z., Huang, D., Luo, Q., Zhang, C., Guo, J., Tan, L., Ge, L., Mu, C.,Li, D. Immunomodulatory multifunctional janus collagen-based membrane for advanced bone regeneration. *Nature Communications* **2025**; *16*(1), 1–18.

[325] Li, Z., Zhu, Y.,Matson, J. B. pH-responsive self-assembling peptide-based biomaterials: designs and applications. *ACS applied bio materials* **2022**; *5*(10), 4635–4651.

[326] Sobczak, M. Enzyme-responsive hydrogels as potential drug delivery systems—state of knowledge and future prospects. *International journal of molecular sciences* **2022**; *23*(8), 4421.

[327] Di Spirito, F., Giordano, F., Di Palo, M. P., Ferraro, C., Cecere, L., Frucci, E., Caggiano, M.,Lo Giudice, R. Customized 3D-Printed Mesh, Membrane, Bone Substitute, and Dental Implant Applied to Guided Bone Regeneration in Oral Implantology: A Narrative Review. *Dentistry Journal* **2024**; *12*(10), 303.

[328] Li, P., Zhu, L., Ding, Y., Long, Z., Yang, Y., Pan, J., Gu, M., Wang, W.,Yang, Z. RF energy harvesting for intraoral orthodontic force monitoring. *Nano Energy* **2024**; *121*, 109244.

[329] Wang, K.-N., Li, Z.-Z., Cai, Z.-M., Cao, L.-M., Zhong, N.-N., Liu, B., Zhou, K., Huo, F.-Y., Cai, B.,Bu, L.-L. The applications of flexible electronics in dental, oral, and craniofacial medicine. *npj Flexible Electronics* **2024**; *8*(1), 33.

[330] Panahi, O. Bridging the Gap: AI-Driven Solutions for Dental Tissue Regeneration. *Austin J Dent* **2024**; *11*(2), 1185.

[331] Batra, A. M.; Reche, A. A new era of dental care: harnessing artificial intelligence for better diagnosis and treatment. *Cureus* **2023**; *15*(11)

[332] Mahdi, S. S., Battineni, G., Khawaja, M., Allana, R., Siddiqui, M. K.,Agha, D. How does artificial intelligence impact digital healthcare initiatives? A review of AI applications in dental healthcare. *International Journal of Information Management Data Insights* **2023**; *3*(1), 100144.

[333] Surdu, A., Budala, D. G., Luchian, I., Foia, L. G., Botnariu, G. E.,Scutariu, M. M. Using AI in Optimizing Oral and Dental Diagnoses—A Narrative Review. *Diagnostics* **2024**; *14*(24), 2804.